Towards a global sulphur dioxide forecast capability for aviation

Authors: Claire Witham, Nina Kristiansen, Frances Beckett and Franco Marenco

Forecasting Research Technical Report No. 648

Met Office, UK

October 2021

© Crown Copyright 2021, Met Office

Publication Details

Title: Towards a global sulphur dioxide forecast capability for aviation

Written by: Met Office on behalf of the London VAAC

Reviewed by: Matthew Hort (Hd of Atmospheric Dispersion and Air Quality)

Date: October 2021

Suggested citation: Witham C., Kristiansen N., Beckett F., and Marenco F., 2021, Towards a global sulphur dioxide forecast capability for aviation, Forecasting Research Technical Report 648, Met Office, October 2021.

Met Office
FitzRoy Road
Exeter
Devon
EX1 3PB
United Kingdom

© Crown Copyright 2021, Met Office

Executive Summary

Volcanic activity can release large quantities of sulphur dioxide (SO_2) into the atmosphere from explosive and effusive eruptions. Elevated concentrations of SO_2 pose a potential health hazard and may impact aircraft components and hence maintenance cycles. The exposure and level of potential risk to air traffic is determined by the extent and concentration of volcanic SO_2 plumes. The aviation industry would like to better understand the frequency and level of potential exposure and what would be required to deliver a suitable forecast capability, to inform if and what a future forecast service requirement might be.

Following a request from the International Civil Aviation Organization's work stream on volcanic ash and sulphur dioxide, this review outlines the capabilities required to provide an operational forecast for aviation of the presence and amount of volcanic SO_2. It makes recommendations on the components needed to deliver such a service and assesses their current operational readiness. The forecast process for volcanic SO_2 is very similar to that for forecasting quantitative volcanic ash, so many of the identified requirements and challenges are similar and not new.

The report presents the current state of the art in modelling, satellite retrievals, and techniques for combing models and observations known as data fusion. This shows that:

- A model capable of representing the chemistry and transport of the SO_2 plume is needed.
- Satellite observations are essential for detecting and constraining the SO_2 release and for validating the forecast.
- Data fusion techniques add considerable value for refining the eruption source parameters and improving the forecast. One or more data fusion methods will likely prove essential to achieve accurate SO_2 forecasts.

With respect to the current capabilities in these areas:

- A variety of suitable models exist, but all will require some degree of optimisation to meet the requirements of an operational forecast.
- Existing satellite sensors and related data tools provide a solid foundation, but a greater focus on geostationary satellite retrievals of SO_2 is needed to help meet the timeliness requirements of an aviation forecast. Planned future satellite missions should add value here.
- Most of the currently available data fusion methods have been developed in the research arena and very few have been tested operationally for volcanic eruptions. Development and validation work will be needed to ensure that techniques are fit for purpose and meet operational delivery requirements.

The impact of applying different SO_2 concentration thresholds on the requirement to produce SO_2 forecasts for aviation has also been assessed. The lowest SO_2 threshold evaluated is 0.175 ppm, which is the World Health Organization's (WHO) short-term threshold for exposure to SO_2. Six higher thresholds have been evaluated based on recommendations by the Volcanic Ash Science Advisory Group and the levels of SO_2 observed by satellites.

Detailed model simulations for eight different historic eruptions have been used to calculate the area and time over which the SO_2 thresholds are exceeded. The eruptions considered are classified as small, moderate, or large based on the amount of SO_2 released, as well as the release height and duration. The findings show that:

- The 0.175 ppm (WHO) threshold is exceeded for all the historic eruptions considered.

© Crown Copyright 2021, Met Office

- The highest SO_2 threshold, 4.375 ppm (WHOx25), is only exceeded for the large explosive eruptions.
- The time and area over which the thresholds are exceeded vary and depend on the eruption characteristics (i.e., the amount, duration and height of the SO_2 which is released).
- A single Dobson Unit (DU) threshold cannot be applied equally to all eruptions, as the corresponding atmospheric concentration is highly sensitive to the height and thickness of the SO_2 plume. The use of a DU threshold in a global forecast system is consequently not advised and thresholds should be expressed in ppm.
- Plume extents defined by the WHO threshold can be considerably larger than the Volcanic Ash Advisory areas issued for the same eruption.

Finally, a trial of a volcanic SO_2 global forecast was conducted for eruptions of Etna and La Soufriere St Vincent using the tools and data that were available at the Met Office at the time. The findings help demonstrate the current capabilities for producing a volcanic SO_2 forecast and identify gaps and areas where further development work would be required.

© Crown Copyright 2021, Met Office

Contents

Executive Summary 2
1 Introduction 6
1.1 Context of this report 6
1.2 Overview of the Required Capability Components 6
2 Background to Volcanic Sulphur Dioxide 8
2.1 Sulphur Dioxide 8
2.2 Volcanic Activity 8
2.3 Atmospheric and Chemical Processes 9
3 Models 11
3.1 Current Modelling Capabilities – The State of the Art 11
3.1.1 Model Frameworks 11
3.1.2 Meteorology and Topography 11
3.1.3 Representing Chemical Processes 14
3.1.4 Output Resolution and Extent 14
3.2 Validation 15
3.3 Considerations for an Operational Model 16
3.3.1 Source Parameters 16
3.3.2 Meteorological and Topographical Datasets 19
3.3.3 Representing Chemical Processes 20
3.4 Current Operational Models 21
3.5 Summary 24
4 Satellites 25
4.1 Spectroscopy 25
4.2 A few decades of satellite observations 26
4.3 Detecting eruptions 29
4.4 The plume height 30
4.5 Estimation of eruption source parameters 32
4.6 Limitations 34
4.7 Summary 35
5 Data Fusion 36
5.1 Trajectory techniques 38
5.2 Inversion methods 40
5.3 Data Insertion 43
5.4 Data assimilation 44
5.4.1 Four-dimensional variational assimilation (4D-Var) 45

© Crown Copyright 2021, Met Office

5.4.2 Ensemble-based data assimilation 46
5.5 Comparing and combining data fusion methods 48
5.6 Model and observation data requirements 48
5.7 Summary and operational considerations 50
6 Thresholds 52
6.1 The proposed thresholds 52
6.2 Historic aircraft encounters and measurements of volcanic SO_2 54
6.3 Eruptions considered in the analysis 54
6.4 Model simulations 55
6.5 Evaluation of ppm thresholds 57
6.6 Evaluation of Dobson Unit thresholds 69
6.7 Comparisons of SO_2 and ash plume extents 73
6.8 Summary 74
7 Forecasting Systems 80
7.1 Detection and Communication 80
7.2 Forecast Delivery 80
8 Forecast Trial 82
8.1 Case-study 1: 28 Feb 2021 eruption of Etna 83
8.2 Case-study 2: 9 April 2021 eruption of La Soufriere 86
8.3 Findings from the trial 92
8.3.1 Alerting 92
8.3.2 Estimation of source parameters 92
8.3.3 Modelling 94
8.3.4 Comparison to ash forecasts 95
8.3.5 Forecast Validation 95
8.3.6 Availability of satellite data 96
9 Recommendations 97
Acknowledgements 102
References 102
Appendix A – List of Acronyms 113

© Crown Copyright 2021, Met Office

1 Introduction

Volcanic activity can release significant quantities of gas, including sulphur dioxide (SO_2), into our atmosphere (Bluth et al., 1993). Sulphur dioxide is a colourless gas with a pungent odour and can cause serious health problems. Between 1980 and 2008 there were at least 15 incidents where aircraft reported encounters with sulphur dioxide, many in the form of detection of sulphurous smells in the cabin (Guffanti et al., 2010). The 2008 eruption of Kasatochi is particularly striking due to dozens of reported encounters as the volcanic gas plume moved over North America.

When volcanic SO_2 enters an aircraft, its odour can cause distress to passengers and crew, and it may represent a significant health hazard. Predominant short-term effects of SO_2 are irritation of the eyes and respiratory tract, and airway constriction in asthmatics (Hansell and Oppenheimer, 2004). Sulphur dioxide and its chemical products can also cause 'crazing' on aircraft windscreens and sensor apertures, premature fading of protective paint, and corrosion issues in hot parts of the engine. Since 2013 the ICAO Working Group on Meteorological Information and Service Development (WG-MISD) has taken an interest in volcanic SO_2, with a focus on identifying and quantifying health risks to aircraft occupants.

1.1 Context of this report

On 20 November 2019, the fifth meeting of the ICAO Meteorology Panel (METP) WG-MISD Volcanic Ash and Sulphur Dioxide (VASD) Work Stream (METP/WG-MISD/VASD/5) agreed the following action relating to sulphur dioxide (SO_2):

> *Action 5/2 - Sulphur dioxide (SO2) information and forecasts – phase 2*
>
> *That, London VAAC is invited to develop and trial a global SO2 forecast capability using the thresholds provided by the VASAG, share the product with the Ad Hoc group, and report back to the next meeting with a view for developing and formulating preliminary functional and performance requirements*.

The discussion in the immediately subsequent Volcanic Ash Science Advisory Group (VASAG) and Volcanic Ash Advisory (VAAC) Best Practice meetings was that the work should explore the "art of the possible", with the outputs needing to be suitable to inform the "development and formulation of preliminary functional and performance requirements" by the WG-MISD, but not presenting a fully functional operational forecast.

This report summarises the work conducted by the Met Office on behalf of the London VAAC to meet Action 5/2 and the resulting recommendations for a future SO_2 forecast capability.

1.2 Overview of the Required Capability Components

An initial evaluation of the components needed to build a global forecast system highlighted that the following categories need to be considered:

1. Detection and awareness that an eruption has occurred
    a. Global notification from volcano observatories
    b. Automated satellite detection of volcanic SO_2
    c. Automated eruption detection from other monitoring data (both local and distal)
2. Satellite data to inform the location and quantity of the plume at the analysis (T+0) timestep
3. Quantification of SO_2 eruption source term parameters

© Crown Copyright 2021, Met Office

    a. Amount of SO_2 emitted
    b. Timing, height, and depth of emission
4. Modelling of the SO_2 plume to produce a forecast
5. Fusion of observations and models to improve source terms and forecast
6. Definition of appropriate thresholds for forecast products
7. Forecast validation
    a. Using satellite data
    b. Using other observations
8. Provision of forecast data to customers

This report focuses on the first six items. A schematic of how the different components fit together is given in Figure 1.1. There is considerable commonality here with quantitative volcanic ash forecasting requirements.

The report starts with a summary of volcanic emissions and the chemical properties of SO_2, and then addresses the requirements and state of the art in models, satellite data, and data fusion approaches. A review of potential concentration thresholds is given in Section 6, before consideration is given to more general forecast system requirements. Section 8 reports the findings of a "forecast trial" using two real eruptions. The report concludes with a set of recommendations. A list of acronyms used throughout the report is provided in the Appendix.

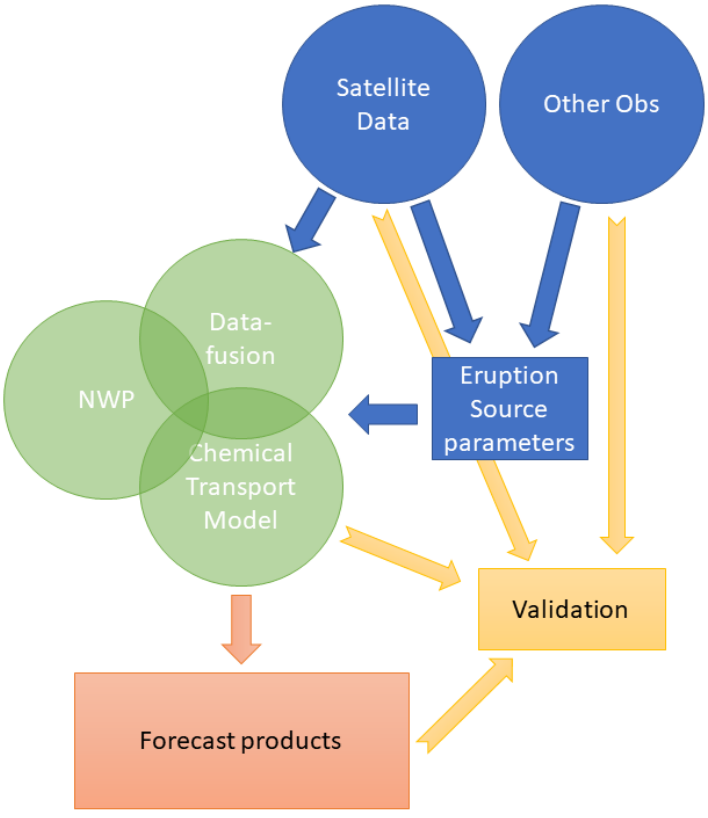

Figure 1.1: Simplified overview of the forecast process and components required.

© Crown Copyright 2021, Met Office

2 Background to Volcanic Sulphur Dioxide

2.1 Sulphur Dioxide

Sulphur dioxide (SO_2) is a colourless toxic gas with a pungent odour and is released into the atmosphere by volcanic activity and industrial processes (fossil fuel combustion and copper extraction). Atmospheric SO_2 can impact human health and the natural environment, and it was one of the primary causes of acid rain. Today, background concentrations of SO_2 in clean air are very small (~1 ppbv, Theys et al., 2013); however, they can increase dramatically in a volcanic event when SO_2 will often reach the upper troposphere and lower stratosphere region (UTLS).

The atmospheric abundance of SO_2 can be expressed in a number of ways. Here, we will mainly refer to: (1) volume mixing ratios in parts per million by volume (ppmv), which are used for health exposure thresholds; (2) atmospheric column loadings in Dobson Units (DU), which are commonly used to express satellite retrievals; and (3) total emitted mass for an eruption, expressed in teragrams (Tg) or kilotonnes (kt) (where 1 Tg = 1000 kt).

2.2 Volcanic Activity

The emission of SO_2 is associated with volcanic activity across all scales. Volcanic gases can be released into the atmosphere through persistent passive degassing, effusive and explosive eruptions (Figure 2.1). The various types of activity need to be addressed when considering the potential hazard to aviation from volcanic SO_2 clouds and when assessing the application of SO_2 concentration thresholds.

Persistent degassing passively releases gas at the surface and is not accompanied by any significant volcanic ash or lava emission. This mechanism represents a significant source of gases to the global atmospheric budget. At least 100 persistently degassing volcanoes were identified by satellite measurements between 2005 and 2015 (Carn et al., 2017). The largest emitter, Ambrym (Vanuatu) released a total of 4581 kilotons (kt) of SO_2 in 2010 (Carn et al., 2019), which translates to a daily SO_2 emission flux of ~12 kt/day. The smallest passive degasser, Merapi (Indonesia), emitted ~0.32 kt/day (Carn et al., 2017). On average, over the past decade, a total of ~63 kt/day of SO_2 has been released due to passive degassing from the world's volcanoes (Carn et al., 2017).

Effusive eruptions, such as the spectacular fissure eruption of the Bárðarbunga-Veiðivötn volcanic system which took place at the Holuhraun lava field in Iceland during 2014-2015, release large quantities of gas alongside lava flows and fire fountaining. The daily SO_2 flux for Holuhraun was between 60-120 kt/day (Schmidt et al., 2015) and a total of ~11,0000 kt of SO_2 was released over the course of this 6-month long eruption, which is approximately two times higher than the total anthropogenic emissions from the European Economic Area in 2011 (Gislason et al., 2015). The resulting SO_2 cloud was transported significant distances within the troposphere and was detected by surface air quality monitoring stations as far away as Austria (Schmidt et al., 2015). The maximum SO_2 concentration measured by surface stations in Iceland was ~1500 $\mu g/m^3$ and in Ireland ~500 $\mu g/m^3$ was measured (Schmidt et al., 2015).

Large explosive eruptions can inject huge quantities of SO_2 into the troposphere and stratosphere, where it can remain for days to weeks (Carn et al., 2016, Mills et al., 2016, Zhu et al., 2020). For example, the eruption of Kelut (Indonesia) in 2014 injected SO_2 up to an altitude of ~26 km and the resulting volcanic SO_2 cloud was tracked using Infrared Atmospheric Sounding Interferometer (IASI) on board the MetOp polar orbiting meteorological satellites for almost 10 days, as it crossed the whole of the Indian Ocean into Africa (Athanassiadou et al., 2016). The eruption of Raikoke (Kuril

© Crown Copyright 2021, Met Office

Islands) in 2019 released around 1500 kt of SO_2 over ~9 hours, which was observed by satellites for several weeks (de Leeuw et al., 2021).

The SO_2 fluxes from passive degassing volcanoes are much smaller than the fluxes from effusive and explosive eruptions. For example, the daily emission flux from the largest passive degasser (Ambrym) is around 10% of the emission flux from the effusive 2014 Holuhraun eruption. Because SO_2 fluxes from passive degassing are small and the release occurs at the surface, it is unlikely that this type of activity constitutes a significant risk for aircraft operations at cruising altitude, and therefore passive degassing emissions are not considered further in this report.

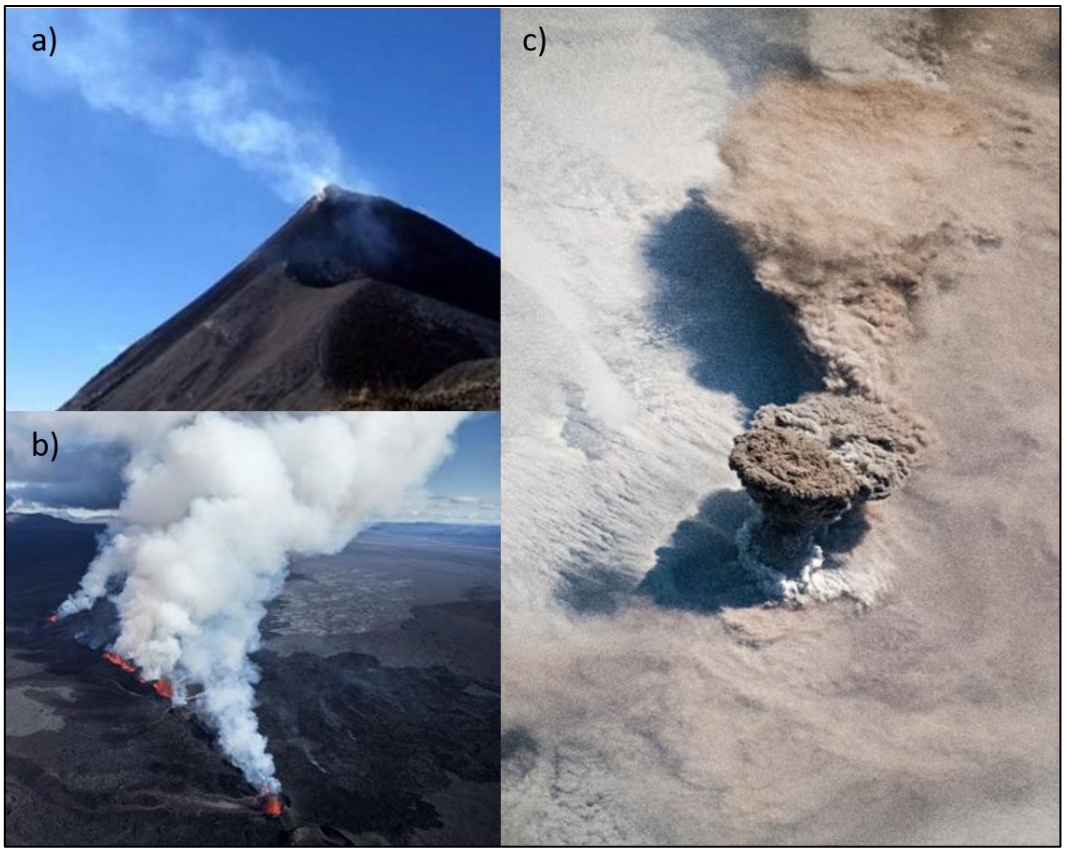

Figure 2.1: Examples of the release of volcanic gases from a) persistent passive degassing at Fuego, Guatemala (accessed from https://volcano.si.edu/showreport.cfm?doi=10.5479/si.GVP.BGVN200912-342090), b) the effusive eruption of Holuhraun, Iceland (accessed from https://guidetoiceland.is/best-of-iceland/15-incredible-photographs-of-the-holuhraun-volcano-in-iceland), and c) the explosive eruption of Raikoke, Kuril Isles, in 2019 which injected SO_2 into the stratosphere (accessed from https://eoimages.gsfc.nasa.gov/images/imagerecords/145000/145226/iss059e119250_lrg.jpg).

2.3 Atmospheric and Chemical Processes

Once in the atmosphere volcanic SO_2 is transported by the wind, dispersed, and removed by atmospheric and chemical processes. In atmospheric science the 'lifetime' or 'e-folding time' of a species is defined as the time taken for concentrations to fall to 1/e of its previous value. The number e, also known as Euler's number, is a mathematical constant approximately equal to 2.71828, i.e., the 'lifetime' is the time it takes for concentrations to fall to approximately 37% of its initial value. The e-folding time of SO_2 is typically reported to vary between hours to days (Carn et

© Crown Copyright 2021, Met Office

al., 2016), and there are several documented cases where volcanic SO_2 clouds have been observed to remain in the atmosphere for weeks to months (e.g., Athanassiadou et al., 2016, de Leeuw et al, 2021).

A number of 'sinks' act to remove SO_2 from the atmosphere, reducing concentrations and the extent of its transport. These include dry deposition (encountering the land surface) and, when in the troposphere, wet deposition, due to the scavenging of particles by precipitation, both within and below cloud. SO_2 also undergoes depletion through chemical processes and can be adsorbed onto volcanic ash (Zhu et al., 2020).

Oxidation processes occur in the gas phase and the aqueous phase, converting SO_2 into particulate sulphate (SO_4). In the gas phase the dominant reaction is with the hydroxly radical (OH). The abundance of OH depends on the atmospheric composition and meteorological factors such as humidity, UV radiation, and temperature (Zhao et al., 2019). Further, because the hydroxyl radical (OH) is formed through photolytic reactions it therefore has diurnal and seasonal cycles (Pattantyus et al., 2018). Concentrations of OH also decrease with altitude as the air becomes cooler and drier and decrease with latitude as water vapour concentrations and sunlight intensity decrease towards the poles. As such, e-folding times in the stratosphere tend to be longer than in the troposphere. In most circumstances the limiting agent in the production of sulphate will be SO_2. However, when SO_2 concentrations are very high, for example in conditions near Halema'uma'u Crater (Hawaii), OH can be completely depleted and could be the limiting agent (Pattantyus et al., 2018).

If there are significant amounts of liquid in the volcanic cloud, or if the SO_2 encounters a meteorological cloud, then it can be taken up in cloud water and undergo oxidation via aqueous phase pathways (Martin et al., 2014). The solubility of SO_2 is dependent on the pH and temperature of the solution (Berglen et al. 2004). In the aqueous phase, SO_2 is oxidized to sulphate by hydrogen peroxide (H_2O_2), ozone (O_3) and O_2 catalysed by TMI (Transition Metal Ions, Martin et al., 2014). Ozone reactions are highly pH dependent and only become the leading oxidant at pH > 5.5 (Pattantyus et al., 2018). As liquid phases in the volcanic cloud are likely acidic, SO_2 oxidation by O_3 is therefore not expected to be significant (Martin et al., 2014). When SO_2 concentrations are very high in volcanic clouds H_2O_2 may be consumed very quickly, and hence only a small fraction of SO_2 might be oxidised via this reaction (Martin et al., 2014). Therefore, most of the volcanic sulphate will probably be produced via gas phase oxidation by OH and/or via O_2-TMI aqueous oxidation (Martin et al., 2014). In the stratosphere the lack of water content tends to favour gas phase oxidation of SO_2 (Martin, 2018). However, very large eruptions producing water-rich volcanic plumes could provide locally significant amounts of water to the stratosphere and aqueous phase oxidation by O_3 could also then play a role (Martin, 2018).

SO_2 can also be adsorbed onto the surface of volcanic ash (Witham et al. 2005). This chemisorption process has been relatively under-studied and there is some debate as to its importance as a 'sink' process. Some laboratory work suggests that this is probably a negligible process in comparison with oxidation of SO_2 by aqueous and gas phase reactions in the atmosphere, except in the case of very high volcanic ash concentrations close to the vent (Maters et al. 2017, Urupina et al. 2019). However, using model simulations and observational data others suggest that, if fine low-density ash persists in the atmosphere, then the lifetime of SO_2 may be dominated by its uptake onto the ash, rather than due to oxidation with the OH radical (Zhu et al., 2020).

© Crown Copyright 2021, Met Office

3 Models

Atmospheric models are an important part of the forecast production process. The choice of model may influence what is required from the other system components. We start by providing an overview of the current 'state-of-the-art' models which can be used to simulate SO_2 clouds. We then discuss the operational considerations that would be required to provide a timely forecast of the presence of volcanic SO_2 clouds to the aviation industry and assess the modelling efforts needed to provide this service.

3.1 Current Modelling Capabilities – The State of the Art

Many atmospheric models have been developed by the global community to simulate the transport and transformation of pollutants in the atmosphere. Table 3.1 provides a list of current models which can be used to model volcanic SO_2. Each model has a slightly different design, for example there are differences in model frameworks (Eulerian or Lagrangian), the atmospheric and chemical processes they represent, the meteorological data they use, and whether they incorporate feedbacks with the meteorology (online vs offline), as well as different choices of horizontal and vertical grid resolution and extent (regional vs global and tropospheric vs stratospheric). As such different models have different qualities when considering their ability to simulate the transport of volcanic SO_2.

3.1.1 Model Frameworks

Most models use either a Lagrangian or Eulerian framework. The two approaches differ in the way they define the flow field. In a Eulerian framework the calculation of the species concentrations is performed at every grid point and emissions are instantly mixed within a grid box, as such peak concentrations are dependent on the grid resolution. In Lagrangian, or trajectory, models the concentration of a species is described for a fluid element as it travels with the flow and output is independent from the resolution of the input data, but can suffer from uncertainty in regions with low particle concentrations. Lagrangian models typically require less computing time and fewer initialization data than Eulerian models, however representing chemical processes in Lagrangian models is more challenging as newly created reaction products must be assigned to Lagrangian particles, and this can introduce errors.

3.1.2 Meteorology and Topography

To represent the transport, dispersion, and removal of a pollutant, a model must accurately represent the meteorological conditions. Three-dimensional wind fields are needed to model the advection of the gas, and information on clouds, their location, total cloud column water content and phase, as well as information on precipitation intensity and phase are also required to represent wet deposition (e.g., Pisso et al., 2019). Two different approaches are used to couple models with meteorological data. Offline models use meteorological fields which have been generated independently from a Numerical Weather Prediction (NWP) model. Alternatively, the NWP model itself can include the treatment of the transport and dispersion of pollutant, an Online approach. For example, the online Composition-Integrated Forecasting System (C-IFS) at the European Centre for Medium-Range Weather Forecasts (ECMWF) provides global forecasts of atmospheric composition, including SO_2 concentrations (Flemming and Inness, 2013, Peuch et al., 2015), as part of the Copernicus Atmospheric Modelling service (CAMs). Online models have the advantage that they can directly incorporate the impact of the pollutant on the weather, for example ICON-ART represents the effect on radiative heating (Muser et al., 2020). Further, the pollutant transport is directly tied to the temporal and spatial resolution of the NWP model. This helps to avoid inaccuracies associated

© Crown Copyright 2021, Met Office

Table 3.1: Current models which include chemistry schemes and have been used to simulate the atmospheric transport and dispersion of volcanic SO_2. If the model is associated with an operational centre (defined as providing real time forecasts) the centre is also listed but note that this does not imply that SO_2 forecasts are currently being generated at that centre. Where models use independent meteorological fields (Offline approach) examples of the meteorological datasets are given, but it should be noted that the examples given are not exhaustive. Significant references relating to each model are also provided.

Model	**Online/ Offline**	**Eulerian/ Lagrangian**	**Associated Operational Centre**	**Significant References**
CALPUFF	Offline Datasets: ECMWF	Lagrangian (Gaussian Puff model)	IMO (Iceland)	Scire et al. (2000); Barsotti et al. (2020)
CESM	Offline Datasets: MERRA (Reanalysis) Climate Model	Eulerian + Lagrangian	-	Mills et al. (2016)
CHIMERE	Offline Datasets: WRF/GFS	Eulerian	-	Boichu et al. (2013,2014,2016)
C-IFS	Online	Semi-Lagrangian	ECMWF (Europe)	Flemming and Inness (2013); Puech et al. (2015)
CMAQ	Offline Datasets: WRF NAM (North American Met)	Eulerian	US National Weather Service's Daily AQ Forecasts NAQFC (NOAA Air Quality Forecasting)	Wong et al. (2012); Tang et al. (2020)
EMEP	Offline Datasets: WRF / ECMWF	Eulerian	UK Centre for Ecology and Hydrology (policy research) Norwegian Met Institute	Vieno et al. (2010); Simpson et al. (2012); Steensen et al. (2016, 2017)
FLEXPART	Offline Datasets: ECMWF / GFS	Lagrangian	ZAMG (Austria)	Eckhardt et al. (2008); Pisso et al. (2019)
GEOS-CF	Offline Datasets: GEOS-FP / MERRA-2 (Reanalysis)	Eulerian	NASA 5-day atmospheric composition forecasts (US)	Ge et al. (2016); Hughes et al. (2016)

© Crown Copyright 2021, Met Office

HYSPLIT	Offline: Datasets: NCEP/GFS/WRF	Lagrangian HYSPLIT-Chem component uses a Lagrangian-Eulerian (mixed) approach.	VAACs: Darwin (Australia), Wellington (New Zealand), Anchorage + Washington (US)	Rolph et al. (1993); Stein et al. (2000); Stein et al. (2015)
ICON-ART	Online	-	German Weather Forecasting Service	Muser et al. (2020)
IFS-CB05-BASCOE-GLOMAP (ICBG)	Online	Semi-Lagrangian + Eulerian	-	Remy et al. (2019); Huijnen et al. (2016)
MOCAGE	Offline Datasets: ARPEGE / IFS	Semi-Lagrangian	Toulouse VAAC (France)	Lamotte et al. (2020)
NAME	Offline Datasets: UM / ECMWF	Eulerian + Lagrangian Options	London VAAC (UK)	Heard et al. (2012); de Leeuw et al. (2021)
SILAM	Offline Datasets: IFS	Eulerian + Lagrangian	Finnish Met Institute	Vira et al., (2017)
UM-UKCA	Online	Eulerian	UK Met Office	Dhomse et al. (2014); Malavelle et al. (2017); Walters et al. (2019)
WRF-Chem	Online	Eulerian	NCAR/ NOAA (US)	Egan et al. (2014)

© Crown Copyright 2021, Met Office

with the handling of atmospheric processes occurring on timescales smaller than the typical coupling intervals used between offline dispersion and NWP models (Marti and Folch, 2018). However, online models are more computationally demanding than offline models, it is not yet clear how uncertainties in the emissions and modelled concentration of the pollutant might result in poorly constrained feedbacks, the spatial resolution of the NWP can limit the representation of small plumes, and it is challenging to set the extent of the domain in the online approach when the transport of the plume is not yet known i.e., for forecasting purposes.

Climate models are also able to represent the transport, dispersion, and atmospheric chemistry of SO_2. However, they are designed to predict future climatological conditions and are not used with operational forecast meteorological datasets, although they have also been used ('nudged') with reanalysis meteorological datasets to study past events (Online approach). For example, Malavelle et al. (2017) used the global climate model HadGEM3 with UKCA to study the impact of volcanic SO_2 from the 2014-2015 eruption of Holuhraun (Iceland) on aerosol-cloud interactions.

3.1.3 Representing Chemical Processes

Many Eulerian models now include a full treatment of the chemical processes of many species, including SO_2. For example, chemistry modules appropriate for the troposphere, stratosphere, mesosphere, and lower thermosphere have been merged into a unified 'TSMLT' mechanism for the Whole Atmosphere Community Climate Model (WACCM, Mills et al., 2016). The TSMLT chemical scheme is more complex than many schemes and includes 158 photochemical species, 2 invariant species, 117 photolysis reactions, 331 gas-phase reactions, 2 aqueous phase reactions in cloud droplets, 4 heterogenous reactions on tropospheric aerosols and 6 heterogeneous reactions on stratospheric aerosol (Mills et al., 2016).

The Lagrangian atmospheric dispersion model NAME has a simpler approach. Its chemistry scheme includes parameterisations that represent the conversion of SO_2 into sulphate aerosols (SO_4) in the gas phase, via the reaction with the hydroxyl radical (OH), as well as conversion in the aqueous phase via the reaction with hydrogen peroxide (H_2O_2) and ozone (O_3), and both are represented at all levels in the atmosphere (Redington et al., 2009). The concentrations of H_2O_2 and O_3 in the atmosphere are pre-defined using monthly-mean background fields obtained from the UM-UKCA model (Unified Model coupled to the United Kingdom Chemistry and Aerosol model). This model has, though, still proved very capable of representing the transport of volcanic SO_2 clouds (e.g., Schmidt et al., 2015, de Leeuw et al., 2021).

3.1.4 Output Resolution and Extent

To balance computational time with output resolution, predictions over large global domains tend to be output on coarser output grids. For example, the atmospheric composition model C-IFS outputs data on a horizontal grid with resolution of ~80 km but can generate forecasts over global spatial extents. The Community Earth System Model (CESM), a global climate model with interactive atmosphere (represented by WACCM), ocean, land, and sea-ice components, is run on a 1.9° latitude × 2.5° longitude (~210 x 278 km at the equator) horizontal grid.

An alternative approach is to use nested grids with varying resolution. The offline European Monitoring and Evaluation Programme (EMEP) chemistry-transport model has been used to provide global output, but also local scale predictions, at higher (~5 km) horizontal resolutions, over the UK and Europe in the EMEP4UK project (Vieno et al., 2010, Simpson et al. 2012). This uses a 1-way nesting of the high-resolution meteorological datasets within a coarser outer domain, such that the results of the large-scale runs are used as boundary conditions for the higher resolution scale (Vieno et al., 2010, Simpson et al. 2012). The standard version of EMEP has just 20 vertical levels reaching

© Crown Copyright 2021, Met Office

up to 100 hPa (~ 16 km), but a more flexible version, used for volcanic emissions, has also been developed, referred to as emergency EMEP (eEMEP). This includes meteorological data from additional vertical levels with a model top height of 32 km (Steensen et al., 2017).

3.2 Validation

A few studies have attempted to validate the different modelling approaches by comparing output to observations of volcanic SO_2 clouds. Tang et al. (2020) compared simulations of volcanic SO_2 from the 2018 eruption of Mt. Kilauea volcano (Hawaii) using CMAQ, a Eulerian model with a comprehensive chemistry scheme, to satellite data and surface air quality measurements. They found that the model results generally agreed well with both the satellite data and in-situ measurements over Hawaii Big Island, although short-lived peak values of SO_2 were not always captured. They suggest that discrepancies were probably due to coarse temporal (e.g., daily volcanic emissions) and spatial resolutions (12 km) in the meteorology over complex terrain.

Forecasts of hourly SO_2 concentrations from the Holuhraun fissure eruption (Iceland) using the CALPUFF model (Figure 3.1) were compared with real-time ground-based measurements at air quality monitoring stations across Iceland (Barsotti et al., 2020). CALPUFF is a Lagrangian dispersion model and represents chemical reactions of SO_2 (both in the aqueous and gas phases) with an assumed set of transformation rates. Some mismatch was observed between model results and measurements and explanations included: the spatial resolution of meteorological data field, the capability to reproduce chemical reactions of SO_2 in the atmosphere, and the reduced extent of the numerical domain used.

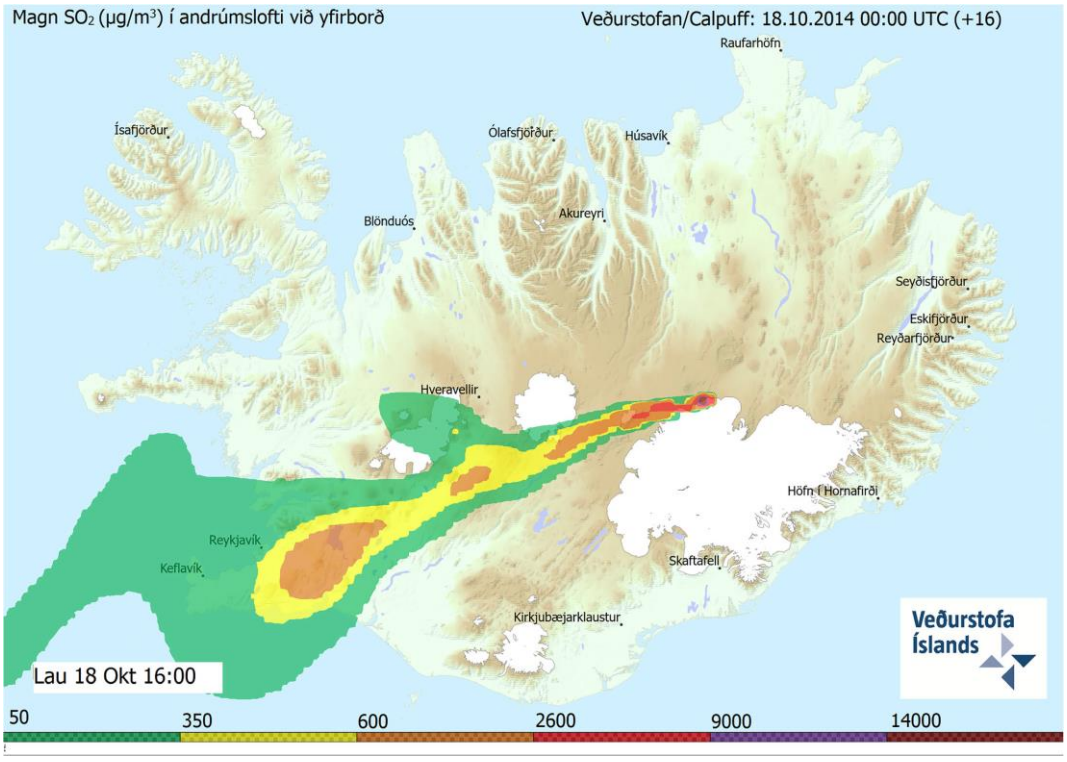

Figure 3.1: An example of a CALPUFF forecast of ground level SO_2 concentrations (ug/m^3) issued on the 18th October 2014. These forecasts were displayed on the Iceland Met Office (IMO) website during the Bárðarbunga-Veiðivötn effusive eruption. The six levels in the coloured legend correspond to air quality thresholds indicated by the EAI (Environmental Agency of Iceland). Taken from Barsotti, (2020).

© Crown Copyright 2021, Met Office

Another study of the Holuhraun SO_2 cloud using CHIMERE, a Eulerian model, also suggested that an accurate representation of the planetary boundary layer dynamics is important when modelling large scale volcanogenic air pollution (Boichu et al., 2016). Whilst simulations of the Raikoke 2019 SO_2 cloud using NAME highlighted the importance of correctly representing mesoscale motions in the atmosphere (de Leeuw et al., 2021). A comparison of simulations using the online WRF-Chem model of the SO_2 cloud from eruption of Kasatochi in 2008 to remote sensing retrievals from the Ozone Monitoring Instrument (OMI) pointed to the importance of capturing the emission source parameters (Egan et al., 2014). Indeed, all the studies mentioned above highlighted the importance of representing source parameters, in particular emission rate and plume height, as they strongly influence the accuracy of the simulation.

3.3 Considerations for an Operational Model

To produce an operational forecast of the presence of volcanic SO_2 in the atmosphere a model must be able to deliver timely and accurate information and be robust enough to guarantee the delivery of up-to-date information multiple times per day. Many of the model capabilities needed to generate a volcanic SO_2 forecast are the same as those needed to generate a quantitative volcanic ash forecast (Table 3.2). However, there are some differences which should be noted.

To initialize a model simulation of a volcanic ash or SO_2 cloud requires near real time information on the source parameters, and the modelling system must be able to react quickly to changing conditions. Models may be initialized by setting eruption source parameters or through direct assimilation of observation data (see Section 5). When initializing an SO_2 forecast fewer parameters are required, simply the plume vertical distribution and the flux of gas into the atmosphere at the source, as information on particle characteristics (used to represent the sedimentation of ash) are not needed (Table 3.2). As observations are not always available there must be processes in place to estimate the source parameters in their absence.

To represent the onwards transport and dispersion of the SO_2 there are also some differences in the model capabilities required, the most significant being that once in the atmosphere volcanic SO_2 is depleted by chemical processes.

We now discuss in more detail how we might set source parameters for volcanic SO_2 clouds and optimal model setup options, including meteorological and topographical datasets, and how we might represent chemical processes, given the time-constraints on operational forecasting.

3.3.1 Source Parameters

To initialise a model simulation, we need to know the location of the SO_2 release (which volcano is erupting), the timings of the release, the vertical extent over which it is being injected into the atmosphere, and the amount being released, the mass flux (e.g., kg/hr). Importantly, to produce an optimal forecast, the modelling system must also be able to capture variations in these parameters with time, specifically changes in plume height and mass flux. Many of the world's volcanoes are too remote for ground or air-based observations and remain completely unmonitored locally, but significant improvements in satellite coverage mean that volcanic eruptions rarely go completely un-detected.

© Crown Copyright 2021, Met Office

Requirement	Volcanic Ash	Volcanic SO_2
Source Parameters		
Plume Height (vertical distribution of mass)		
Mass Flux		
Particle Size Distribution		
Particle Density		
Particle Shape		
Model Capabilities		
Topography		
Horizontal wind advection		
Vertical wind advection		
Horizontal Atmospheric Diffusion		
Vertical Atmospheric Diffusions		
Particle Sedimentation		
Other Dry Deposition Processes		
Wet Deposition		
Chemical Processes		

Table 3.2: The source parameters and model capabilities required for quantitative volcanic ash and SO_2 forecasts. Green indicates a requirement, whereas white indicates where the item is not applicable.

A variety of techniques have been developed to detect, and constrain the properties of, volcanic SO_2 clouds from satellite retrievals, including mass loadings and plume height, as discussed in Section 4. Satellite retrieved observations can be used with Data Fusion approaches (Trajectory Techniques, Inversion Methods, Data Insertion, and Data Assimilation), which are discussed in Section 5. These methods use satellite observations to either automatically constrain the source term (at the volcano) or to correct the modelled down-wind volcanic cloud to better match the observations. For example, Inversion and Data Assimilation Techniques have been used with SILAM and C-IFS respectively to improve model predictions (post-event) of the volcanic SO_2 cloud from the eruption of Eyjafjallajökull in 2010 (Flemming and Inness 2013, Vira et al. 2017). However, it should be noted that all the methods used to retrieve properties of volcanic clouds from satellite data, and the Data Fusion techniques themselves, are prone to several limitations (see Sections 4 and 5).

If the area around the volcano is accessible, ground-based monitoring may be used to measure fluxes in real-time. During the effusive Bárðarbunga-Veiðivötn eruption ground–based DOAS (Differential Optical Absorption Spectroscopy) was used to measure the emission rate of SO_2 from the beginning of the eruption (Gislason et al., 2015). However, it can be challenging to maintain ground-based measurements close to hazardous sites. At the Alaska Volcano Observatory (AVO) they monitor volcanic gases using airborne surveys (Lopez et al., 2013). During the explosive eruption of Mount Redoubt in 1991 11 gas observations flights were conducted in conjunction with satellite overpasses. During each flight SO_2 column density was measured. These were integrated across the plume and multiplied by the wind speed to provide an estimate of the SO_2 flux (Lopez et

© Crown Copyright 2021, Met Office

al., 2013). However, airborne surveys are costly, require good flying conditions (favourable weather), can be difficult to carry out during explosive eruptions due to the associated hazards, and only generate data over the duration of the flight (measurements are not continuous).

If no direct observations of the mass flux are available the magnitude of an eruption tends to be a good indicator, with larger eruptions generating more ash and gas (Newhall and Self, 1982, Schnetzler et al., 1997, Halmer et al., 2002). The London, Toulouse, Montreal, and Wellington VAACs use empirical estimates of the flux of volcanic ash based on the observed plume height, referred to as the 'Mastin Relationship' (Mastin et al., 2009). This approach is based on classic buoyant plume theory which dictates that the height of a plume should increase with the fourth root of the eruption rate (Morton, 1956). We have explored whether a similar approach could be employed to estimate the flux of SO_2 from an observed plume height.

Figure 3.2 shows the plume heights and SO_2 mass fluxes from 505 explosive eruptions with a VEI >2, using data from the Multi-Satellite Volcanic Sulphur Dioxide Database Long-Term L4 Global (MSVOLSO2L4) compiled by Carn (2019). The dataset includes information on the eruption, including the plume height, and the observed mass of SO_2 in the atmosphere for events between 1978 and 2019. We convert total mass observed to mass fluxes by assuming the mass retrieved per day has been released over the 1-day period. The mass flux (M) increases with plume height (H), described by a power-law relationship, although the best-fit to the data suggests slightly lower mass fluxes for a given plume height than buoyant plume theory would predict:

$$M = 0.289\, H^{\frac{1}{0.184}}$$

However, it should be noted that there is likely significant uncertainty on the plume height and mass loading measurements, and this should be constrained to understand the spread in the data. Further, as is the case when this empirical approach is applied to volcanic ash plumes, it assumes there is no significant meteorological interaction i.e., that the plume is not overly influenced by the wind (bent over). Calculated volcanic ash fluxes using the Mastin Relationship have roughly an order of magnitude uncertainty (Mastin et al., 2009). Further research would be needed to constrain the uncertainty on SO_2 fluxes using this empirical approach, this initial work would suggest they could be significant, 1 – 2 orders of magnitude, and this would directly translate into the uncertainty on the model forecast of SO_2 concentrations in the cloud. However, even with significant uncertainties, this approach could prove very useful during the early stages of an eruption when observations are limited, or as an a priori estimate for more complex data fusion methods (see Section 5).

A variety of eruption column models have also been developed to simulate the eruption dynamics at the source, based on buoyant plume theory, which account for interaction of the plume with the atmosphere (see the intercomparison study of Costa et al., 2016), and although these have been designed for volcanic ash plumes, they could, in principle, also be developed for volcanic SO_2 plumes.

© Crown Copyright 2021, Met Office

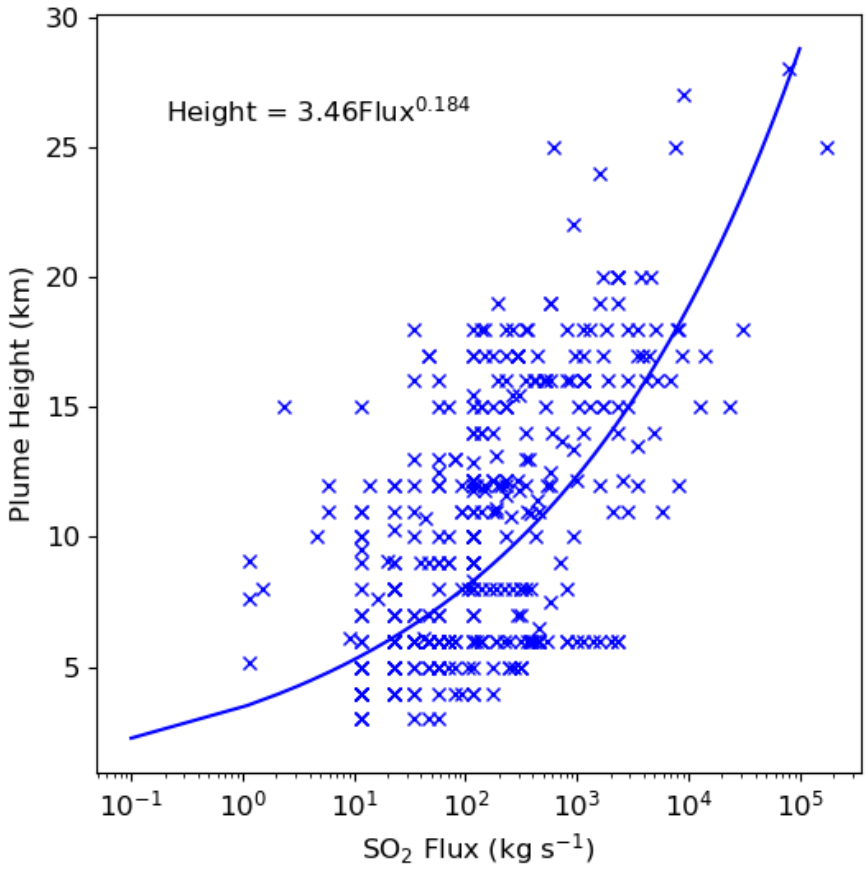

Figure 3.2: Plume height (km) versus log erupted SO_2 flux (kg s^{-1}) for explosive eruptions with a VEI > 2, taken from the Carn (2019) database. The solid line is the best-fit curve through the data, the relationship, indicating how plume height varies with SO_2 flux, is given on the Figure.

3.3.2 Meteorological and Topographical Datasets

Any future operational modelling system for volcanic SO_2 clouds will need to use forecast meteorological datasets. Volcanic ash forecasts are required to have a horizontal resolution of 0.25° (Table 3.3). To generate an optimal model simulation the resolution of the meteorological data should, at a minimum, have this resolution too. As SO_2 can be released close to the ground (effusive eruptions) as well as at high altitudes (from violent explosive eruptions) the setup of the model domain extent and resolution (both in the horizontal and vertical) and the choice of meteorological and associated topographic datasets may require a flexible approach. Passive degassing and effusive eruptions, which generate smaller plumes releasing gas close to the surface may be best represented by limited area higher resolution meteorology and topography data nested in a coarser larger domain (e.g., Beckett et al., 2015). Using a limited domain may help to preserve fast run times while using higher resolution data but will require the model to represent the transport and dispersion of the volcanic SO_2 and background species into and out of the domain over the forecast period. Large explosive eruptions will require that the transport of SO_2 and chemical processes are represented in both the troposphere and stratosphere and may require global model domains and meteorological datasets to fully represent the long-range transport of the SO_2 cloud.

© Crown Copyright 2021, Met Office

Requirement	Volcanic Ash	Volcanic SO_2
Forecast Requirements		
Horizontal Resolution	0.25° (lat-lon, regular grid)	
Vertical Resolution	50FL, 5000 ft (surface to FL600)	
Temporal Resolution	3 Hourly	
Forecast Period	24 Hours	
Issue Times	6 Hourly	
Outputs	Gridded Format	

Table 3.3: Model output requirements for quantitative volcanic ash forecasts. Note the issuance requirements for volcanic SO_2 have yet to be agreed.

3.3.3 Representing Chemical Processes

The atmospheric and chemical processes which occur inside a volcanic SO_2 cloud are complex (as discussed in Section 2.3) and challenging to represent in a model. An initial study by D'Amours et al. (2010) used an interact tracer (no chemistry or deposition processes) to represent the long-range transport of volcanic SO_2 clouds from the 2008 eruptions of Okmok and Kasatochi using the Lagrangian model MLDP0. In a retrospective study of the volcanic SO_2 clouds from the 2011 eruption of Grímsvötn (Iceland) and the 2010 eruption of Eyjafjallajökull (Iceland) Flemming and Inness (2013) found they were able to represent well the spread of the clouds by representing chemical loss of SO_2 by reaction with the OH radical simply by applying a constant e-folding time of 10 days. However, the e-folding time will depend on the height at which the SO_2 resides in the atmosphere and would be difficult to define in 'real-time' for an operational system. Further, a recent study by de Leeuw et al. (2021) of the volcanic SO_2 cloud from the eruption of Raikoke in 2019 using NAME highlighted that inaccurate representation of chemical processes can lead to a significant over-estimation of the mass of SO_2 in the downwind cloud over timescales greater than a few days, suggesting that it is important to represent these processes when predicting concentrations in the atmosphere (Figure 3.3).

To initialize a chemistry scheme, the background composition of the atmosphere must be known. Operational air quality models often use a prior run (e.g., yesterday's forecast) to initialize the succeeding run (Ryan 2016). Alternatively, climatology can be used to quantify background fields, for example NAME uses monthly averaged 3-dimensional background fields provided by the UKCA model (Redington et al., 2009) and FLEXPART uses monthly averaged OH fields from GEOS-Chem (Eckhardt et al., 2008, Pisso et al., 2019).

An operational chemistry scheme would need to be computationally efficient and able to represent chemical processes at all latitudes and altitudes (from both low-level passive and effusive eruptions and high-altitude plumes from explosive eruptions), and for all seasons (see Section 2.3). Inclusion of comprehensive chemistry schemes can impose a significant burden on computational resource; exact run times will depend on the model setup but will also depend on the amount of computing resources used. As such comprehensive testing would be required to assess both the suitability and computational resource requirements of any model for operational forecast use.

© Crown Copyright 2021, Met Office

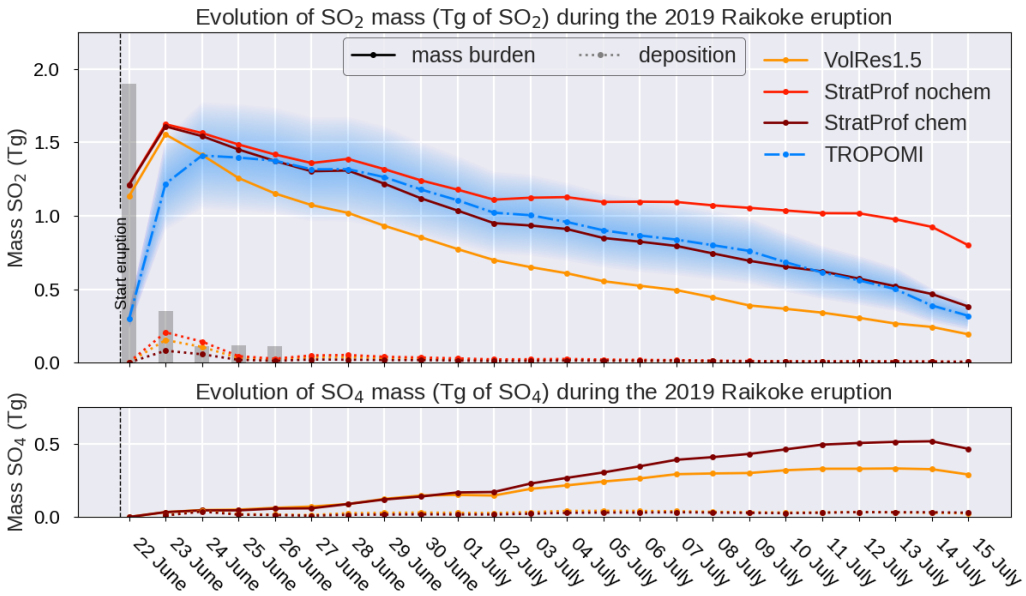

Figure 3.3: To show the impact on predicted mass of SO_2 in the atmosphere when chemical reactions are not represented in the modelling system. Here retrieved mass loadings of the Raikoke 2019 SO_2 cloud using the satellite instrument TROPOMI are compared to the modelled total mass in the atmosphere using NAME. When chemical reactions are not represented (bright red line) the total mass is over-estimated, and no SO_4 is produced (bottom plot). When chemical reactions are included (dark red line) the modelled mass better matches the observations. Modified from de Leeuw et al. (2021) and reproduced with kind permission from H. de Leeuw.

3.4 Current Operational Models

Presently none of the modelling systems used by the VAACs are set up to deliver volcanic SO_2 forecasts, but in some cases the centres are using a model which does have the capability to do so (Table 3.4). The NAME model used by the London VAAC has recently been used to study the transport and dispersion of the SO_2 cloud from the 2019 eruption of Raikoke volcano (de Leeuw et al. 2021) and has been used to simulate regional air quality (Heaviside et al., 2021). MOCAGE, used by Toulouse VAAC, is used in the regional ensemble forecasting system developed by CAMS, to provide air quality forecasts. It has also been used in a recent study to model volcanic SO_2 clouds from persistently active passively degassing volcanoes, to understand their impact on the tropospheric sulphur budget (Lamotte et al., 2020).

There are also two other modelling systems, not used by the VAACs, which have been used to provide real-time forecasts of volcanic SO_2 clouds. The CAMs service is using the C-IFS Online Eulerian model with a comprehensive chemistry scheme to provide global 5-day forecasts, with a 3 hourly temporal resolution, of total column mass loadings (g m^{-2}) of atmospheric SO_2, with an output horizontal resolution of ~80 km (Figure 3.4). To initialize their simulations, they use Data Assimilation of satellite retrieved mass loadings of SO_2. The Lagrangian atmospheric dispersion model CALPUFF was used to provide daily 72-hour forecasts of volcanic SO_2 over Iceland during the Holuhraun effusive eruption (2014-2015) and for the effusive eruption in the Krýsuvík-Trölladyngja volcanic system, close to Fagradalsfjall on the Reykjanes Peninsula in 2021 (Figure 3.5). Forecasts of the Holuhraun volcanic SO_2 cloud used ECMWF meteorological data with a resolution of ~2 km and the model output had a horizonal resolution of 4 km (Barsotti 2020). However, these operational forecasts did not include representation of chemical reactions in the volcanic cloud.

© Crown Copyright 2021, Met Office

Model	Met Datasets	Chemistry Scheme?	Eulerian/ Lagrangian	VAAC	Significant References
FALL3D	ETA / SMN	No	Eulerian	Buenos Aries	Folch et al. (2020)
HYSPLIT	NCEP / GFS / WRF	Yes	Lagrangian	Darwin, Wellington, Anchorage, Washington	Rolph et al. (1993) Stein et al. (2000) Stein et al. (2015)
JMA GATM	Global Spectral Model (JMA)	No	Lagrangian	Tokyo	Ishii et al. (2018)
MLDP0	GEM	No	Lagrangian	Montreal	D'Amours et al. (2010)
MOCAGE	ARPEGE / IFS	Yes	Semi-Lagrangian	Toulouse	Lamotte et al. (2020)
NAME	UM / ECMWF	Yes	Eulerian + Lagrangian Options	London	Heard et al. (2012) de Leeuw et al. (2021)

Table 3.4: The current offline atmospheric dispersion models used by the VAACs for volcanic ash forecasts. Although none of the centres currently provide volcanic SO_2 forecasts, some of the models being used do have the capability to represent atmospheric chemistry, and hence the ability to model volcanic SO_2 clouds in the atmosphere.

© Crown Copyright 2021, Met Office

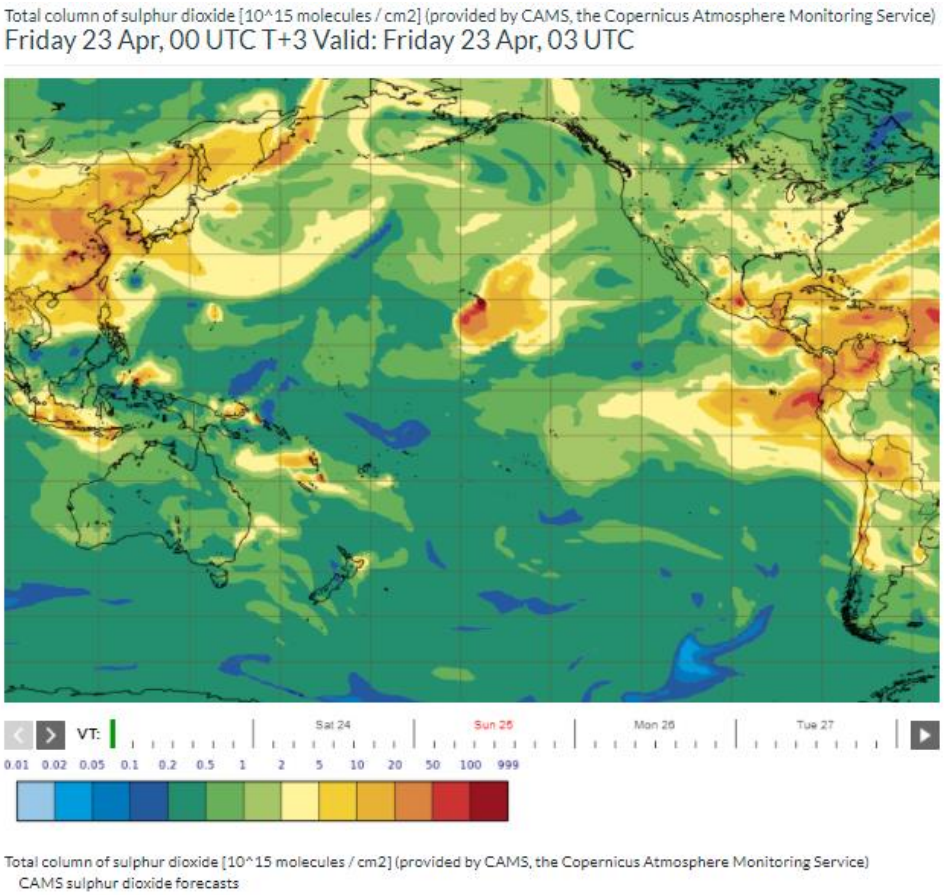

Figure 3.4: An example of a CAMs daily SO_2 forecast, accessed from their website on the 23rd April 2021, https://atmosphere.copernicus.eu/charts/cams/sulphur-dioxide-forecasts. Note the high predicted loadings of SO_2 around Hawaii from ongoing outgassing of volcanoes here, and over the Caribbean following the eruption of La Soufrière (St Vincent).

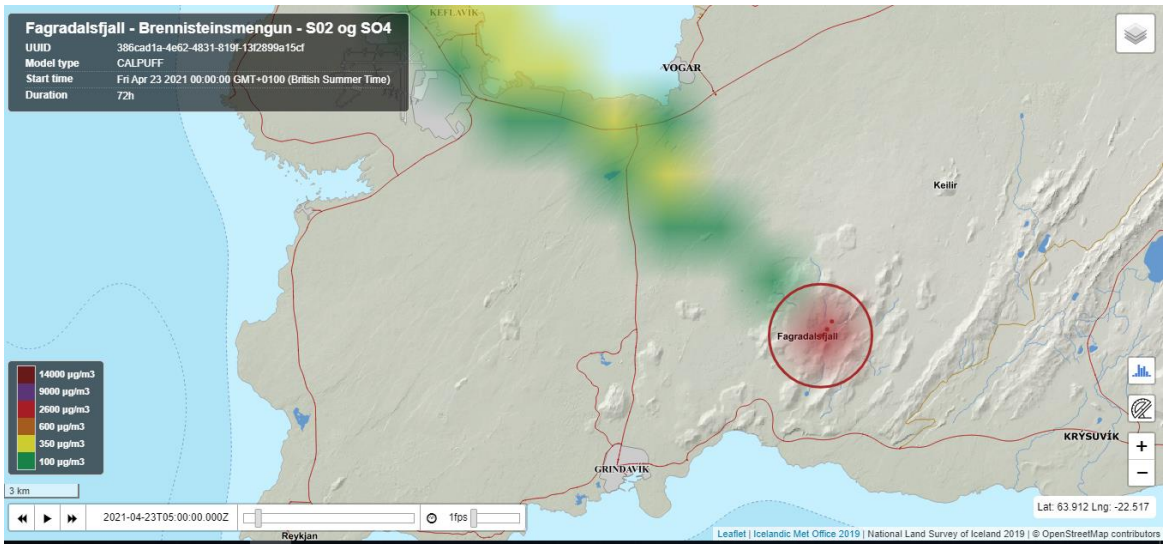

Figure 3.5: An example of a CALPUFF forecast showing atmospheric concentrations of volcanic SO_2 from the eruption of Krysuvik (also rereferred to as Fagradalsfjall), accessed from the IMO website on the 23rd April 2021, https://dispersion.vedur.is/.

© Crown Copyright 2021, Met Office

3.5 Summary

We have reviewed the model capabilities required to provide operational forecasts to the aviation industry. The requirements are similar to those needed to deliver volcanic ash forecasts: the modelling system must represent the atmospheric transport and dispersion of the volcanic cloud, and processes which act to remove it (sinks), but there are some differences which need to be considered:

- Volcanic SO_2 can be released from ground level sources (passive degassing and effusive eruptions) and explosive events. The transport of low altitude SO_2 clouds may be strongly influenced by the local topography, whereas to forecast well the transport and dispersion of a high-altitude explosive release will require accurate representation of the meteorological fields in both the troposphere and stratosphere. A flexible approach to setting meteorological and topographical fields, as well as model domains, which allows the system to generate forecasts at the best possible horizontal resolution, would be ideal.
- The model must include an accurate representation of chemical processes in the atmosphere, which convert SO_2 into SO_4 (sulphate), effectively acting to reduce concentrations of this gas. Chemical processes are different in the troposphere and stratosphere and this will need to be reflected in the model.

To deliver an accurate forecast the source location, the vertical extent of the injection, how much gas is being emitted and the timings of the release need to be known. These parameters may be set directly by the user in the initialization of the model run or incorporated into the modelling system through data fusion techniques. In the absence of any observations, default parameters based on scientific advice will be needed.

An operational modelling system will also need to balance complexity in the chemistry scheme, the horizontal resolution of the output, and the forecast length, which all increase computational load, with reasonable model run times to ensure the delivery of optimal forecasts multiple times per day.

Historically, atmospheric dispersion models have been used by the VAACs to provide operational forecasts of the presence of volcanic ash in the atmosphere. To deliver a volcanic SO_2 forecast the VAACs would need to develop their current modelling systems, primarily to enable them to represent atmospheric chemical processes. Some of the models used already possess this capability, others would need more substantial development, or the centre would need to adopt a different model.

Significant progress has been made in the development of model capability to simulate the transport and dispersion of volcanic SO_2 in the atmosphere. However, there are still outstanding limitations, for example the role of chemisorption is still poorly constrained, and future research will need to address these issues. Operational modelling systems will also need to evolve to ensure they represent the latest scientific and technical developments, and comprehensive verification studies should be conducted to ensure the accuracy of forecasts.

© Crown Copyright 2021, Met Office

4 Satellites

Sulphur dioxide absorbs light in the ultraviolet and infrared parts of the electromagnetic spectrum and these spectroscopic properties can be exploited for remote sensing. Satellite observations of SO_2 started in 1978 with the Total Ozone Mapping Spectrometer (TOMS) instrument, and currently a dozen sensors exist providing global coverage: it is therefore unlikely that nowadays a significant eruption could go undetected. This section presents efforts on the measurements of this gas, led by NASA, ESA and Copernicus, using multispectral and hyperspectral instruments, and the outlook based on the next generation satellites. A brief discussion on assumptions and limitations is provided in general terms, and in particular the fact that in most remote sensing retrievals the plume altitude and columnar abundance are highly interlinked. Spaceborne sensors can be exploited to estimate the source parameters needed to initialise forecast models, to set up systems for eruption detection globally and for model validation.

4.1 Spectroscopy

Satellite SO_2 measurements exploit absorption bands in the ultraviolet (UV), infrared (IR), and microwave (MW) (Carn et al., 2016). In the UV, absorption bands between 300 and 340 nm are exploited; this spectral range is shared with ozone's Huggins band, and both gases need to be retrieved simultaneously; the ozone signal can, moreover, affect the sensitivity of the SO_2 retrievals (Figure 4.1).

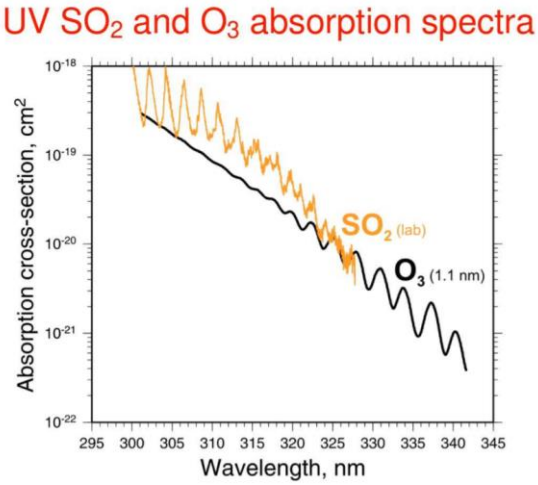

Figure 4.1: Sulphur dioxide and ozone and absorption in the UV.

In the thermal IR, the absorption bands associated with the vibrational motions of the SO_2 molecule are usually exploited (Figure 4.2). In particular, satellite remote sensing in the IR is usually based on the v1, v3 and v1 + v3 bands (Clarisse et al., 2012). Of these, the v3 band centred at 7.3 µm provides the greatest sensitivity due to the stronger absorption gradient, and it is moreover the one that is less affected by the simultaneous presence of volcanic ash. It is often used for measurements in the upper troposphere and above. Due to water vapour absorption, this band lacks sensitivity in the lower troposphere (< 3 − 5 km), but on the other hand it is little dependent on surface properties. The v1 and v1 +v3 bands, on the other hand, are located in atmospheric windows and can help retrieve the lower tropospheric SO_2, however radiance observed in these bands is dependent upon other variables such as emission from the surface, clouds, solar reflection (for the shorter wavelength of the v1 + v3 band) and volcanic ash (for v1).

© Crown Copyright 2021, Met Office

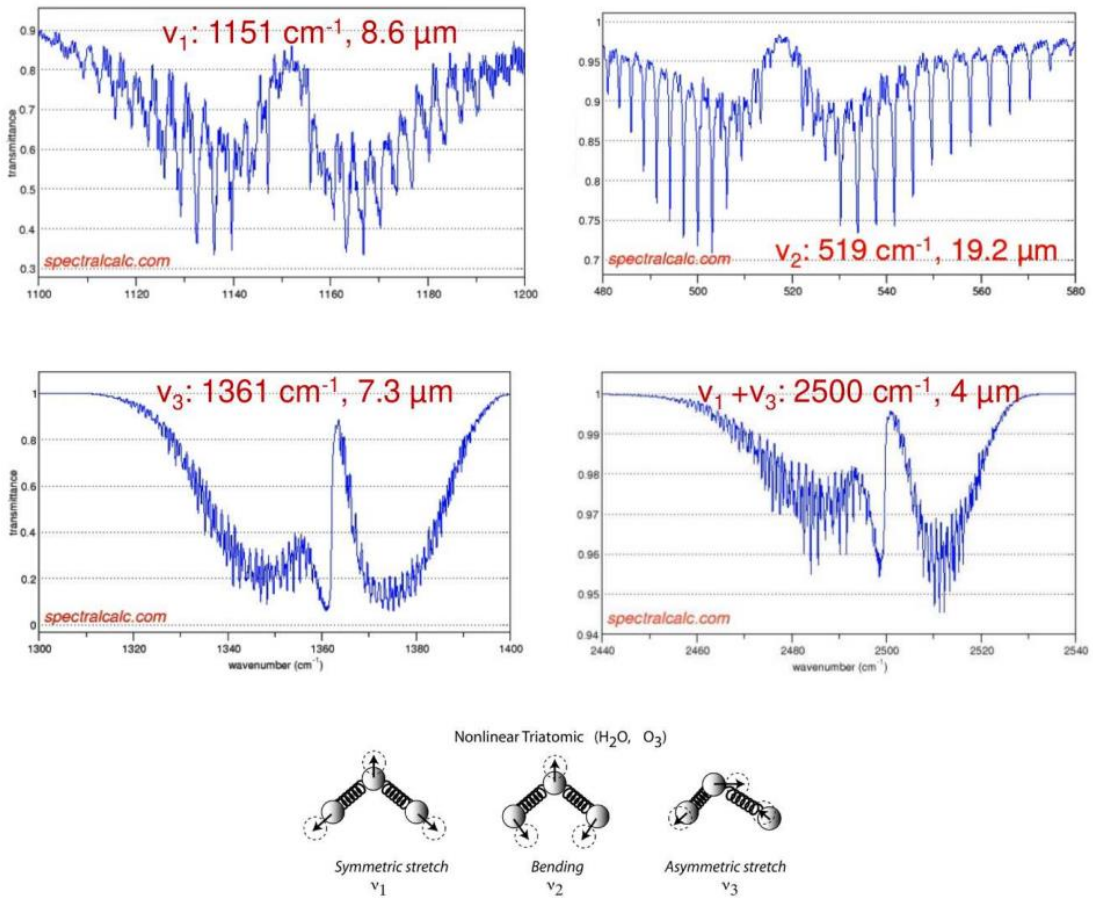

Figure 4.2: Sulphur dioxide IR absorption bands due to vibrational motions.

In the MW, the rotational absorption bands around 200–240 GHz have also been exploited, mainly for limb sounding.

Some satellite sensors, for example IASI, are classified as 'hyperspectral' and measure the electromagnetic signal with high spectral resolution over hundreds or thousands of narrow band channels. These instruments are also often known as 'sounders' because the high spectral resolution can help in profiling atmospheric parameters. Conversely, other sensors such as MODIS and SEVIRI are 'multispectral'. These measure in a smaller number of spectral channels (on the order of 10-50), with a broader bandwidth than hyperspectral instruments. Spectral and spatial resolution are often the result of a compromise, with the multispectral instruments in general having a better horizontal resolution than the hyperspectral ones. For this reason, they are often known as 'imagers'. As sensors improve in both spatial and spectral resolution, the distinction between imagers and sounders will become less important.

4.2 A few decades of satellite observations

Spaceborne remote sensing of SO_2 has been available since 1978, using a number of methods, and several improvements have been made since, thanks in particular to hyperspectral UV and IR instruments. Currently, more than a dozen daily observations exist, taken with a number of methods. It is therefore unlikely, nowadays, that a significant volcanic emission can go undetected.

© Crown Copyright 2021, Met Office

One of the difficulties with the remote sensing of atmospheric species is that their abundance can span several orders of magnitude, and current retrievals tend to show biases towards one or the other end of the range of observable concentrations. SO_2 does not escape this rule and, according to Carn et al. (2016) it can vary over at least five orders of magnitude. We shall follow here the review by the latter paper, as it is quite complete, and in particular their Table 1 and Section 2. References specific to each mission can be found therein. Please note that hereby we mainly refer to instruments observing at the nadir, unless explicitly specified differently.

A multi-decadal series of SO_2 observations has been provided by exploiting the UV spectral range, through TOMS (4 missions, 1978–2005), OMI (2004–present), and OMPS (2011–present). Note that TOMS and OMPS were NASA missions, whereas OMI is provided by the Dutch Space Agency NIVR, on-board a NASA platform. As is expected, the observations have been continuously evolving: TOMS provided observations with a limited spectral and spatial resolution (39–50 km), and its observations were substantially limited to episodes of a large abundance; OMI is a hyperspectral instrument providing increased sensitivity to smaller abundances associated with passive degassing and small eruptions, and has a spatial resolution of 13 × 24 km at nadir; and OMPS also has a comparable sensitivity and it can provide two spatial resolutions, 50×50 km and 10×10 km. OMPS will provide continuity of measurements into the future, being part of the instrument kit for the JPSS meteorological satellites. It is also worth noting that a long series of UV observations has also been provided by NOAA through the SBUV instrument (11 missions, 1979–present), although it has a coarser resolution than TOMS and it is limited by sensitivity to only give quantitative information for the largest eruptions.

A parallel series of UV observations has been provided through ESA with GOME (1995–2003), SCIAMACHY (2002–2012) and GOME-2 (2006–present). However, it seems that this series appears problematic for climatological studies, due to the fact that an inventory of GOME mass loadings has not yet been reported, that SCIAMACHY was limited in spatial coverage as it was alternating between two modes of measurement (limb and nadir sounding), and GOME-2 displays a lower sensitivity compared to OMI (see Figure 4.3). The European contribution is now evolving through the new Copernicus Earth Observation Programme with TROPOMI (Sentinel-5P, 2017–present) and Sentinel-5 (launch ≥ 2023 with MetOpSG), which are hyperspectral instruments with a spectral resolution of 0.5–0.55 nm in the 300–340 nm spectral band, and with a horizontal resolution of 7 km. They will be complemented by Sentinel-4 in geostationary orbit (launch ≥ 2023 with MTG-S), which will have a similar spectral and horizontal resolution.

In addition to the methods based on the UV spectrum, a number of IR instruments have been exploited as well for SO_2. An advantage of this part of the spectrum, obviously, is the addition of night-time coverage. An approach makes use of multi-spectral sensors such as HIRS (1978–present), MODIS (2000–present), and ASTER (2000–present). The latter two are imagers with a high spatial resolution (1 km and 90 m, respectively, see Figure 4.3), and they have also been used in combination, as they share the same platform (Terra). The high spatial resolution has the obvious advantage of resolving localised plumes better, but on the other hand it comes with larger data volumes, and therefore these sensors have been used sporadically rather than for long-term monitoring. The multispectral approach can be extended to the main geostationary imagers that are used (SEVIRI, AHI, ABI, and FCI in the future), as they all offer channels in the v1 and v3 bands (see, e.g., Doutriaux-Boucher et al., 2006; Corradini et al., 2009). As for all observations from geostationary orbit, the advantage is in the continuous coverage with high temporal resolution; however, the SO_2 column from these sensors is not currently disseminated operationally.

© Crown Copyright 2021, Met Office

Hyperspectral IR sounders have an obvious advantage over the multi-spectral approach, as spectral features can be better captured and in principle different parts of the spectrum can be exploited, to adapt the sensitivity to the concentration and plume height. The sensors used with this approach are AIRS (Aqua, 2002–present) and IASI (MetOp, 2007–present). AIRS provides robust measurements of SO_2 in the UTLS, using the 7.3 µm band, and there is room for further exploitation as the instrument spectral range also covers the 4 µm and part of the 8.6 µm bands. Observations of SO_2, as well as other volcanic species, have also been obtained with IASI by a number of groups, among which are the Earth Observations Data Group (Oxford University) and the Spectroscopy, Quantum Chemistry and Atmospheric Remote Sensing group (Universite Libre de Bruxelles).

The various satellite sensors have different sensitivities to SO_2 in the atmosphere as illustrated in Figure 4.3 for an SO_2 plume at 12 km altitude as measured by thermal IR imagers, thermal IR hyperspectral sounders and UV-VIS instruments. The two most sensitive instruments with lowest pixel areas are IASI and TROPOMI (S-5P). This is useful as they are complementary instruments measuring in the IR and UV spectrum, respectively.

Table 4.1 lists a selection of current and future spaceborne sensors that could be exploited for a global forecast system.

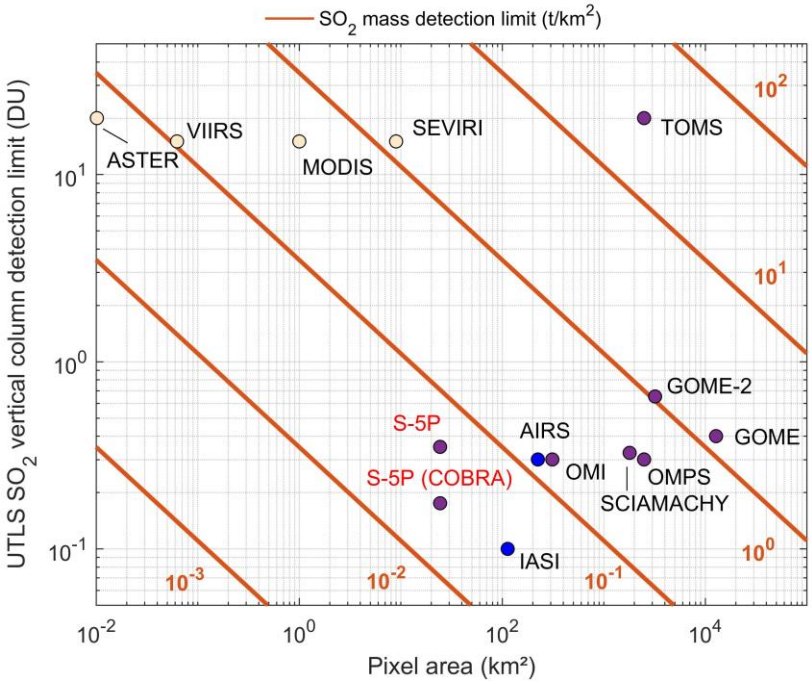

Figure 4.3: Detection limits for SO_2 vertical column for a plume at Upper Tropospheric Lower Stratospheric (UTLS) level (12 km altitude) as a function of pixel size (in km²) for space nadir sensors. Pale orange points are used for thermal infrared imagers (ASTER, VIIRS, MODIS, SEVIRI). In blue; thermal infrared hyperspectral sounders (IASI, AIRS). In purple; UV-VIS instruments (TOMS, GOME, SCIAMACHY, GOME-2, OMPS, OMI, TROPOMI (labelled S-5P for current operational product and S-5P COBRA for a new improved scientific algorithm). The orange curves are the corresponding iso-lines of SO_2 mass detection limit (t/km²). (Figure provided by N. Theys, Royal Belgian Institute for Space Aeronomy (BIRA-IASB), adapted from Figure 2 of Theys et al. (2019)).

© Crown Copyright 2021, Met Office

Hyperspectral sounders						
Satellite	**Availability**	**Orbit**	**Instrument**	**Band**	**Coverage**	**Resol (km)**
SNPP, JPSS	Until ≥ 2038	LEO	OMPS	UV	global 2x/day	50
Aqua	Until ≥ 2021	LEO	AIRS	IR	global daily	14
Sentinel-5P	Until ≥ 2024	LEO	TROPOMI	UV	global daily	7
MetOp	Until ≥ 2027	LEO	IASI	IR	global 2x/day	12–48
MetOp-SG	2024–2044	LEO	Sentinel-5	UV	global daily	7
			IASI-NG	IR	global 2x/day	12–48
MTG-S	2023–2038	GEO	Sentinel-4	UV	Europe every 60'	8
			IRS	IR	full disk every 4h Europe every 30'	4–10 Europe: 6–8

Multispectral IR geostationary imagers					
Satellite	**Availability**	**Longitude**	**Instrument**	**Coverage**	**Resol (km)**
MSG	Until ≥ 2033	0E, 41.5E	SEVIRI	full disk every 15'	3
Himawari-8	Until ≥ 2030	141E	AHI	full disk every 10'	2
GOES	Until ≥ 2036	75W, 137W	ABI	full disk every 15'	2
MTG-I	2022–2040	0E	FCI	full disk every 10'	2

Table 4.1: Some of the current and future spaceborne sensors that are used (or can be used) to monitor SO_2 globally. Note that this list is not exhaustive (see text for a more complete coverage of SO_2 measurements). Infrared (IR) sensors operate at all times, whereas ultraviolet (UV) sensors only measure in daylight (and therefore, in the polar regions they miss the full winter season). LEO: Low Earth Orbit. GEO: Geostationary Equatorial Orbit.

4.3 Detecting eruptions

Not all volcanoes feature the presence of a nearby observatory, nor are they all equipped with a set of dedicated instruments. With a view to a more global approach, this section covers the field of eruption detection using satellites. As volcanic ash and sulphur dioxide are often emitted together, both are considered.

The following satellite indicators can be used to detect when an eruption has occurred:

- the detection of an ash and/or SO_2 plume
- detection of a hotspot on the surface
- rapid cloud growth
- the proximity of any of the above with one or more known volcanic vents and/or the existence of a prior eruption warning for the location of interest

© Crown Copyright 2021, Met Office

It is to be noted, however, that some of the above indicators may be linked to other causes as well as eruptions (e.g., hotspots due to fires, cloud growth caused by convection, etc.). Therefore, an optimal system should make use of them in combination, so as to strengthen knowledge on any potentially detected event.

The NOAA Cooperative Institute for Meteorological Satellite Studies (CIMSS) operates an experimental system called VOLcanic Cloud Analysis Toolkit (VOLCAT), able to generate a number of real-time volcanic cloud products (Mike Pavolonis, personal communication, January 2021; VOLCAT: https://volcano.ssec.wisc.edu/). VOLCAT is extensively used by some of the VAACs, and it is scheduled to become an operational system by 2023. VOLCAT includes of a collection of sensor-agnostic algorithms for detecting, tracking, and characterizing volcanic ash and SO_2, providing concurrent alerting and monitoring dashboards. VOLCAT makes use of the probabilistic approach to retrieve SO_2 properties (Hyman and Pavolonis, 2020). Global coverage is ensured by using a range of geostationary and polar orbiting satellites, and the aim is to capture the lifecycle of volcanic clouds from emergence to dissipation. It includes an alerting service for official users of the system, based on four categories: (1) sudden changes in thermal output (hotspots), (2) newly detected ash emissions, (3) newly detected rapidly developing clouds near known volcanic vents, and (4) newly detected SO_2 emissions. Thanks to the early detection and its cloud tracking capability, VOLCAT can automatically generate eruption source information, and work is under way to automatically derive SO_2 fluxes (Hyman et al., 2021).

Another alerting system is provided by the Support to Aviation Control Service (SACS) (https://sacs.aeronomie.be/), funded by ESA and based at the Royal Belgian Institute for Space Aeronomy (Brenot et al., 2014). SACS uses SO_2 observations from a number of polar orbiting satellite instruments (OMI, OMPS, GOME-2, IASI, AIRS, and TROPOMI), and like VOLCAT it is primarily aimed at supporting the VAACs. By combining multiple sensors with different overpass times, a timely monitoring of volcanic plumes on a global scale is enabled: when exceptional SO_2 concentrations are detected, a notification is issued, where the concentration chart for the event is highlighted. SACS is optimised to avoid false alerts while at the same time limiting the number of notifications in case of large plumes. The system is automated and runs unattended in real time, despite not being operational yet.

4.4 The plume height

Most often, quantitative information on atmospheric SO_2 retrieved from satellites is expressed as a column loading in Dobson Units (DU) (Figure 4.4, left panel). Retrievals will generally require inverting the radiative transfer equation, which can be done using an optimal estimation scheme together with a radiative transfer model, or through look-up tables representing the observed radiances under a number of conditions. It has to be noted, however, that column loading is a two-dimensional field representing the spatial distribution, and it does not include information on the plume altitude.

© Crown Copyright 2021, Met Office

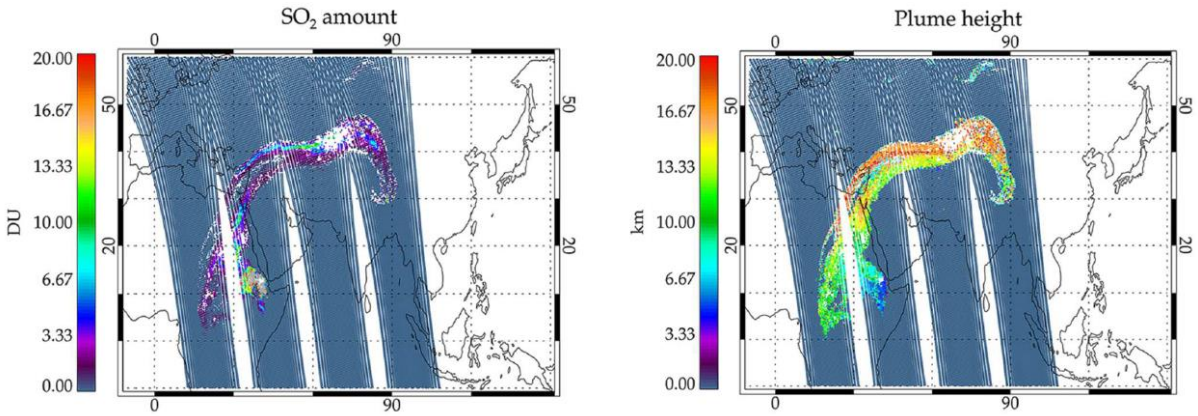

Figure 4.4: Example SO_2 column loading (left) and plume height (right). These charts have been obtained from four IASI orbits, following the eruption of Nabro in June 2011 (Carboni et al., 2016).

Altitude information on atmospheric constituents is available through a number of methods and is of great importance to complement the information on the columnar abundance. For instance, the SO_2 plume height is essential for aviation safety, and for evaluating the impact on climate, and plans exist to improve this information operationally. (See e.g., the SENTINEL-5P+ INNOVATION SO_2 Layer Height Project: https://eo4society.esa.int/projects/sentinel-5p-innovation-so2-layer-height-project/). Hyperspectral measurements at nadir in the UV and IR represent a method to retrieve altitude information, but these should ideally be complemented with the best available prior information to inform the retrievals. Plume altitude and columnar abundance are highly interlinked and need to be retrieved together as in Figure 4.4 (right): an error in estimating the altitude of the layer is usually associated with a corresponding error in the columnar density, and vice versa. To overcome the issue, current algorithms developed for GOME-2, OMI, IASI, TROPOMI, etc., attempt a quantification of column loading for a number of pre-defined layer heights, thus yielding more than one estimate (Theys et al., 2013). It is to note that some of the advanced methods tend to retrieve the SO_2 column loading and altitude probabilistically (Hyman and Pavolonis, 2020). It is moreover foreseeable that model estimates and satellite retrievals may be combined together operationally, similarly to the data assimilation of temperature and humidity for NWP, so as to arrive at the best estimate of the SO_2 plume parameters (see Section 5).

Plume altitude information is also available through satellite sensors looking at the limb rather than at nadir, as e.g., with sensors such as MLS, OSIRIS, MIPAS, SCIAMACHY, ACE and OMPS. Solar occultation is another similar technique available e.g., with SAGE-II and SAGE-III. However, it is worth noting that the viewing geometry used for limb sounding implies a very coarse horizontal resolution, and there is also a considerable probability that radiances may be affected by clouds along the path.

The most straightforward source of information on plume height and also plume thickness could in principle be given by active sensors such as lidar and radar; however, neither the existing spaceborne sensors (e.g., CALIOP, CloudSat and Aeolus) nor those currently planned (e.g., EarthCARE) have a capability to detect SO_2 directly. Instead, they can be used to infer the height of aerosols and hydrometeors present in volcanic plumes, and therefore the derived height of the SO_2 plume is indirect, based on the assumption that the volcanic aerosols and gases are co-located. A similar caveat applies to multi-angle observations such as from MISR and 3MI, as once again aerosols and hydrometeors have to be taken as proxies.

© Crown Copyright 2021, Met Office

4.5 Estimation of eruption source parameters

Satellite retrievals can be used to quantify the source activity including the total amount of SO_2 released into the atmosphere, injection height or profile, and emission flux (amount per unit time). This is useful for volcanology and climate (Theys et al., 2013) but the main reason of interest here is the for initialisation of models to forecast the dispersion of the plume.

Total emitted mass: A method to evaluate the total amount of SO_2 released is a 2-D horizontal integration of measured columnar densities over the pixels of a scene observed by satellite (Prata et al., 2019). A scene can be a single image or a composite of several images. The process involves retrieving the Vertical Column Density (VDC, measured in molecules cm^{-2} or g m^{-2} or Dobson units) in each pixel affected by SO_2, followed by multiplication by the area of the pixel and finally summing these up. The underlying assumptions of this method are:

- The scene is captured after the eruption is complete
- The whole plume is within the area covered by the scene
- No portion of the plume is obscured by clouds, aerosols, or volcanic ash
- Sinks between the beginning of the eruption and the acquisition of the scene can be neglected
- There are no significant additional sources of SO2 within the scene considered.

In practice, the above conditions are not fully met, and each of them causes an underestimation: the exception is for the last assumption, which causes overestimation (however it will be rare to have several significant sources emitting simultaneously in the same region). To overcome the risk of underestimation, a time series of scenes from multiple satellites can be considered, and the maximum of that series can be used as the best estimate of the total erupted mass, as e.g., in Figure 4.5.

Additionally, for some of the retrieval methods large column loadings can lead to biases: in those cases, it is better to wait until the plume has dispersed a little, rather than observing it at the moment of the eruption.

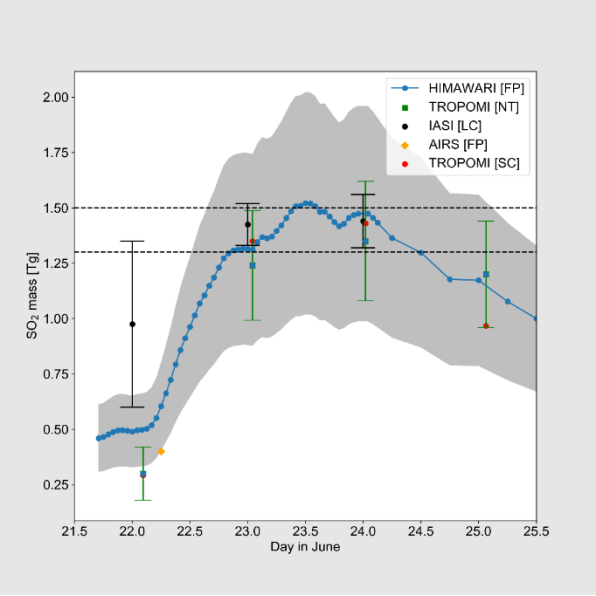

Figure 4.5: Total SO_2 mass as a function of time, estimated from various satellite sensors for the eruption of Raikoke in June 2019, according to Prata et al. (2019). A value of 1.5±0.2 Tg is suggested as the SO_2 mass injected into the UTLS for this eruption.

© Crown Copyright 2021, Met Office

Injection height: Details on estimating the altitude of the plume are given in the previous section. A plume emission profile can be estimated by combining all the retrieved heights of the plume in the proximity of the source, obtained from several pixels and/or from subsequent scenes; see e.g., Prata et al. (2019).

Emission fluxes: Estimating fluxes is notoriously difficult and implies more than applying crude scaling laws to the measured column loadings and total SO_2 masses, because transport and losses following the release into the atmosphere need to be accounted for (Theys et al., 2013). Strong and long-lasting volcanic eruptions are particularly challenging, as they produce a vertically distributed and time-varying emission profile, in response to the instantaneous eruptive power. The dispersion being different at every location and time, according to the wind fields, the plume ends up being inhomogeneous and stretched over distances of the order of thousands of kilometres, with the likely formation of multiple layers which are generally harder to retrieve.

Theys et al. (2013) provide a survey of methods used for flux estimation from a scene or a sequence of scenes, obtained with satellite observations. For all methods, an estimate of the loss term is required, and it can be accounted for in terms of an e-folding time τ; however, the latter is strongly dependent upon poorly controlled and highly variable atmospheric conditions (cloudiness, humidity, the availability of atmospheric oxidants, aerosol surfaces enabling heterogeneous chemistry, etc.). For these reasons, estimates of τ span from a few hours (ash-rich plume, boundary layer, tropical) to a few months (dry, cold, stratospheric plume). For a plume persisting for a sufficiently long time after the end of the eruption ($\sim \tau$ or longer), τ can be estimated from how the total observed mass residing in the atmosphere decays in time; the caveat being that this can only be estimated after the fact (which is of limited operational use), and that only a global average value can be found, neglecting local variations.

Four methods are proposed in the above-mentioned article, with increasing complexity. The first three are limited to cases where (a) SO_2 is injected at a single altitude to minimise errors related to the plume height, and (b) the SO_2 plume has a simple geometry and/or is well covered by the satellite sensors and not obscured by clouds or volcanic ash:

1. Box method: within a single scene, a circle is drawn around the source, with a radius corresponding to the estimated distance travelled in a day (which can be determined e.g., with a trajectory model). The flux is then given by the mass within the circle per day, after applying a correction for the loss term.
2. Traverse method: within a single scene, a vertical surface through the plume is considered and the flux through it is evaluated by integration of concentration and wind vector along the surface. By constructing multiple traverses across the plume at increasing distance within the scene, and accounting for losses, one can reconstruct the flux history at the source. The wind vector can be obtained from an NWP model, or estimated by tracking the volcanic plume itself. As most satellite observations are expressed as column loadings, however, the vertical variation of the wind cannot be easily accounted for.
3. Delta-M method: successive scenes are considered, and the flux at the source is determined as the time-derivative of the total mass in each of them, after a correction for the losses. In this method, the knowledge of the wind field is not required.
4. Inverse modelling: in this approach, SO_2 observations are coupled to a dispersion model, in an optimal estimation framework, to determine the most likely emission flux and altitude that enable to reproduce the observations. See Section 5.

© Crown Copyright 2021, Met Office

4.6 Limitations

Satellite retrievals are based on a number of assumptions and are prone to the following limitations:

- Determinations using channels within the solar spectrum will be limited to daytime conditions, and this means exclusion of the polar regions for the respective winter months.
- Determinations using channels in the thermal infrared are generally poorer in the lower troposphere and boundary layer.
- Different methods exist, making use of different instruments, different channels within a given instrument, and different retrieval algorithms. This can lead to discrepancies in the retrieved abundances, and ideally each method should be accompanied with a robust estimate of its biases and uncertainties.
- The atmosphere is a complex system, and SO_2 retrievals are influenced by several other parameters such as aerosols and clouds, other trace gases such as ozone and water vapour, the vertical profile of temperature and pressure, or the surface properties. Each of these can lead to complications and ambiguities that cannot always be resolved.
- The accuracy of retrievals does depend on which channels are chosen within the absorption spectrum. Channels where the absorption cross-section is stronger will generally be very sensitive to small abundances but will become less useful when the absorption optical depth increases, and vice-versa channels with weak absorption are optimal to sense the very large concentrations. For this reason, for instance, the TROPOMI retrieval considers three different spectral ranges with different sensitivities, and selects the most appropriate one, based on the SO_2 abundance (BIRA-IASB, 2020).
- Plume altitude and columnar abundance need to be retrieved together so, as noted above, an error (or assumption) in estimating the altitude of the layer is usually associated with an error in the columnar density, and vice versa.
- It is reported that several methods may only be reliable below a certain column loading (quantified to be of the order of 100–200 DU) and that larger retrieved values need to be treated with suspicion, due to difficulties leading to uncharacterised biases, usually resulting in underestimation (Yang et al., 2009; Prata et al., 2019). Biases in the presence of large amounts of SO_2 are caused by assumed approximate relationships being extended outside their range of validity and/or an absorption optical depth that is too large (sometimes referred to as a saturation of the absorption band). These issues lead to a non-linear response of the retrieved SO_2 column to the actual atmospheric content. This problem is not a fundamental one, and it can in principle be overcome with improved and better characterised algorithms, such as e.g., in Yang et al. (2009); Clarisse et al. (2012).
- Satellite observations of SO_2 cloud thickness (or depth) are rare and only currently possible indirectly through satellite-based lidars assuming that the volcanic aerosols and gases are co-located. Such lidar observations have very limited coverage. Information on SO_2 cloud thickness is crucial for some Data Fusion techniques (e.g., data insertion and data assimilation as described in more detail in Section 5), and also essential for converting between total column and concentration as explained in Section 6.

© Crown Copyright 2021, Met Office

4.7 Summary

Observing volcanic SO_2 from space has been possible since the late 1970s. Currently a dozen satellite sensors exist, and several future instruments are planned, which can be exploited for volcanic SO_2 clouds.

The most commonly retrieved quantitative satellite product is the total (atmospheric) SO_2 column abundance (a 2D field), which is highly interlinked with the SO_2 plume altitude and both must be considered together. Satellite observations of SO_2 cloud thickness (or depth) are rare and can only currently be inferred from satellite-based lidar which detect the associated sulphate aerosol. Such satellite-based lidar observations also have very limited coverage.

Satellite observations of volcanic SO_2 can be used for a number of purposes, namely 1) detecting and alerting that an eruption has occurred, 2) tracking and characterizing volcanic SO_2 during transport, 3) estimating source parameters for dispersion model initialisation, 4) use within data fusion techniques (see Section 5) and 5) for model validation.

© Crown Copyright 2021, Met Office

5 Data Fusion

Data fusion methods are methods that incorporate observations with modelling. The methods apply a form of "calibration" of the model by integrating observations to reduce model uncertainties.

Several data fusion methods exist for combining models and observation data with the aim of improving the forecasts of volcanic clouds (Figure 5.1). Some methods have been applied to volcanic SO_2 clouds, while other methods have been more extensively developed and tested for volcanic ash for which some of the most significant work is discussed in this section. Some techniques have been developed and applied more broadly to other atmospheric composition problems, and while applications to volcanic problems leads to certain unique issues and needs, the wider use and validation provide evidence of the reliability of these methods. The methods are not atmospheric transport model specific and have been developed using a range of different atmospheric transport models. More details on the dispersion models can be found in Section 3.

The observations can guide and correct the model where the observations are of good quality. Most current data fusion methods use satellite observations to adjust the model forecast, either by estimating an improved source term at the volcano location, or by correcting the modelled volcanic cloud at the location of the satellite observations downwind from the volcano. By using data fusion methods, some of the limitations of satellite retrievals (see Section 4) can be overcome by integrating model simulations and vice versa. The combination of observation and model data can provide a more continuous and accurate data set in space and time, by for example filling in the gaps in the observation data due to sampling frequency or due to cloud cover obscuring the satellite signals.

Four types of data fusion methods (trajectory, inversion, data insertion and data assimilation) are described in this report, with details on the required input, output, advantages, and limitations. The methods are summarized in Table 5.1.

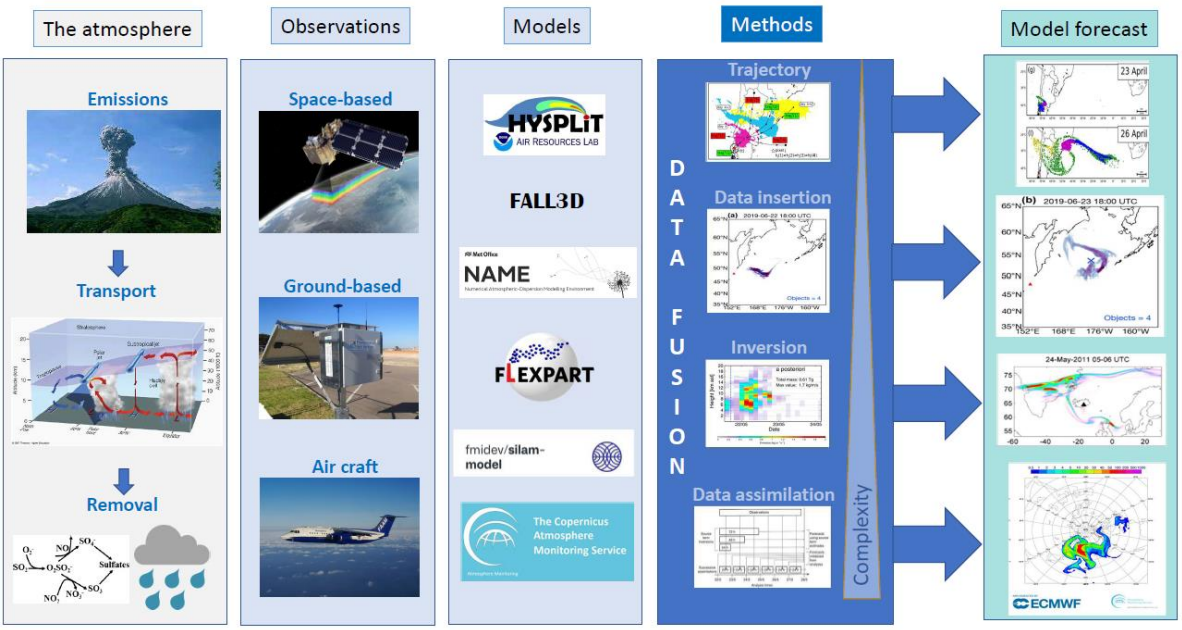

Figure 5.1: Illustration of data fusion methods to combine observations and model forecasts.

© Crown Copyright 2021, Met Office

Technique	Input	Output	Advantages	Limitations	References
Trajectory	Satellite data, modelled trajectories	Revised source term at volcano location	Quick, simple, only one satellite image needed, no assumptions on eruption time needed	Defining minimum arrival distance from volcano for back trajectories, sufficient wind shear needed, error characteristics	*Schoeberl* et al. (1993); *Prata* et al. (2007); *Maerker et al. (2008);* *Krotkov* et al. (2010); *Hughes* et al. (2012, 2016); *Gorkavyi* at al. (2021) *Pardini* et al. (2017, 2018)
Inversion	Satellite total column loading, modelled total column loading, first guess source term (some schemes)	Revised source term at volcano location	Quick, robust. Tested on a range of eruptions	Sufficient wind shear needed, averaging kernel (satellite height sensitivity) needs to be applied to model data, error characteristics	*Eckhardt* et al. (2008); *Boichu* et al. (2013,2014); *Theys* et al. (2013); *Moxnes* et al. (2014); *Zidikheri & Potts* (2015); *Heng* et al. (2016); *Vira* et al. (2017)
Data Insertion (DI)	Satellite total column loading, cloud height and thickness	Revised modelled downwind volcanic cloud location and mass	Simple, quick, provides results with a single satellite image	Information on cloud height and thickness needed, error characteristics	*Wang et al. (2013);* *Folch et al*. (2020); *Prata* et al. (2021)
Data Assimilation (DA)	Satellite total column loading, cloud height and thickness, initial model forecast	Corrected modelled downwind volcanic cloud location and mass	Uncertainties in both source term, meteorology and model accounted for.	Input on cloud height and thickness needed, computational cost, error characteristics	*Flemming & Innes* (2013); *Kristiansen* et al. (2017); *Vira* et al. (2017); *Mingari et al. (2021);* *Innes et al. (2021)*

Table 5.1: Methods used for combining observations and model data to improve source terms and forecasts of volcanic SO_2 clouds. References included in the table refer to studies which have applied these methods to volcanic SO_2.

Simple trajectory techniques have been used for volcanic SO_2 clouds since at least the early 1990s, but more advanced trajectory methods have since been developed which allow quantitative estimation of the emission flux and emission heights. Data insertion and inversion methods have been developed and validated for volcanic SO_2 in several research studies, while data assimilation methods have been developed for volcanic ash (not yet for SO_2) mainly in the last 5 years.

Many research studies have demonstrated the benefit of these various techniques and shown that the forecasts are improved by applying a data fusion approach. Most methods have been developed in research mode and have the potential to be used in an operational setting, but this will require additional resources and work. A global SO_2 forecast system would greatly benefit from the use of one or more data fusion methods to achieve more accurate forecasts.

A detailed literature review of four data fusion methods applied to volcanic clouds is given below. The review does not cover all available publications but describes and illustrates a wide range of different approaches.

© Crown Copyright 2021, Met Office

5.1 Trajectory techniques

Trajectory techniques use modelled trajectory calculations (forward and/or backward) and satellite data to estimate source term parameters, which is typically a mean emission height and emission time, and for more advanced trajectory techniques also an emission flux.

The ability to infer source parameters from trajectory analyses depends on the vertical wind shear along the transport path. If the wind speeds and directions vary sufficiently with altitude, then emissions at different altitudes will be transported in different directions and to various distances from the source. This leads to differences in the horizontal transport patterns and thus different modelled trajectories, which when compared to the SO_2 cloud observed from satellite observations, can be used to infer the vertical location.

Trajectory methods vary in complexity. Some of the simpler approaches involves estimating the injection height (the height of the eruption plume at the location of the volcano) by running model trajectories forward from the volcano starting at various altitudes. Then by overlaying the trajectories onto satellite images, the trajectory which best matches the observations can be identified, as illustrated in Figure 5.2. The height at which this trajectory started at the volcano is the injection height. Schoeberl et al. (1993) demonstrated the ability to resolve the height of the 1991 Cerro Hudson SO_2 cloud and Prata et al. (2007) estimated an injection height to be 20 km for the 2006 Soufriere Hills eruption (Figure 5.2).

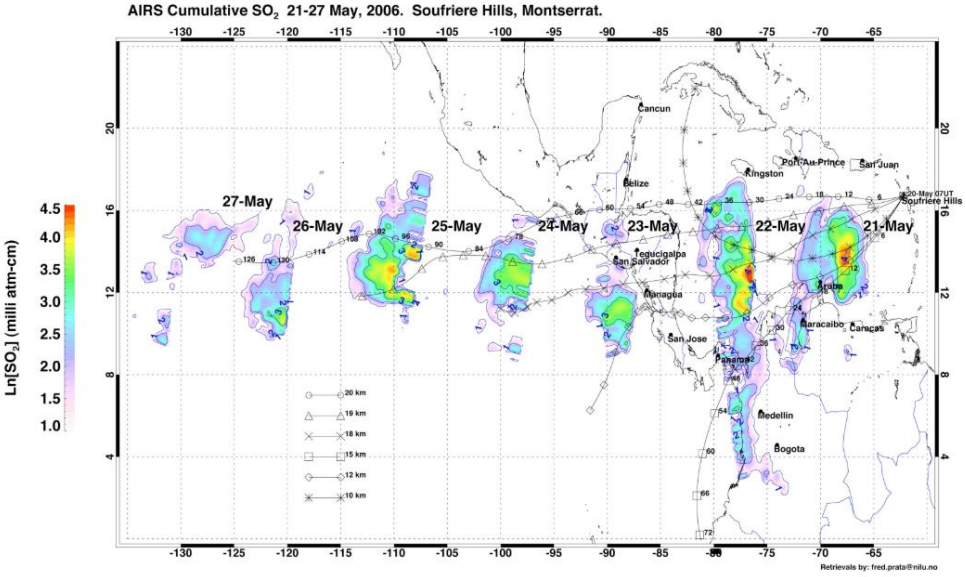

Figure 5.2: Simple trajectory method. Satellite SO_2 observations (colours) and model trajectories (black lines) starting at six different altitudes above the volcano. The trajectory at 20 km matches the satellite observations best. Figure from Prata et al. (2007).

Trajectory methods can also use backward model trajectories starting at the location of the observations, or a combination of both forward and backward trajectory modelling. Maerker et al. (2008) used a backward trajectory matching technique with the FLEXPART model to determine the origin of an SO_2 plume and the effective emission height. Krotkov et al. (2010) used a forward and backward trajectory analysis with the Goddard Trajectory Model to similarly estimate the height and emission time of an SO_2 cloud by looking at the trajectories that track the volcanic cloud back to the

© Crown Copyright 2021, Met Office

volcano. Hughes et al. (2012, 2016) extended this method using several consecutive days of observations and statistical analysis and included the use of near-real-time lidar measurements of the volcanic aerosol height to correct the trajectory-based estimates, which improved the volcanic SO_2 forecast with the global Eulerian GEOS-5 model. The modelled dispersion patterns were more accurate and distinct stretching characteristics as seen in satellite measurements were reproduced by the model. Also, the modelled height of the SO_2 cloud agreed with spaced-based lidar observations. The technique, however, does not estimate the emission flux and thus the modelled concentration values are not optimized.

More recently, more advanced trajectory techniques have been developed which are able to estimate several source parameters including the emission flux. The PlumeTraj scheme developed by the University of Manchester (Pardini et al. 2017, 2018, Queißer et al., 2019) can retrieve multiple source parameters including the emission flux and the plume altitude at the volcano and at the measurement location. Model trajectories performed using the HYSPLIT model are started at the location of the satellite observations (this can be several hundreds to thousands of pixel locations) and followed backwards in time. The scheme then finds which back trajectories approach the volcano. The time at which a back trajectory reaches the volcano is the 'injection time', and the height of the trajectory as it reaches the volcano is the 'injection height'. An SO_2 flux is calculated by matching the injection time for a trajectory with the observed SO_2 column amount in the satellite pixel it was initiated from. If more than one back trajectory approaches the volcano, then a mean injection height, time and flux is calculated. More robust results can be obtained by additional screening of the trajectories with the use of multiple satellite images and a combination of forward and backward trajectory modelling. Further improvements to the scheme include improved error quantification, graphics, and automation (M. Burton, Pers. Comm., April 2021). Figure 5.3 shows an example of the SO_2 source parameters derived with PlumeTraj.

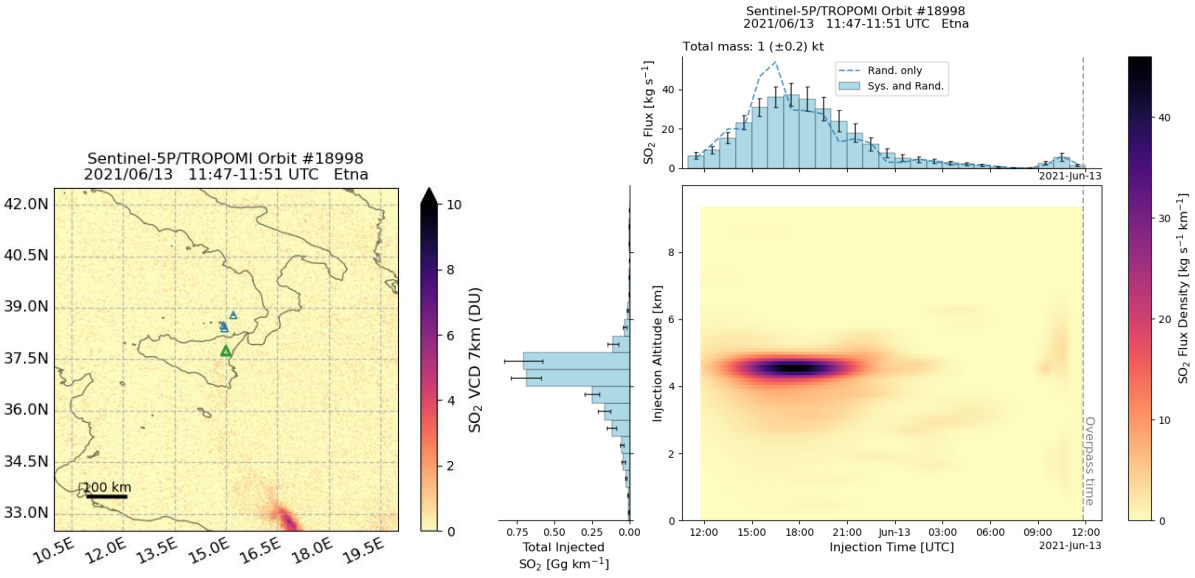

Figure 5.3. Advanced trajectory method. Results from the PlumeTraj method. Left: Satellite images used as input to scheme. Right: Estimated SO_2 flux and injection altitude for Etna volcano. Figures from http://dailyetna.eps.manchester.ac.uk/, accessed 14.06.2021.

© Crown Copyright 2021, Met Office

An additional major strength of PlumeTraj is that the satellite observed vertical columns are corrected based on the estimated plume height at the measurement location. As satellite retrievals of SO_2 are strongly dependent on the assumption of the height of the SO_2 cloud, Pardini et al. (2018) proposed a way to correct the satellite retrieved SO_2 column amount by using the SO_2 plume heights estimated from PlumeTraj to re-calculate the satellite total column (TC) values. By interpolating between the different satellite retrieval products provided using different plume height assumptions, a new and more accurate satellite total column is achieved. This can in turn be fed back into the data fusion method for improved results.

A limiting factor with back trajectory methods, is that it is not expected that the trajectories will arrive back at the exact location of the volcano. This is due to the temporal and spatial resolutions of the trajectories. Therefore, the method requires a minimum arrival distance from the volcano (sometimes called a threshold radius) to constrain which back trajectories reach close 'enough' to the volcano. Determining this distance is often tricky. It can be done by visual inspection of satellite imagery (e.g., Pardini et al., 2017) or by statistical analysis (e.g., Hughes et al., 2012), but it is not trivial to generalize or automate.

Also, the trajectory methods are dependent on vertical wind shear. When wind shear is weak, back trajectories from numerous altitudes can return to close to the volcano, meaning there is a greater uncertainty in the estimated emission height. When there is strong wind shear, a small change in height or error in the wind field can result in a significant difference in the speed and direction of the trajectory, leading to a greater uncertainty in the emission time and emission rate.

5.2 Inversion methods

Inversion methods use more advanced model dispersion calculations instead of simple trajectory calculations, and often a more advanced mathematical solver. The aim is to find the optimum emission source parameters that give the best model agreement with observations. For volcanic cloud modelling it means finding the combination of the eruption source term parameters that bring the model into best agreement with the satellite data. This is done using numerical optimization methods which search for the optimum model parameters (for example the emission flux, emission time and the vertical distribution of the emissions).

The basic principle of the inversion method is illustrated in Figure 5.4. Several model forecasts are initiated each with emissions at a different altitude above the volcano. These forecasts are run forward in time simulating the transport of the emission cloud for a specific emission altitude. When satellite observations are available the different model simulations are compared in order to find which combinations of the forecasts, and hence which combinations of the emissions give the best match to the satellite observations. The inversion finds the optimum emission combination using a numerical optimisation solver. In this case the vertical profile of the emissions above the volcano is obtained. By repeating the forecast for different emission times, the source term as a function of both height and time can be estimated.

© Crown Copyright 2021, Met Office

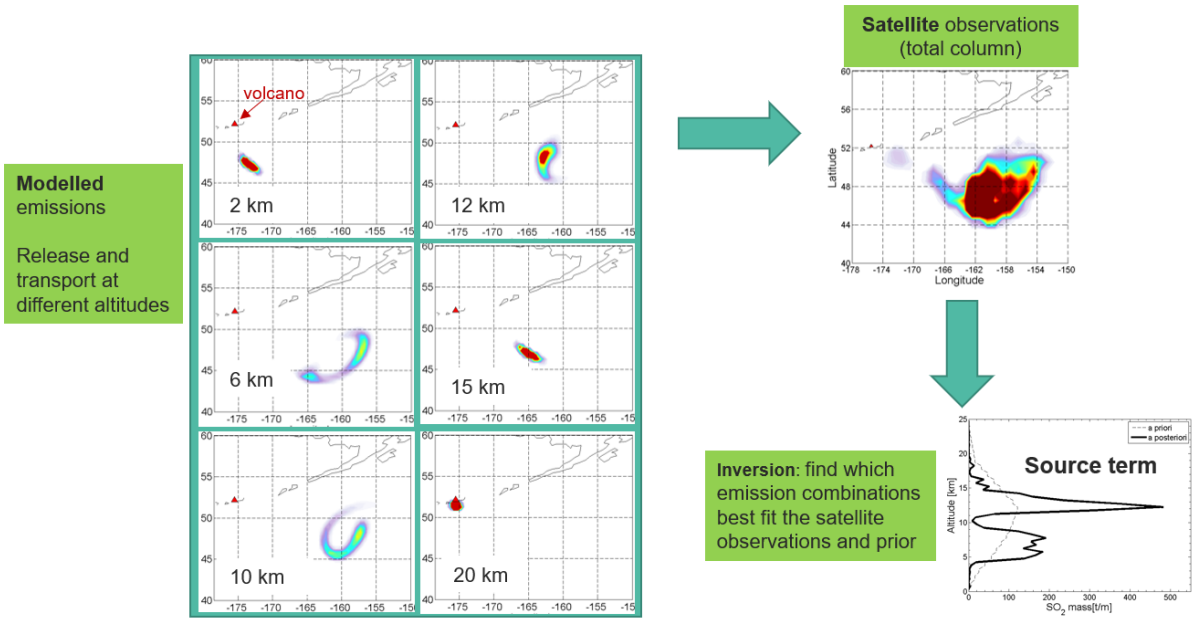

Figure 5.4: Simple schematic illustrating the principle of the inversion method.

Because the observations are often limited and/or don't carry enough information in order to find a unique solution (i.e., many emission combinations can explain the observations equally well), additional information in the form of a first guess (a priori) source term is often needed (see the black dashed line in the plot on bottom right corner of Figure 5.4). As with the trajectory technique, the inversion methods are most robust if strong wind shear exists, which transports emissions in different directions depending on emission altitude.

Eckhardt et al. (2008) first developed an inversion scheme specifically aimed at deriving volcanic emissions and demonstrated its use by successfully retrieving the vertical profile of the SO_2 emissions from the 2007 eruption of Jebel at-Tair (Yemen), constrained by satellite data from a range of sensors (Figure 5.5). The same scheme has been applied to other case studies such as the Kasatochi 2010 eruption (Kristiansen et al., 2010) and Grímsvötn 2011 (Moxnes et al.,2014).

Similar schemes have also been used to derive SO_2 emissions from the Eyjafjallajökull 2010 eruption (Boichu et al., 2013,2014; Vira et al., 2017), the Merapi 2010 eruption (Zidikheri and Potts, 2015), the Nabro 2011 eruption (Heng et al., 2016) and for Kilauea (Tang et al., 2020). A simpler inversion scheme was used by D'Amours et al. (2010) in which model calculated source-receptor relationships were coupled with maximum observed total column values to derive emission estimates. Several inverse methods have been developed to estimate volcanic ash emission parameters (Stohl et al., 2011; Denlinger et al., 2012; Pelley et al., 2015; Chai et al., 2017 and Zidikheri et al., 2018).

© Crown Copyright 2021, Met Office

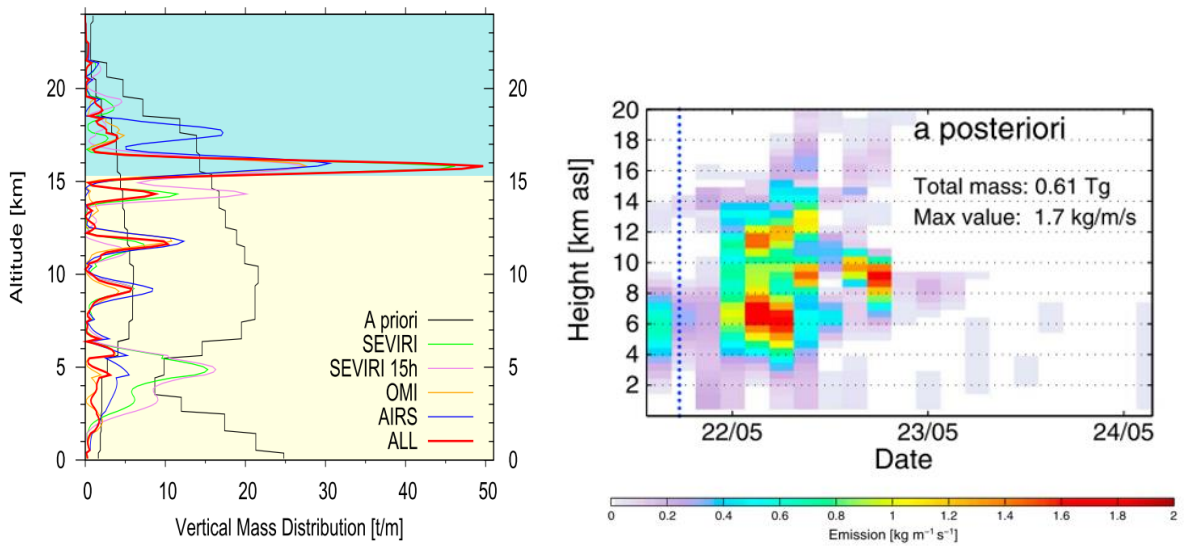

Figure 5.5. Inversion method examples. Left: figure from Eckhardt et al. (2008) showing the SO_2 vertical mass distribution for the 2007 Jebel at Tair eruption estimated by inverse modelling. Right: figure from Moxnes et al. (2014) showing the time, altitude, and strength of the SO_2 emissions for the 2011 Grímsvötn eruption, also estimated by inverse modelling.

One consideration with inverse techniques is that the computational effort is related to vertical and temporal resolution of the source which is being estimated. This is because the number of model simulations needed are dependent on the source resolution. A coarse source resolution will be quicker to run but might not provide the details needed for an accurate forecast, while a very fine source resolution will be more computationally costly. However, the computational cost of each model simulation can be considered relatively low, and the simulations can also easily be parallelised if an appropriate system like a supercomputer is available.

The inverse methods applied to volcanic SO_2 calculate the optimum source term by comparing modelled and satellite observed total column SO_2 values. The SO_2 satellite retrievals have a variable sensitivity to SO_2 at different altitudes in the atmosphere, and it is important that this sensitivity is considered when calculating the modelled total SO_2 column values. This is done by applying the SO_2 satellite averaging kernel operator to the model data (e.g., Eckhardt et al., 2008; Theys et al., 2013). This does not need to be considered for volcanic ash as the satellite retrievals do not have an equivalent height sensitivity.

Inverse methods implicitly assume that the dominating uncertainty is related to the source term. As the volcanic cloud gets transported farther from the source, this assumption could be violated as errors in meteorology and/or model parametrizations become dominant. Recent work using ensemble meteorology in combination with inverse methods attempts to assess the uncertainty in the meteorological situation (Harvey et al., 2020, Zidikheri and Lucas, 2020).

© Crown Copyright 2021, Met Office

5.3 Data Insertion

Data insertion (DI) methods initialise a model run from satellite data by creating a downwind source term for the model which matches the horizontal extent of the satellite observed volcanic cloud. Several studies have shown that the model simulations initialised with data insertion consistently improved the agreement with satellite retrievals (e.g., Prata et al., 2021; Crawford et al., 2016; Wilkins et al., 2014, 2016, Wang et al., 2013). An example of data insertion in shown in Figure 5.6.

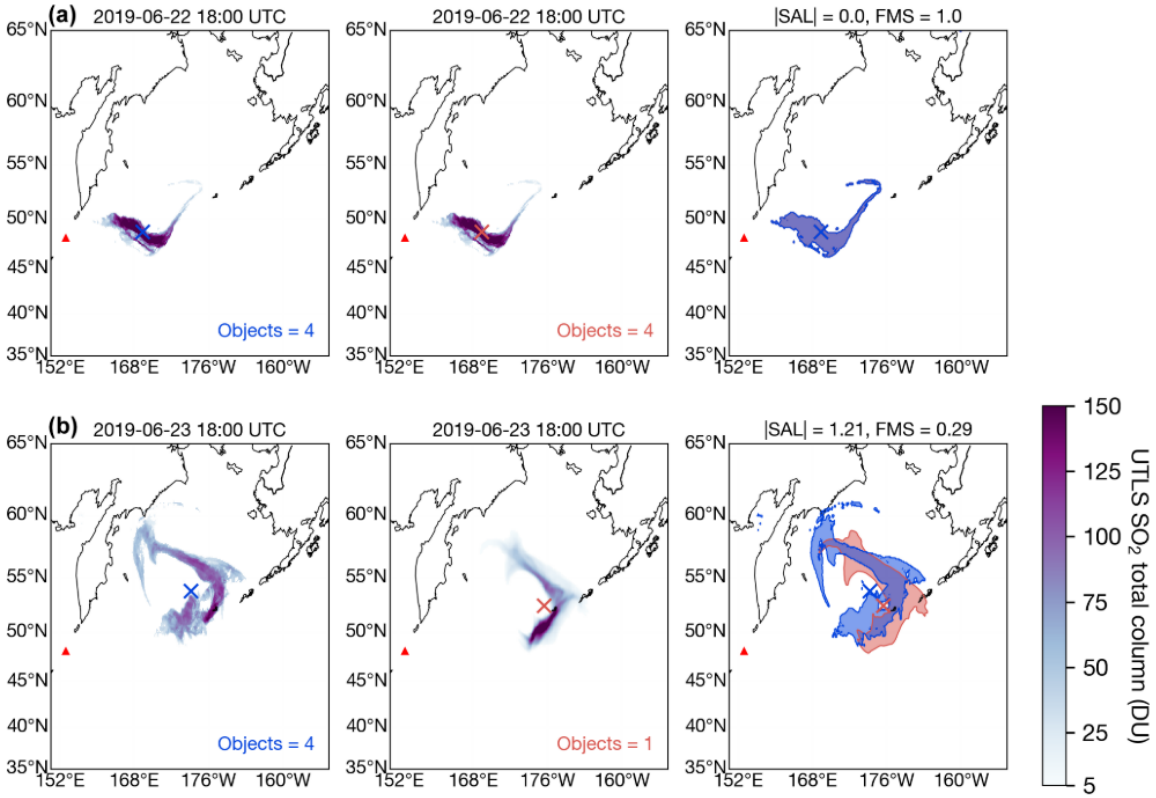

Figure 5.6: Data insertion. Figure from Prata et al. (2021) showing satellite observations (left column), FALL3D model simulations (middle column) and spatial overlap of model shaded in red vs. observed shaded in blue (right column) for the Raikoke-2019 eruption on (a) 22 June 2019 at 18:00UTC (data insertion time, i.e., time when the model forecast is initialised from the observations) and (b) 23 June 2019 at 18:00UTC.

Information on the height and thickness of the volcanic cloud at the observation points is also required for initialising the model forecast at the correct altitude. Aircraft measurements, space-based lidar observations or satellite derived cloud top heights can be utilised, but in cases where such data are not available assumptions must be made.

The method does not require any information on the eruption source parameters from the volcano itself as the forecasts starts downwind. However, assumptions on the emissions from the volcano after the time of the data insertion calculation are needed. The method is relatively simple and computationally quick and can provide results from a single satellite image. One limitation with the method is that the data insertion forecasts may be less robust than simulations initialized from the eruption source because (parts of) volcanic clouds obscured by meteorological cloud or below detection threshold are not modelled.

© Crown Copyright 2021, Met Office

5.4 Data assimilation

Data assimilation (DA) originates in the field of Numerical Weather Prediction (NWP). It is increasingly being widely applied in air quality forecasting, although still in the early stages of development. For example, the nine models contributing to the Copernicus Atmosphere Monitoring Service (CAMS) operational regional air quality ensemble system all include data assimilation (https://atmosphere.copernicus.eu/regional-air-quality-production-systems).

The general principle of data assimilation is to provide the most accurate model forecast by knowing the initial state of the atmosphere as accurately as possible. This initial state is based on observational data and is used as initial conditions for sequences of model runs. In each sequence, a forecast from the previous model forecast is used as a first guess which is then adjusted to be in better agreement with the observations (see Figure 5.7). In general, the simulated concentration fields are changed according to the observations, and not the underlying emission source term.

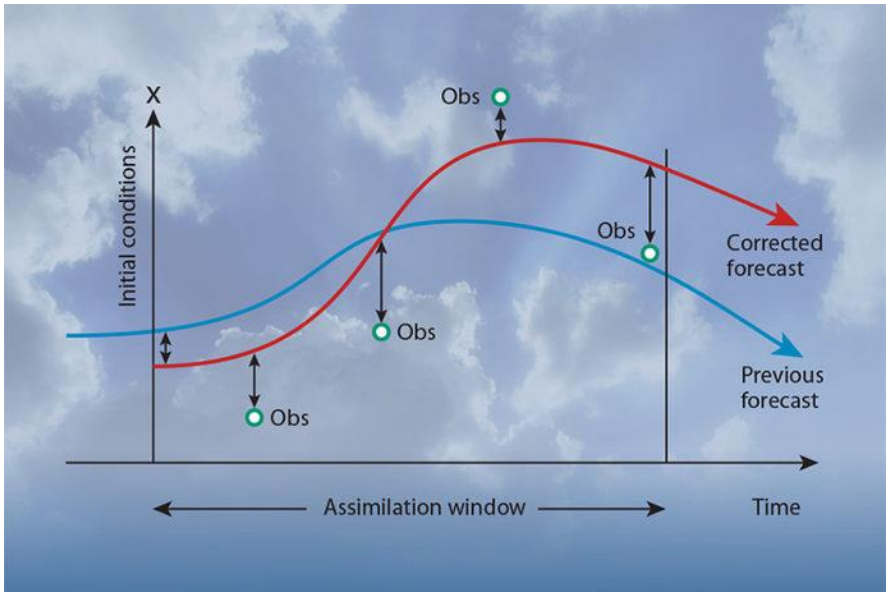

Figure 5.7: Illustration of data assimilation. First a short-range forecast is run (blue line), then once all observations (green circles) within an assimilation window are received, the previous forecast is adjusted based on the observations to create an 'analysis' (red line). This analysis is used as initial conditions for the next forecast which is then run beyond the assimilation window to provide the best possible forecast. Figure and description from https://www.ecmwf.int/en/about/media-centre/news/2017/20-years-4d-var-better-forecasts-through-better-use-observations.

The application of data assimilation techniques to volcanic SO_2 cloud dispersion is limited to only a few research studies (e.g., Mingari et al., 2021; Innes et al., 2021; Flemming and Innes 2013; Kristiansen et al., 2017; Vira et al., 2017). Some further development has been done for volcanic ash, particularly in the last 5 years (e.g. Pardini et al. 2020; Osores et al. 2020; Fu et al. 2015, 2016, 2017; Lu et al. 2016, 2016b, 2017; Lin et al. 2016; Schmehl et al. 2012; Benedetti et al. 2011), but it is still a relatively new application with ongoing research, and to date only one application (CAMS) has been fully tested and used in an operational context for real eruption cases (further discussion on this application will follow later in this section).

© Crown Copyright 2021, Met Office

It should be noted that the definition of DA is ambiguous and is often used in a broad sense covering any method that incorporates observations into modelling i.e., some of the methods mentioned previously are sometimes referred to as DA methods although they are often much simpler than the type of DA applied in NWP modelling. There is also not always a clear separation of data assimilation and source term estimation via inversion methods. For example, in air pollution modelling, data assimilation schemes have been extended to cover source term estimation.

The two most common advanced DA methods are four-dimensional variational assimilation (4D-Var) and Ensemble-based data assimilation. Each of these two assimilation methods are described in more detail below including examples of applications to volcanic clouds.

5.4.1 Four-dimensional variational assimilation (4D-Var)

The general idea of four-dimensional variational assimilation (4D-Var) is illustrated in Figure 5.7 and is a way of correcting the modelled forecast concentrations in space and time using observations within a set assimilation window. 4D-VAR methods have been applied to volcanic SO_2 clouds by Innes et al. (2021), Flemming and Innes (2013) and Vira et al. (2017), and to volcanic ash clouds by Lu et al. (2016, 2016b, 2017). 4D-VAR methods require user input for the model uncertainty and are less sensitive to unaccounted model errors than other methods, but more sensitive to wrong observations (e.g., false alerts). In 4D-Var the modelled SO2 concentrations are adjusted based on satellite observations.

An example of the use of 4DVar for volcanic clouds is the operational Copernicus Atmosphere Monitoring Service (CAMS) SO_2 forecast (https://atmosphere.copernicus.eu/charts/cams/sulphur-dioxide-forecasts). These forecasts use a 4D-Var data assimilation system, and one set of observations which are assimilated is volcanic GOME-2 and TROPOMI SO_2 satellite data (Innes et al., 2021, CAMS, 2020). The volcanic flag provided with the satellite data is used and all data that are flagged as volcanic origin are assimilated. The satellite data is total column values of SO_2 from a retrieval which uses a plume height assumption of 6 km (the middle troposphere product). In the assimilation step the satellite data is used to correct the forecasted SO_2 concentrations. The correction is applied via the ‘background errors’ of the system. The ‘background’ is a priori information which comes from a previous model forecast. If a model grid point doesn’t contain any SO_2 then it will be 'created' based on the relative weight of the background and observation errors of the assimilation system. I.e., SO_2 concentrations can be added and adjusted even for locations where SO_2 is not present in the previous model forecast. Because the satellite data do not provide information on the plume altitude and vertical distribution of SO_2 within the atmosphere, the assimilation does not know at which altitudes the SO_2 concentrations need to be corrected. Therefore, an assumption must be made about the plume altitude and vertical distribution. The current operational CAMS configuration assumes a plume altitude of 5 km and the correction is applied at that altitude in the model. More correctly, the background error standard deviation profile peaks around 5 km and thus a vertical distribution which peaks at 5 km is assumed. The impact of this assumption is that if in reality the volcanic plume is located at say 15 km rather than at 5 km (where the correction was applied), the SO_2 might be transported to the wrong location in the forecast if the winds at 15 km differ from the winds at 5 km altitude. Innes et al. (2021) recently tested the assimilation of SO_2 layer height (plume height) from TROPOMI in the CAMS system. This is making use of the satellite retrieved plume height information to place the SO_2 increments at a retrieved altitude, rather than at the assumed 5 km altitude as in the current operational configuration. Assimilation tests have shown that the additional layer height information leads to improved SO_2 forecasts compared to using the operational CAMS configuration.

© Crown Copyright 2021, Met Office

5.4.2 Ensemble-based data assimilation

The ensemble-based data assimilation is built on an ensemble of numerical simulations instead of a single model simulation. The state of the system is then described in a statistical way from the ensemble. More precisely, many slightly different model forecasts are run. Each of the forecasts are initialised with different model inputs or set up. The various forecasts can for example be using different meteorological data such as different wind directions. This will represent the uncertainty of the meteorological data which drive the dispersion model. The different model forecasts can also use different source parameters, such as a range of different eruption column heights, which then represents the uncertainty on this source parameter. And lastly the forecast can also use different model schemes for, for example wet scavenging which is also an uncertain parameter in the forecasts.

By running many realistic but slightly different forecasts an ensemble of model realisations is obtained. From the ensemble, statistical variables such as the ensemble mean and covariances are calculated. Once satellite observations are available, the ensemble filter combines the statistical information from the ensemble with the observations and the result is a new model forecast which is corrected with observations and therefore is in better agreement with the observations and less uncertain. This corrected forecast forms the initial state for the next forecast.

One type of ensemble filter is the Ensemble Kalman Filter (EnKF). EnKF methods have to date mainly been applied to volcanic ash clouds (e.g., Pardini et al., 2020; Osores et al. 2020; Fu et al., 2015, 2016, 2017, 2017b) and only very recently to volcanic SO_2 (Mingari et al., 2021). When applying ensemble data assimilation techniques, it is important to construct the ensemble members from a realistic distribution, otherwise unphysically biased prior ensemble plumes can result in a DA algorithm that cannot reconstruct physical plume estimates. An advantage of the ensemble approach is that model uncertainty, which is often difficult to handle in other schemes, can be included by perturbing the ensemble. A second advantage is that the ensemble standard deviation can be used as a reasonable estimate for the uncertainty.

An example of the application of EnKF to volcanic clouds is the work of Pardini et al. (2020) who developed an ensemble data assimilation method which they showed significantly improved volcanic ash forecasts (Figure 5.8). An ensemble of HYSPLIT model simulations based on perturbations of the wind and eruption column heights was used in the DA system. By using free open-source software environments for the data assimilation routines and for the numerical model, they show that the assimilation procedure can relatively easily be implemented with any dispersion model. They highlight that their approach could also be effective for volcanic SO_2 clouds, can be used operationally in near real time, and can represent a real breakthrough for improving assessments of volcanic hazards. Mingari et al. (2021) use a similar approach and show that their ensemble based Kalman filtering technique may lead to nonphysical solutions, but that a truncated state yields a dramatic improvement of forecast quality when compared to simulations without assimilation.

© Crown Copyright 2021, Met Office

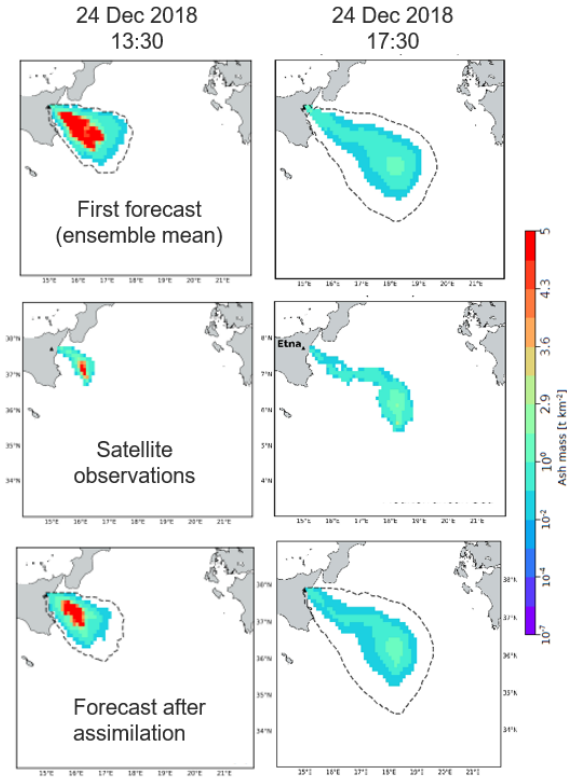

Figure 5.8: From Pardini et al. (2020) demonstrating the use of ensemble data assimilation

Advantages and limitations of data assimilation

The advantage of DA over other data fusion methods is that for most DA methods no accurate information on the eruption source parameters is needed. Also, since the volcanic cloud is corrected during transport, the uncertainties related to the eruption source parameters, meteorological data and model parameterizations are all considered together. Another advantage over the inversion approach is that DA can in principle handle non-linear processes (e.g., chemistry) better.

A challenge with DA is that when assimilating satellite derived total column values of ash or SO_2, information or assumptions on the plume height and thickness is required to locate the plume at the correct vertical level in the model. Plume height information can be retrieved from satellite data itself, in fact the total column SO_2 loading and the plume height are interlinked in the satellite retrievals. Some studies have looked at incorporating plume height information into the assimilation process (e.g., Innes et al., 2021). The remaining unknown is the volcanic cloud thickness, i.e., the vertical depth or distribution which can be difficult to obtain a good estimate for, especially in near-real time. Spaced-based lidar observations from e.g., the CALIPSO instrument can provide such vertical information but the coverage of these instruments is sparse.

Data assimilation methods are the costliest, in terms of compute power, of the methods reviewed in this report. Compared to inversion methods which could relatively easily be parallelised, a 4D-VAR system is essentially sequential and takes longer to run, while an ensemble DA is parallelisable (i.e., all ensemble members can be simulated simultaneously as they are independent) and is thus quicker but involves a significant amount of computational resource due to the number of simulations required for the ensemble. Some work to speed up the DA system has been proposed by *Fu* et al. (2017b), but this is an area which needs further improvements. Lastly, a DA system is inherently more complex than the other methods reviewed here and will require more development efforts.

© Crown Copyright 2021, Met Office

5.5 Comparing and combining data fusion methods

Two research studies have compared model forecast accuracy when applying two different data fusion techniques. Flemming and Inness (2013) found that a combination of data assimilation and emission initialisation provided the best-performing forecasts. Kristiansen et al. (2017) highlight that forecasts initialized using 4D-Var data assimilation based on 2D satellite observations had good skill for short-term forecasts, but that inversion methods provided more robust predictions on longer timescales due to a better representation of the 3D volcanic clouds.

A detailed intercomparison of all the data fusion methods discussed in this report have not been undertaken, and a ranking of the various methods is not possible. However, it is suggested that a combined inversion/data assimilation method could be favourable where both the underlying emission source term is optimised as well as the simulated concentrations fields, with an addition of post-processing tools (e.g., bias correction) which could be applied together with data assimilation as a fully independent approach. Such a system does not yet exist and would need thorough system development work as well as validation.

5.6 Model and observation data requirements

Data fusion schemes have been used with both Lagrangian (e.g., Pardini et al., 2017, 2018; Eckhardt et al., 2008) and Eulerian models (e.g., Mingari et al., 2021; Innes et al, 2021; Boichu et al., 2013,2014; Vira et al., 2017). The complexity of these types of models varies greatly. Further details on the models are given in the Section 3.

The data fusion methods are not directly dependent on the type of model used, but rather on how they are configured and that the model output is comparable to the observations. For example, for methods which compare the model and observations values quantitatively (e.g., inverse modelling), it is important to apply the satellite averaging kernel operator (i.e., a height sensitivity) to the model data prior to the calculations (see e.g., Eckhardt et al., 2008; Theys et al. 2013). The averaging kernel reflects the fact that the satellite retrievals have a different sensitivity to SO_2 at different altitudes in the atmosphere. This sensitivity is specific to SO_2 and is not needed in applications for volcanic ash.

Further it is important to consider the model representation error, which is the difference between the quantity that an instrument observes, and what the model represents. The model output is often on a specific discrete grid with finite resolution and output valid for discrete time steps. The observations should ideally be mapped to the same grid and time steps. Alternatively, the model data can be mapped onto the observation space. The model error should also ideally consider processes that might not be included in the model, or which are parameterised and thus a simplification, as well as limits in resolution in terms of the source description.

An important consideration is whether removal processes for SO_2 including wet deposition and chemical conversion are more important to include in models used with data fusion approaches than when such approaches are not applied. In practice, data fusion schemes estimate an “effective” source term (either at the volcano location or downwind), i.e., the source term needed by the model to best match the observations. If certain removal processes were not accounted for in the model, this could be compensated for in the data fusion scheme by adjusting the estimated source term accordingly, however the uncertainties in the estimated source terms could in this case be larger. If chemical conversion of SO_2 is neglected in the model, the estimated emissions would be lower than for the case when chemistry is included as less is removed during transport to the observation points. No specific study has looked at these effects in detail and further analysis would be needed to fully understand the implications of including or excluding removal processes in the modelling used for data fusion.

© Crown Copyright 2021, Met Office

The observations typically used in current data fusion methods for volcanic SO_2 (and ash) are total column mass loadings of SO_2 (or volcanic ash) from satellite measurements (e.g., Eckhardt et al. 2008; Section 4). The total column is a vertically integrated quantity which gives, for each horizontal pixel, the total mass of SO_2 (or ash) between the Earth's surface and the top of the atmosphere, often expressed in units of g/m^2, or for SO_2 in Dobson Units (DU). With observations in 2D (total column values) it is still possible to estimate the 3D vertical distribution of emissions in the presence of sufficient vertical wind shear which carry the emissions released at different altitudes in different directions and/or to different distances downwind.

Ideally the observations used in any data fusion technique would also contain information about the volcanic cloud altitude, in addition to the column loading. In the last few years, several satellite retrieval products have included volcanic cloud altitude (e.g., Yang et al., 2010; Carboni et al., 2016; Taylor et al., 2019) in addition to the total column values. However, the retrievals resolve a single effective altitude for the entire ash or SO_2 column, and not the vertical distribution within the column. To date, only a few data fusion studies have made use of satellite derived plume altitude information. Wang et al. (2013) used SO_2 column amount and plume height retrieved from OMI to initialize a global chemistry transport model (GEOS- Chem) through a type of data insertion method and found good model performance. Vira et al. (2017) found that including SO_2 plume altitude information in their 4D-Var system in some cases resulted in more vertically concentrated emission profiles, but overall, it only had a small impact. Chai et al. (2017) found that including plume height information did not benefit their inverse model system and deteriorated the subsequent model predictions. Fu et al. (2017) used ash cloud top heights in their ensemble data assimilation approach together with reasonable assumption of the cloud thickness range to map the 2D observations into a 3D space which they found to be more advantageous than the assimilation in 2D space. Innes et al. (2021) found that including SO_2 plume height information in the CAMS assimilation system improved the model forecasts.

Observations on volcanic cloud thickness would also be beneficial in data fusion methods to constrain the vertical distribution of the volcanic clouds. Data insertion methods require assumptions or observation of thickness to define the downwind source term in the vertical (Section 5.3). Data assimilation approaches require information or assumptions on the vertical cloud thickness to adjust the model forecast at the correct vertical levels (Section 5.4). However, observations of cloud thickness are rare, have limited coverage and are often indirect measurements (e.g., lidar observations which detect the associated sulphate aerosol; see Section 4).

A common limitation for all the data fusion schemes is that the quality of the results relies on the satellite data used as input. Limitations in the satellite observations for SO_2 can occur for example due to interference with ice particles, water vapour and volcanic ash, or band saturation caused by extremely high SO_2 column loads etc (e.g., Prata et al., 2021; Section 4). The implications of these limitations are larger uncertainties in the observations, and possibly that part of the volcanic SO_2 cloud is not detected by the satellites. These observation limitations translate directly into larger uncertainties in the data fusion results. It is possible that in some cases the model data are more complete than the satellite data if for example the SO_2 is obscured by meteorological clouds and not seen by the satellite, or if there is no satellite overpass at a given timestep. In those cases, a balance must be found between the model and observations by considering the uncertainty of the observations and the model. It is important to note that only the SO_2 emissions which are observed by satellite will be constrained by any method. Any SO_2 obscured by meteorological clouds or below the satellites' detection threshold will not be constrained but could instead be represented by the model.

© Crown Copyright 2021, Met Office

5.7 Summary and operational considerations

Many of the data fusion methods described in this report have the potential to be used in near real time in an operational setting. This introduces a range of requirements; firstly, the method needs to be easy to implement, automated and suitable for use in real-time. The key operational consideration for the use of data fusion methods in near real time is how timely a scheme can provide improved forecasts. The method must be computationally quick as well as robust. Simple techniques such as trajectory methods usually require less computational efforts than more advanced methods such as certain data assimilation types. A global SO_2 forecast system will require access to a computing facility with adequate capacity, e.g., a supercomputer.

As each data fusion method has its advantages and limitations it is recommended that a forecast system includes not just one but several of the different techniques. For example, simple and quick trajectory techniques might be most useful in the first few hours of the eruption to constrain the source term from a single satellite image, while a more comprehensive and computationally demanding inversion or data assimilation might be most suitable when more observations are available at a later stage.

The observations used must have good spatial and time coverage and be available in near real time. They must be accurate and include uncertainty estimates which should be considered in the data fusion method. Often specific pre-processing of the observations is required (e.g., re-mapping of satellite data onto a grid consistent with the model grid). The errors in both the observations and in the model need to be considered.

Many of the methods already developed are in research mode and are bespoke techniques that have been tuned to certain eruptions or situations. Further 'tuning' on a case-by-case basis might be necessary. A fully automated process might therefore not be recommended, and further 'expert analyses of the results might be necessary in near real time.

A limiting factor for operational centres can be the porting of software. Various open-source software is available to perform EnKF data assimilation algorithms (e.g., as used by Pardini et al., 2020 and Fu et al., 2015) but such software is not always straight forward to implement into already existing operational systems both for licensing and technical reasons.

Most of the data fusion methods developed for volcanic ash are in theory also applicable to volcanic SO_2. For application to SO_2 some methods require the averaging kernel (AK) operator to be applied to the model data. However, the importance of applying the AK operationally needs to be further assessed.

Another important consideration for operational use is how frequently the data fusion method should be applied, i.e., the temporal cycle. This depends on the type of observation data which is being assimilated (e.g., how often data are available). Data from polar orbiting satellites are available at specific times for a specific region, which means that the data fusion methods rely on the overpass time of the satellite and a delay might occur if an eruption occurs several hours before data from an overpass is available. Geostationary satellites provide higher temporal resolution but, to date, with lower quality for SO_2 retrievals (future missions will improve on this aspect, see the Section 4). A combination of data from polar orbiting and geostationary satellites would provide a robust system considering both the timeliness and quality of the satellite observations.

The required temporal cycle also depends on the effective duration of the improved forecasts. This duration has been assessed in some research studies, but it varies greatly (e.g., Fu et al. 2015, 2016, 2017 report between 6 and 24 hours), and can also be longer for regions farther away from the

© Crown Copyright 2021, Met Office

volcano as it depends on the specific case, meteorological conditions and on the atmospheric dispersion model used.

Further consideration needs to be made about how many observations are needed to obtain improvements in the forecast. For example, how many data assimilation cycles are needed and over which time periods before improvements in the forecast are significant. This is likely to be case specific.

A limiting factor with data fusion techniques is that they provide no forecast source term (i.e., into the future for T+6 etc). This means that assumptions of future volcanic activity and source terms need to be made and integrated into the forecast process. However, as more observations become available the data fusion methods can be re-run to provide updated dispersion forecasts. The atmospheric dispersion model used for the forecasts need to be able to accurately represent onwards transport e.g., for SO_2 the model needs to represent loss processes such as deposition and chemistry.

CAMS is the only service currently applying a data fusion method to improve the representation of volcanic SO_2 emissions in the SO_2 forecasts. The University of Manchester runs an experimental service using the PlumeTraj method of Pardini et al. (2017, 2018) to provide daily SO_2 flux estimates for Etna (http://dailyetna.eps.manchester.ac.uk/index.php). Two other centres have currently installed a method for volcanic ash that can be used in an emergency forecasting procedure; 1) a volcanic ash inversion method developed by Pelley et al. (2015) is currently installed at the UK Met Office. However, the system has, to date, not been tested in real time for a real eruption. 2) the volcanic ash EnKF DA system of Pardini et al. (2020) has been parallelised and automized as part of an emergency forecasting procedure at INGV Pisa (Italy). The system can be run in real time for red eruption status but is not yet operative and has to date only been tested and applied to historical eruptions (Pers. Comm. F. Pardini, March 2021). Some centres are working towards operational use of data fusion methods. For example, at the Bureau of Meteorology in Australia, the observation assimilation is expected to be fully operational around the end of 2021 or start of 2022 (Pers. Comm. M. Zidikheri, May 2021). None of the other methods listed in this report has been tested or used in an operational setting.

© Crown Copyright 2021, Met Office

6 Thresholds

A review of SO_2 concentration thresholds for use in a global forecast system has been undertaken. The assessment has analysed volcanic SO_2 from recent eruptions and illustrates the impact of applying different SO_2 concentration thresholds on the requirement to produce SO_2 forecasts. Atmospheric dispersion model data for historic eruptions have been used to calculate the area and time over which the SO_2 thresholds are exceeded. This provides information that allows the MISD to evaluate whether the proposed thresholds are sensible and which to take forward.

6.1 The proposed thresholds

A reminder that the driver for this investigation into SO_2 is the hazard to human health onboard an aircraft. SO_2 is an irritant when inhaled and high concentrations may cause breathing difficulties in people exposed to it. People suffering from asthma and chronic lung disease may be especially susceptible to the adverse effects of SO_2 and, if in high concentrations it may provoke attacks of asthma. Based on the findings from controlled human exposure studies with exercising asthmatics, the World Health Organization (WHO) has recommended a threshold for short term exposure of 500 µg/m^3 over 10 minutes (WHO, 2021).

Concentrations of SO_2 in air can be measured in units of mass per volume (e.g., µg/m^3) or in volumetric units such as parts per million (ppm). At ground level, an SO_2 mass concentration of 500 µg/m^3 equates to a volumetric unit of 0.175 ppm, using a conversion factor based on the molecular weight of SO_2. The advantage of volumetric units is that they are equivalent at different pressures and atmospheric air densities (i.e., they are constant when air expands or contracts, cools or warms) and so can be applied equally at all altitudes, while a mass concentration unit will vary with different atmospheric pressures and therefore with altitude. This mass concentration variation is illustrated in Figure 6.1, which shows that for an SO_2 plume with initial ground-level concentration of 500 µg/m^3, the equivalent mass concentration when the plume is lifted up to 5 km altitude is 300 µg/m^3, and at 10 km the equivalent mass concentration is ~170 µg/m^3. This is due to the atmospheric pressure decreasing with increasing altitude. The disadvantage with a volumetric unit is that many atmospheric models only output in mass units such as g/m^3, and a conversion to ppm would be needed as a postprocessing step using atmospheric pressure and density profiles.

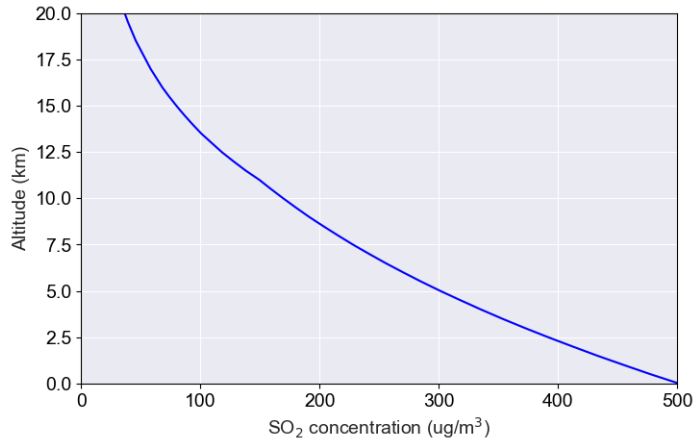

Figure 6.1: The change in SO_2 mass concentration with altitude, for an SO_2 plume with an initial concentration of 500 µg/m^3 at ground level, assuming a standard atmospheric pressure gradient.

To facilitate rapid evaluation when only satellite data is available it might be useful to use thresholds relating to volcanic SO_2 in Dobson Units (DU) (i.e., the atmospheric column load), which is the main quantitative measurement obtained from satellite sensors (see Section 4 Satellites), in addition to air concentrations (either µg/m^3 or ppm) which can be provided by atmospheric forecast models.

© Crown Copyright 2021, Met Office

On 20 November 2019, the ICAO METP WG-MISD/5 (VASD) specifically requested the VASAG to determine the thresholds to be used in the SO_2 trial. Over the two days of the ensuing VASAG meeting, discussion was held between the VASAG members and other meeting observers in the break-out periods to try to reach a consensus. Concerns were raised about the inability to observe or validate concentration measurements and that comparable thresholds in Dobson Units should be evaluated as part of the trial. Previous work for the MISD and VASAG had shown that levels of 50 DU and higher are observed in larger eruptions and that most current satellite retrieval methods have uncharacterised biases above ~200 DU. Conversion between DU and concentration is complex (See Section 6.6 for a detailed explanation). In this work all comparisons of DU to the equivalent concentration were made assuming a 1000 m thick SO_2 plume at an altitude of 10 km. This revealed that 50 DU was approximately the WHO value times 10 and 150 DU was approximately the WHO value times 25 for this plume. For this reason, the thresholds and units given in Table 6.1 were provided by the VASAG as a starting point for evaluation in the trial.

Label	Parts per million (ppm)	Dobson Unit (DU)
WHO	0.175	~5
WHO x 10	1.750	~55
WHO x 25	4.375	~140

Table 6.1: The SO_2 thresholds provided as a starting point for evaluation in the trial.

The conversion from concentration to DU strongly depends on the assumption of the cloud thickness and altitude and is further explored in Section 6.6. It should be noted that there is no medical basis for the choice of WHO x 10 and WHO x 25 by the VASAG.

These thresholds have been considered as the starting point for this investigation. To understand whether other thresholds could provide more useful data, we have also considered additional thresholds at the lower end that may be more pertinent to health endpoints: WHOx2 (0.35 ppm), WHOx4 (0.7 ppm), WHOx6 (1.05 ppm), and WHOx8 (1.4 ppm). A total of seven thresholds (Table 6.2) have been evaluated.

Label	Parts per million (ppm)
WHO	0.175
WHO x 2	0.350
WHO x 4	0.700
WHO x 6	1.050
WHO x 8	1.400
WHO x 10	1.750
WHO x 25	4.375

Table 6.2: The seven SO_2 thresholds considered in the analysis.

The additional lower-end thresholds (WHOx2-WHOx8) are related to the odour detection thresholds of SO_2. Reported odour detection thresholds of SO_2 range from 266 $\mu g/m^3$ (0.1 ppm, WHOx0.5) to 12500 $\mu g/m^3$ (4.7 ppm, WHOx25), with a median threshold of 2770 $\mu g/m^3$ (WHOx5.5) (Kleinbeck et al., 2011). This means that at the WHO concentration threshold most humans are not likely to smell the SO_2 gas but will start smelling it once the SO_2 concentrations reach around a factor 5 over the WHO threshold.

© Crown Copyright 2021, Met Office

The analysis of the thresholds has not considered the time it would take for the cabin to come to equilibrium with the outside SO_2 concentrations, nor considered that the WHO threshold is for a 10-minute exposure duration in relation to an aircraft's typical cruise speed.

6.2 Historic aircraft encounters and measurements of volcanic SO_2

A short review of historic volcanic SO_2 aircraft encounters data has been made. This is to illustrate that there is very limited information on aircraft encounters with volcanic SO_2 plumes, and especially limited information on the encountered SO_2 concentration levels. A few reports on aircraft measurements of volcanic SO_2 plumes have been published, but only a small number of cases include in-situ measurements of SO_2 from explosive eruptions. It is therefore not possible to use measured aircraft encounter data alone to evaluate the proposed thresholds, and hence a need for atmospheric dispersion model data.

During the Eyjafjallajökull 2010 eruption two research aircraft sampled the volcanic plumes at various locations over Europe. The DLR Falcon aircraft (see table 3 in Schumann et al 2011) measured 1.8 nmol/mol of SO_2, which equates to 0.0018 ppm (~WHOx0.01), on the 22 April 2010 over Skagerrak. The highest SO_2 mixing ratio measured during the DLR Falcon flights was 74.9 nmol/mol, which is 0.0749 ppm (~WHOX0.4), sampled on the 2 May 2010 over the North Atlantic. The FAAM research aircraft (Johnson et al., 2012) measured elevated levels of SO_2 of 10-100 ppbv (~WHOx0.05 - WHOx0.6) during the May 2010 phase of the Eyjafjallajökull eruption.

Following the Hekla 2000 eruption, in-situ measurements of plume properties were measured by a NASA DC-8 research plane on 28 February 2000 (one and a half days after the eruption). The airplane flew in the SO_2 plume for 7-10 minutes, during which the on-board instrumentation recorded high concentrations, up to 1 ppm (~WHOx6) (see Figure 7 of Rose et al., 2003).

The aircraft encounters database compiled by Guffanti, Casadevall, and Budding (2010) includes qualitative information on SO_2 encounters for incidents involving commercial aircraft, for the period 1953-2009. No in-situ measurements are available for these encounters, and the association with SO_2 is mainly from the fact that the aircraft crew smelled sulphur gases. This indicates that the odour detection threshold was exceeded. However, this is not a reliable indication of the concentration encountered by the aircraft as the odour detection threshold vary between WHOx0.5 and WHOx25.

6.3 Eruptions considered in the analysis

This assessment has considered atmospheric dispersion model data for eight historic eruptions (Table 6.3) to evaluate how often and to what extent the various SO_2 thresholds (Table 6.2) are exceeded. The eight eruptions span a large range of SO_2 fluxes and plume altitudes. A relative eruption size (small, moderate, large) has been given to each eruption (third column in Table 6.3) which is determined by the average SO_2 flux in combination with the plume altitude.

Both effusive and explosive eruptions are included in this analysis. The effusive eruptions of Holuhraun and Fogo have a much longer duration of SO_2 emissions than the explosive eruptions. Emissions from passive degassing volcanoes are not included in this threshold assessment because SO_2 fluxes from this type of volcanic activity are small and the release occurs at the surface, and it is unlikely that this type of activity constitutes a significant risk for aircraft operations at cruising altitude (see Section 2.2 for more details on types of volcanic activity).

In addition to the eight eruptions in Table 6.3, the 2021 eruption in the Krysuvik/Fagradalsfjall area of Iceland was analysed. The emissions from this eruption were more than 100 times smaller than those during the Holuhraun eruption in 2014, and the results showed that thresholds were only

© Crown Copyright 2021, Met Office

exceeded in a very localised area close to the volcano. Therefore, the results are not illustrated in this report.

	Volcano	Relative eruption size and type	Location (lat, long)	Start date	Eruption duration	Plume altitude (km asl)	Total SO_2 emission (kt)	Average SO_2 flux (kt/day)
1	Kliuchevskoi	Small – Explosive	Russia (56.057, 160.638)	18/10/2013	8 days	6-10	55	7
2	Etna	Small – Explosive	Italy (37.734, 15.004)	30/12/2013	1 day	4	10	10
3	Fogo	Small – Effusive	Cape Verde (14.95, -24.35)	24/11/2014	34 days	7-9	353	10
4	Holuhraun	Moderate - Effusive	Iceland (64.85, -16.833)	31/08/2014	122 days*	3-5	6000	50
5	Merapi	Moderate - Explosive	Indonesia (-7.542, 110.442)	04/11/2010	5 days	12-17	350	70
6	Puyehue Cordon Caulle	Moderate - Explosive	South America (-40.59, -72.117)	04/06/2011	41 hours	11-14	160	95
7	Raikoke	Large - Explosive	Russia (48.3, 153.2)	21/06/2019	9 hours	10-14	1570	**
8	Kasatochi	Large - Explosive	Alaska (52.17, -175.51)	07/08/2008	< 1 hour	7-13	1700	**

Table 6.3: Eruptions considered in the analysis.
* This eruption lasted for ~6 months but present analysis covered the first two months.
** Daily flux not given for eruptions with duration less than a day.

6.4 Model simulations

The Numerical Atmosphere-dispersion Modelling Environment (NAME) (Jones et al., 2007) dispersion model has been used to simulate the dispersion of volcanic SO_2 released from the eight different historic eruptions in Table 6.3. NAME has previously been used for simulating volcanic SO_2 clouds from several different eruptions (Heard et al., 2012; Schmidt et al., 2014, 2015) including most recently a detailed analysis of the 2019 eruption of Raikoke (de Leeuw et al., 2021). These previous studies have found that NAME is able to capture the atmospheric transport, chemistry and removal of the volcanic SO_2 clouds providing an appropriate SO_2 emission flux and meteorological data are used to drive the model.

The simulations use global meteorological input fields from the Met Office Unified Model (MetUM), with a 3 hourly temporal resolution. The horizontal resolution varies between 40 and 10 km depending on the year that the simulation covers.

Source term estimates

The source terms used in the NAME simulations are based on robust values reported in the literature. For Holuhraun, the SO_2 emission estimate from Schmidt et al. (2015) was used, releasing 60-100 kt/day between 1.5 and 3.0 km a.g.l. The NAME simulation used in this current analysis

© Crown Copyright 2021, Met Office

covers part of the eruption period (31.08.2014 until 05.10.2014), releasing a total of 2680 kt of SO_2. For the Puyehue Cordon Caulle eruption, the source term determined from inverse modelling by Theys et al. (2013) was used, while for Kasatochi, the inversion-based source term by Kristiansen et al. (2010) was applied. For Raikoke, the source term estimated by de Leeuw et al. (2021) was used. For the four other eruptions (Fogo, Merapi, Kliuchevskoi and Etna) the source terms were based on daily emissions of SO_2 reported in a long-term database of volcanic SO_2 emissions derived from ultraviolet satellite measurements (Carn et al., 2019). Some further details on the emission fluxes and altitudes for each eruption is given in Figures 6.2 - 6.9 later in this section.

Chemistry and other loss processes

A chemistry scheme to convert sulphur dioxide (SO_2) to particulate sulphate (SO_4) is used in the NAME model simulations (Redington et al., 2009). The scheme includes both aqueous and gaseous phase chemistry and uses pre-defined monthly atmospheric concentration fields of the oxidants: hydrogen peroxide and ozone. SO_2 is also removed from the atmosphere by wet and dry deposition.

Output

The model output was produced on gridded fields with 30 min temporal resolution. The horizontal resolution of the gridded output matches the resolution of the historical meteorological data used to drive the simulation. For the 2008-Kasatochi simulation the resolution is 0.5625° longitude by 0.375° latitude (~40 km), while for the 2019-Raikoke simulation the resolution is about 20 km. Note that current and future operational forecast resolutions are, and will be, higher. The vertical resolution of the output is 500 m up to 20 km asl and 1 km resolution up to 23 km asl, giving a total of 43 altitude levels. This is different to the resolution of the input MetUM data.

Uncertainties and model skill

There are many sources of uncertainty in the results that should be considered. These include uncertainties in the model inputs (both the emissions and meteorology), the model chemistry and other model parameterisations (e.g., mesoscale motions).

Uncertainties exist in the emission for (1) the amount of SO_2 emitted, (2) the timing of the emission and (3) the height of the emissions. Many of the source term estimates are based on satellite data. The satellite derived SO_2 masses are an estimate only. Different satellite instruments have their own uncertainties and give different values for the same eruption. The timing and duration of many of these eruptions are poorly constrained by satellite and local observations, therefore simplifications have been made to the release durations used.

If the SO_2 flux used in the model simulation is too low, the modelled concentrations will be lower than reality, and vice versa, if the assumed flux is too high, the modelled concentrations can be overestimated. Similarly, the height range of the emissions if often not very well known. SO_2 is typically emitted at the top of explosive eruption columns, but for effusive eruptions this is not the case. If the vertical emission range assumed in the model simulation is too large, then SO_2 mass is spread over too large a range, which would lead to under prediction in the model. If the assumed vertical range is too narrow, this can lead to over prediction in the model.

Errors and uncertainties in the meteorological data will affect the transport and positioning of the plume in the model simulations. Although the “analysis” meteorological data used here incorporates the influence of weather observations, there are still uncertainties. For example, incorrect

© Crown Copyright 2021, Met Office

representation of vertical wind shear can lead to the plume being transported in the wrong direction. Such errors will be responsible for offsets between the modelled and observed plume.

All these factors mean that some discrepancies between the model and observed plumes should be expected and that uncertainties in the spatial and temporal location of the plumes should be considered.

Recent work of de Leeuw et al. (2021) found that for Raikoke, NAME accurately simulates the observed location and horizontal extent of the SO_2 cloud during the first 2-3 weeks after the eruption and has skill for 12-17 days for the low-density parts of the SO_2 clouds (SO_2 vertical column densities below 1 DU). However, they also found that NAME performs less well for the denser parts of the SO_2 cloud (vertical column densities greater than 20 DU) with a skill on the order of 2-4 days.

6.5 Evaluation of ppm thresholds

To assess the impact of applying various concentration thresholds on the requirement to produce SO_2 forecasts, the plume area obtained using the seven different thresholds (Table 6.2) has been evaluated.

The horizontal extent of the plume that exceeds a given threshold has been calculated from the 3-dimensional (latitude, longitude, altitude) model output. If the threshold is exceeded at any altitude level for a given horizonal grid box (longitude, latitude), the horizontal area of the grid box is added to the plume area exceeding the threshold. This is subsequently repeated for all horizontal grid boxes in the modelled domain. As such, the current analysis has focussed on the total atmospheric column and the horizontal extent of the SO_2 cloud exceeding various concentration thresholds. Repeating the threshold exceedance analysis for different flight levels in the vertical is beyond the scope of this work.

Figures 6.2 - 6.9 show the resulting horizonal plume extents for each eruption considered in the analysis. On the left side of each figure are the plume areas obtained when applying three of the thresholds: WHO (red plume), WHOx2 (green plume) and WHOx4 (purple plume). Note that the horizontal maps are selected for a time when there are large differences in the plume areas when applying these three thresholds and are not necessarily representative of the entire eruption period

On the right side of each of the Figures 6.2 - 6.9 is a timeline of the plume extent as it evolves after the start of the eruption, when applying the various ppm thresholds. The lowest threshold (WHO threshold, 0.175 ppm: red area and line) is exceeded for all 8 eruptions over a significant time period and over significant areas. The largest threshold (WHOx25, 4.375 ppm: green thick line) is rarely exceeded, and only over small areas for a short duration of time for the largest eruptions.

With each figure is a corresponding table showing the number of hours that the various SO_2 concentration (ppm) thresholds are exceeded, and the corresponding maximum plume area (km^2) that is reached during the simulated time period.

In summary we find:

- The time period and area over which the thresholds are exceeded depend on the size of the eruption (the amount, duration and height of the SO_2 released). Details on the emission flux and emission height for each eruption are given in the bottom right side of each of the Figures 6.2-6.9. Eruptions which release large quantities of SO_2 over a short period of time and at high altitudes give the most extensive plume areas and duration of exceedance.

© Crown Copyright 2021, Met Office

- For the small, explosive eruptions of Etna and Kliuchevskoi, the WHO threshold is exceeded for up to 24 hours over a relatively small area (up to 25.000 km^2 - the size of Sicily) (Figures 6.2 and 6.3, Tables 6.4 and 6.5). The WHOx6 and higher thresholds are not exceeded.

- For the effusive eruptions of Holuhraun and Fogo (Figures 6.4 and 6.5, Tables 6.6 and 6.7) with continuous SO_2 emission throughout the model simulation period, the WHO threshold is exceeded during a large part of the period, and the other 6 thresholds are exceeded for some time periods.

- The moderate, explosive eruptions of Merapi and Puyehue (Figures 6.6 and 6.7, Tables 6.8 and 6.9) resulted in exceedance of 6 of the 7 thresholds, with the WHO threshold exceeded for 3-5 days. The long-range transport of the Puyehue SO_2 cloud is shown (Figures 6.7b, 6.7c) but none of the thresholds were exceeded in the plume after 3 days.

- The large, explosive eruptions of Kasatochi and Raikoke (Figures 6.8 and 6.9, Tables 6.10 and 6.11) show significant areas of exceedance of all thresholds. For Raikoke, the WHO threshold is exceeded for about two weeks, and covers a large area of up to 1.7 million km^2 (the size of Alaska), while the WHOx25 threshold is exceeded over an area of up to 150.000 km^2 (size of England and Wales) and over a period of about 60 hours. In the area of an aircraft encounter with the Kasatochi eruption cloud (Figure 6.8b) the three lowest thresholds were exceeded.

© Crown Copyright 2021, Met Office

Etna Dec 2013

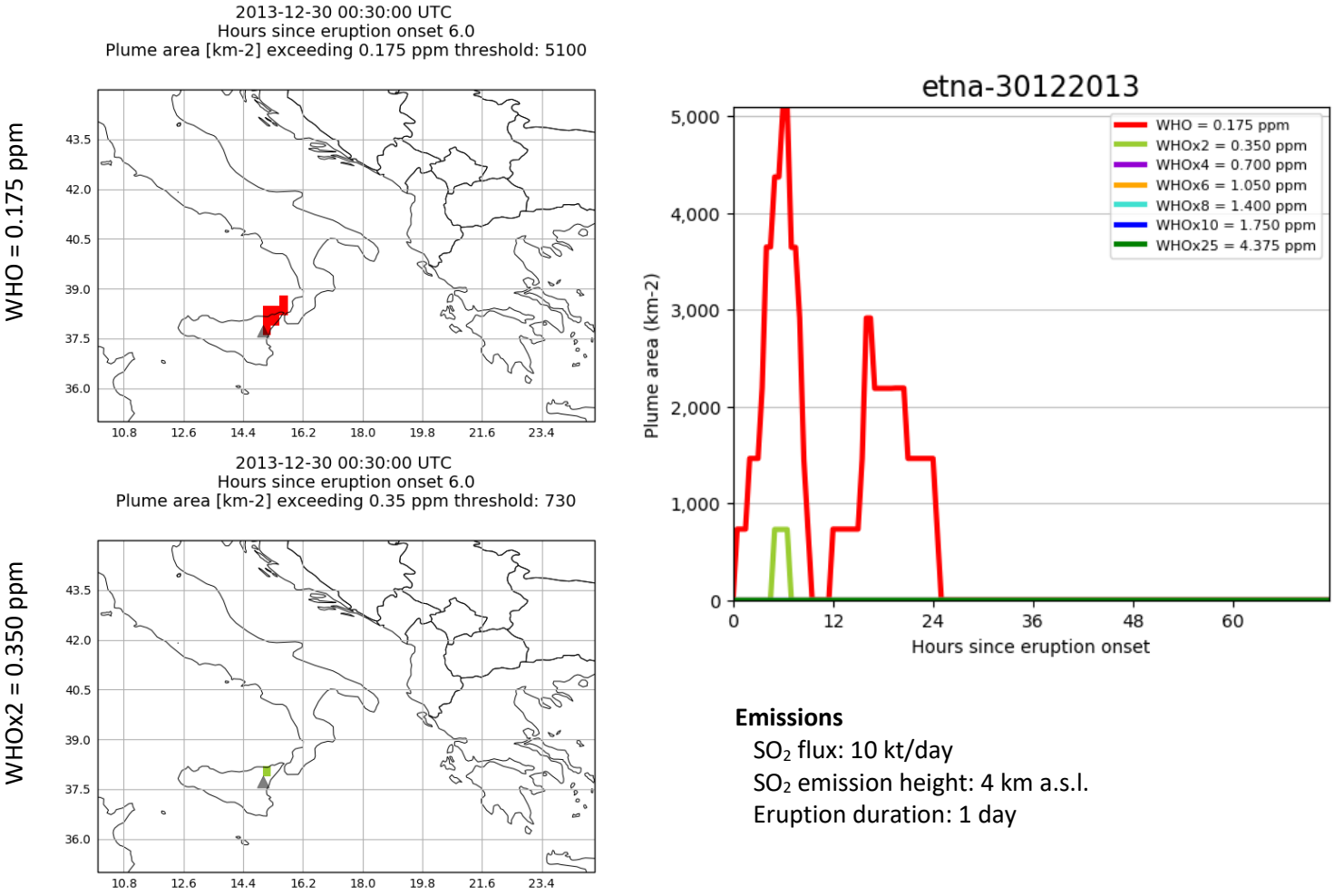

Emissions

SO_2 flux: 10 kt/day
SO_2 emission height: 4 km a.s.l.
Eruption duration: 1 day

Figure 6.2: Maps and time series of the plume area (km^2) which exceeded various SO_2 concentration (ppm) thresholds for the Etna December 2013 eruption.

Threshold (ppm)	Number of hours exceeding threshold	Maximum plume extent (km^2)
WHO	22	5100
WHOx2	2	730
WHOx4	0	0
WHOx6	0	0
WHOx8	0	0
WHOx10	0	0
WHOx25	0	0

Table 6.4: The number of hours exceeding the various SO_2 concentration (ppm) thresholds, and the maximum plume area (km^2), for the Etna December 2013 eruption.

© Crown Copyright 2021, Met Office

Kliuchevskoi Oct 2013

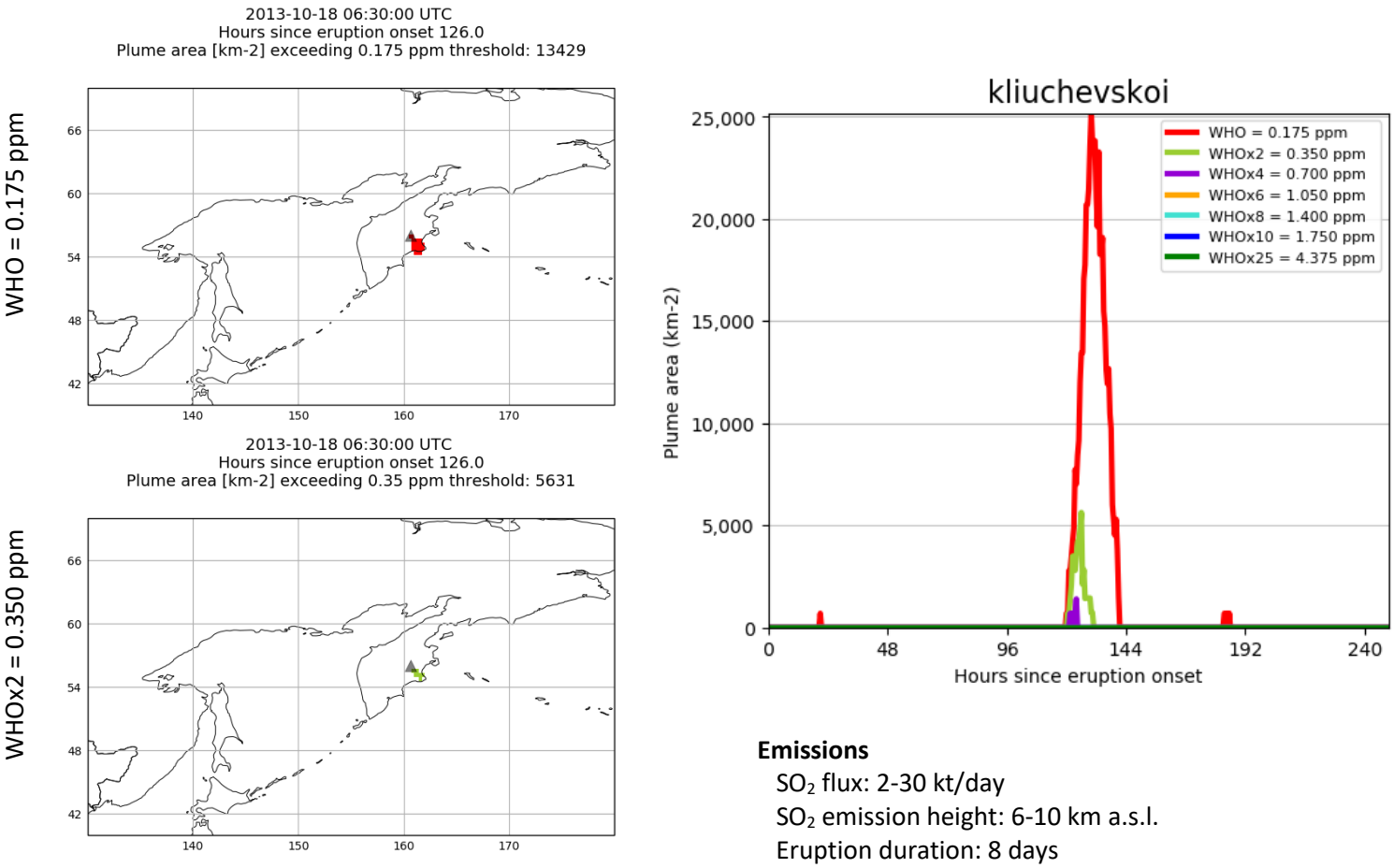

Emissions

SO_2 flux: 2-30 kt/day

SO_2 emission height: 6-10 km a.s.l.

Eruption duration: 8 days

Figure 6.3: Maps and time series of the plume area (km^2) which exceeded various SO_2 concentration (ppm) thresholds for the Kliuchevskoi 2013 eruption.

Threshold (ppm)	Number of hours exceeding threshold	Maximum plume extent (km^2)
WHO	24	25,177
WHOx2	11	5631
WHOx4	3	1397
WHOx6	0	0
WHOx8	0	0
WHOx10	0	0
WHOx25	0	0

Table 6.5: The number of hours exceeding the various SO_2 concentration (ppm) thresholds, and the maximum plume area (km^2), for the Kliuchevskoi 2013 eruption.

© Crown Copyright 2021, Met Office

Holuhraun Aug-Sept 2014

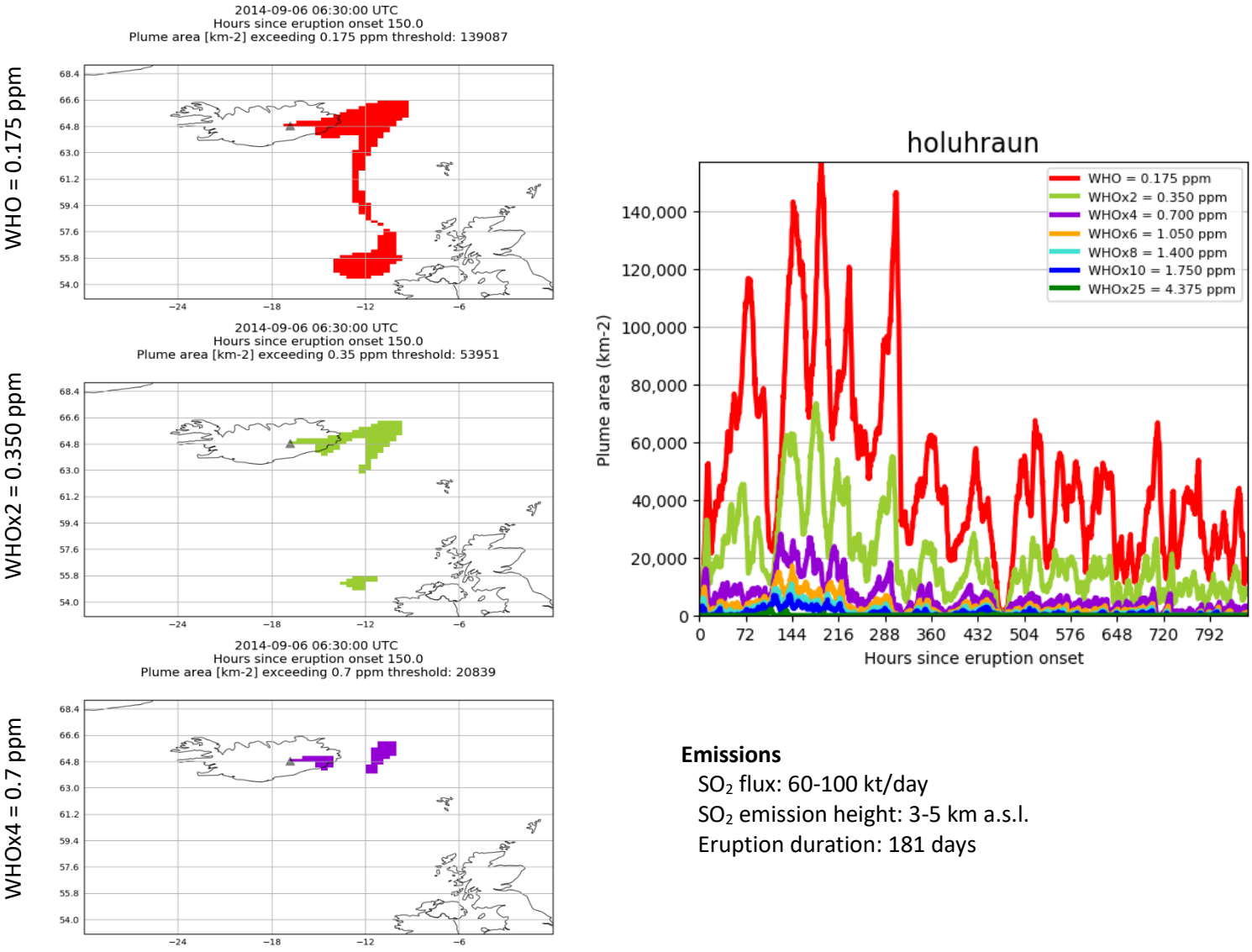

Emissions

SO_2 flux: 60-100 kt/day

SO_2 emission height: 3-5 km a.s.l.

Eruption duration: 181 days

Figure 6.4: Maps and time series of the plume area (km^2) which exceeded various SO_2 concentration (ppm) thresholds for the Holuhraun 2014 eruption.

Threshold (ppm)	Number of hours exceeding threshold	Maximum plume extent (km^2)
WHO	852	157,085
WHOx2	852	73,251
WHOx4	832	28,149
WHOx6	700	17,116
WHOx8	551	10,860
WHOx10	395	7121
WHOx25	49	2132

Table 6.6: The number of hours exceeding the various SO_2 concentration (ppm) thresholds, and the maximum plume area (km^2), for the Holuhraun 2014 eruption.

© Crown Copyright 2021, Met Office

Fogo Nov-Dec 2014

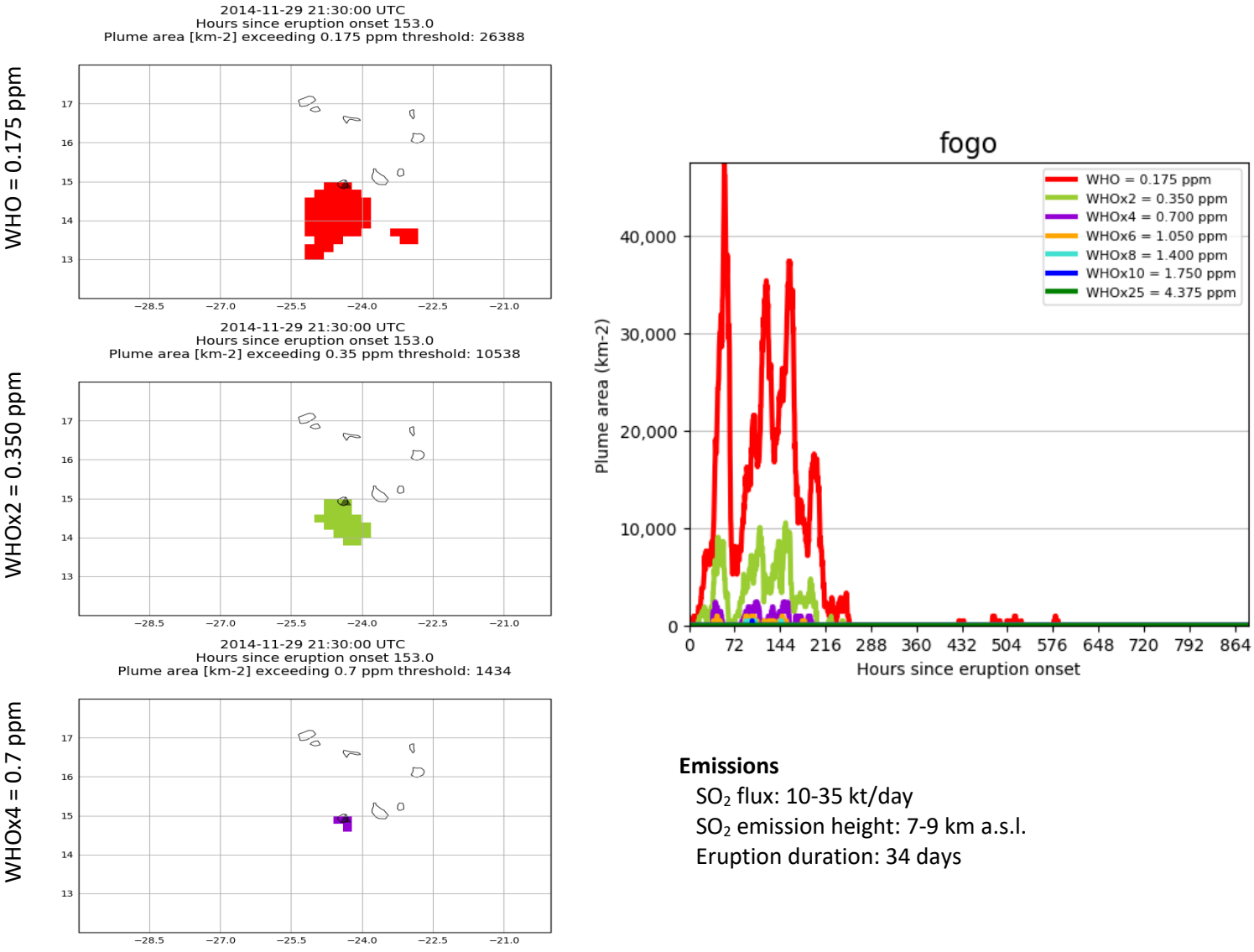

Emissions

SO_2 flux: 10-35 kt/day

SO_2 emission height: 7-9 km a.s.l.

Eruption duration: 34 days

Figure 6.5: Maps and time series of the plume area (km^2) which exceeded various SO_2 concentration (ppm) thresholds for the Fogo 2014 eruption.

Threshold (ppm)	Number of hours exceeding threshold	Maximum plume extent (km^2)
WHO	284	47,563
WHOx2	193	10,538
WHOx4	117	2392
WHOx6	49	956
WHOx8	15	477
WHOx10	0.5	477
WHOx25	0	0

Table 6.7: The number of hours exceeding the various SO_2 concentration (ppm) thresholds, and the maximum plume area (km^2), for the Fogo 2014 eruption.

© Crown Copyright 2021, Met Office

Merapi Nov 2010

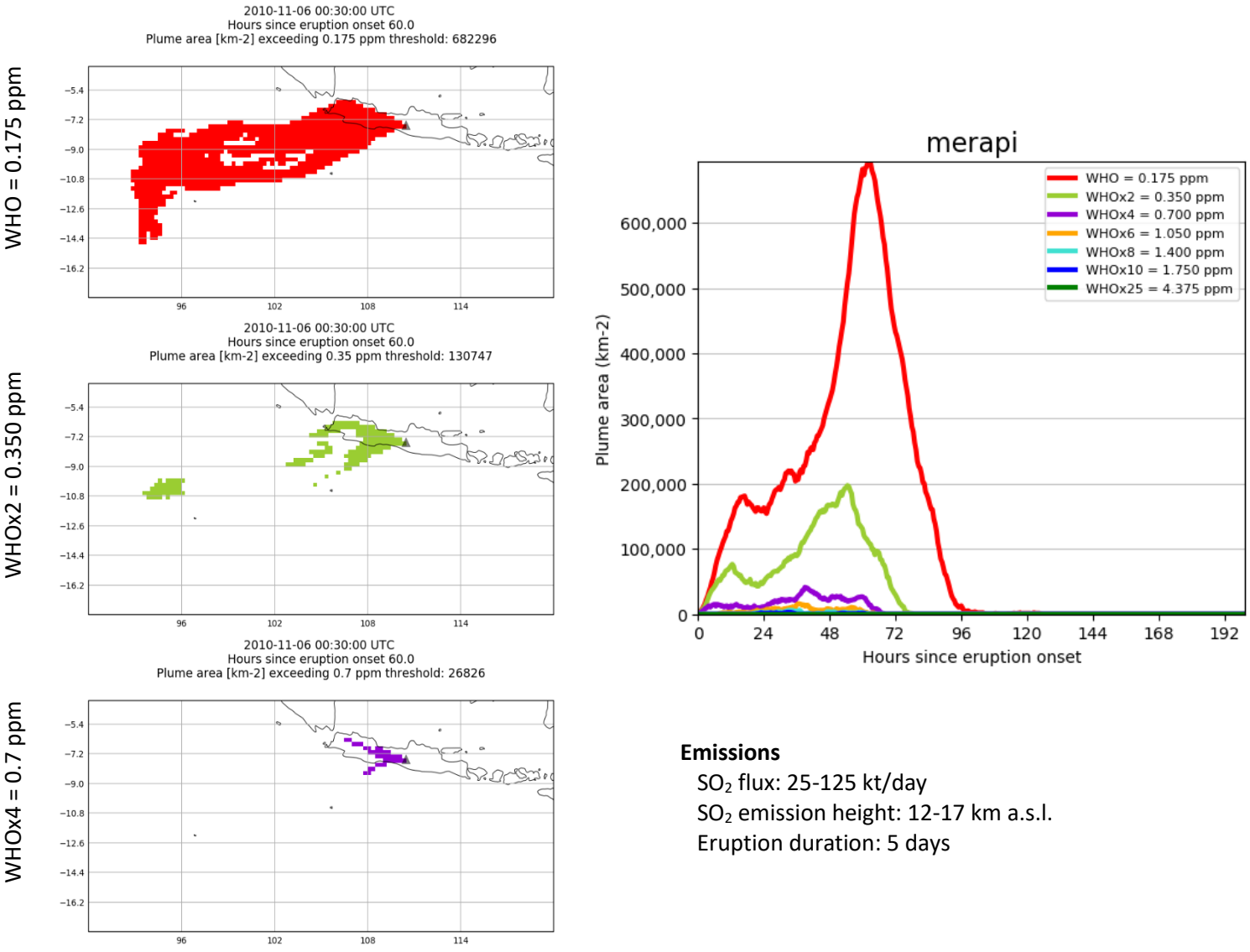

Emissions

SO_2 flux: 25-125 kt/day

SO_2 emission height: 12-17 km a.s.l.

Eruption duration: 5 days

Figure 6.6: Maps and time series of the plume area (km^2) which exceeded various SO_2 concentration (ppm) thresholds for the Merapi 2010 eruption.

Threshold (ppm)	Number of hours exceeding threshold	Maximum plume extent (km^2)
WHO	120	694,526
WHOx2	79	197,306
WHOx4	68	41,360
WHOx6	59	16,087
WHOx8	40	6130
WHOx10	25	3063
WHOx25	0	0

Table 6.8: The number of hours exceeding the various SO_2 concentration (ppm) thresholds, and the maximum plume area (km^2), for the Merapi 2010 eruption.

© Crown Copyright 2021, Met Office

Puyehue June 2011

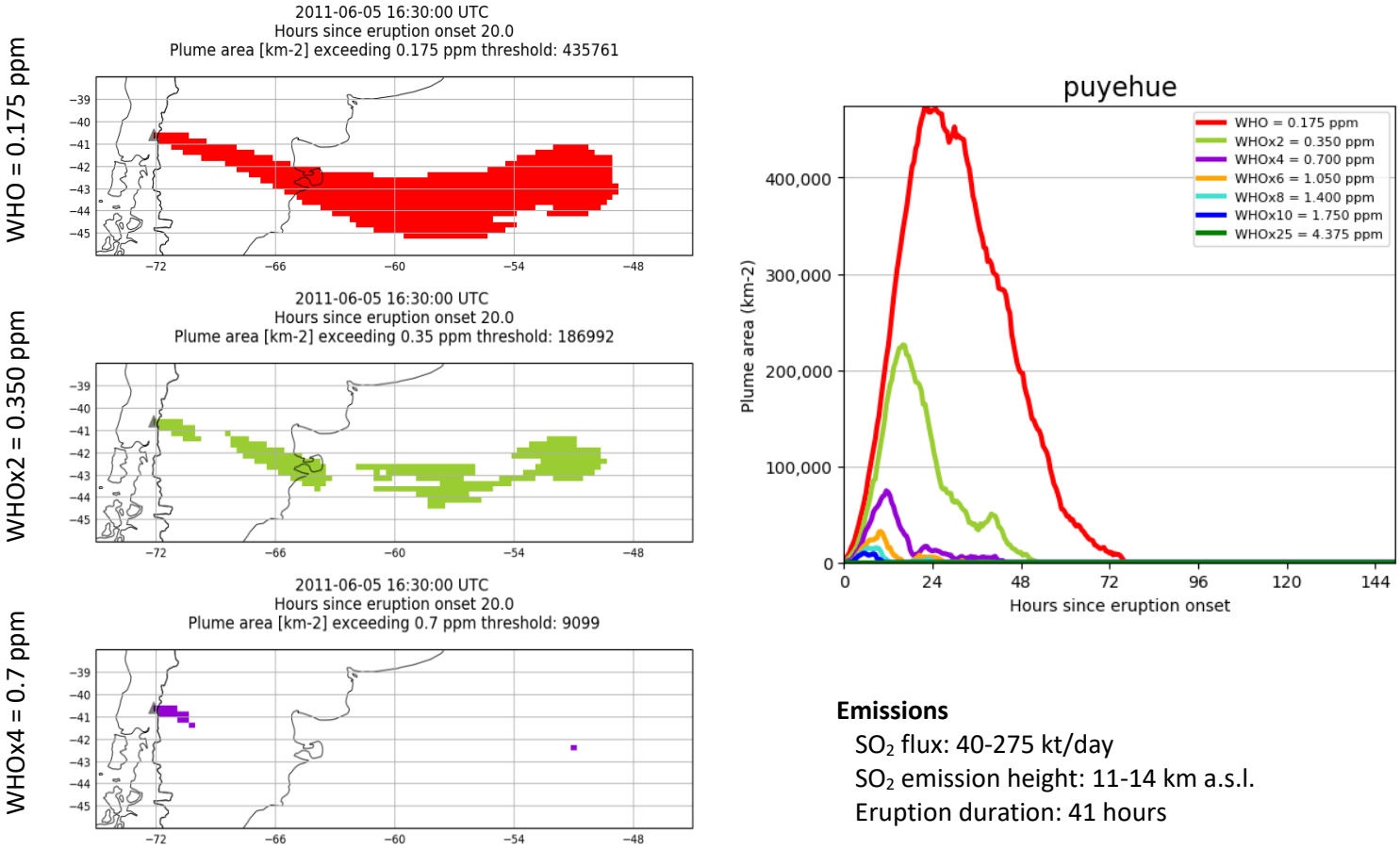

Emissions

SO_2 flux: 40-275 kt/day
SO_2 emission height: 11-14 km a.s.l.
Eruption duration: 41 hours

Figure 6.7a: Maps and time series of the plume area (km^2) which exceeded various SO_2 concentration (ppm) thresholds for the Puyehue 2011 eruption.

Threshold (ppm)	Number of hours exceeding threshold	Maximum plume extent (km^2)
WHO	77	474,896
WHOx2	53	226,236
WHOx4	44	74,517
WHOx6	31	32,297
WHOx8	17	15,218
WHOx10	9	9712
WHOx25	0	0

Table 6.9: The number of hours exceeding the various SO_2 concentration (ppm) thresholds, and the maximum plume area (km^2), for the Puyehue 2011 eruption.

The Puyehue eruption cloud circled the Earth three times between 50–80°S (Klüser et al., 2013; Clarisse et al., 2012) as shown in Figure 6.7b. The first circuit took 9-10 days (Clarisse et al., 2012). Air traffic in both Australia and New Zealand was disrupted.

When applying the WHO threshold, the plume reached 3°W after 77 hours, after which (i.e., further east) all concentration values dropped below the threshold. Thus, the part of the plume exceeding the WHO threshold travelled about 1/3 of the distance between the volcano and Australia, and the remaining part of the plume that reached Australia and further circulated the Earth contained SO_2 concentration values much below 0.175 ppm.

© Crown Copyright 2021, Met Office

After one week of transport the SO_2 plume crossed the International dateline at 180° longitude (Figure 6.7c). Two weeks after the eruption onset the SO_2 plume was spread across all longitudes and after three weeks the plume was mainly located over the Eastern hemisphere. No areas of these old plumes exceeded the WHO threshold.

i) **Satellite observed**

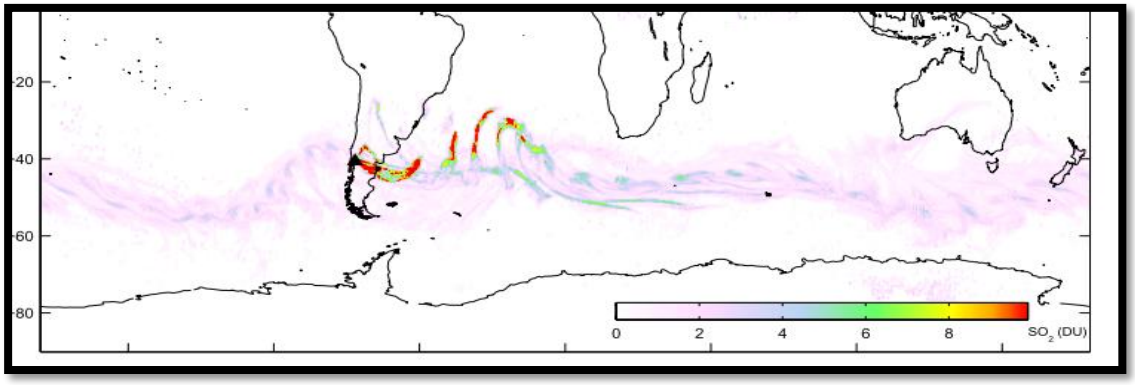

ii) **NAME modelled**

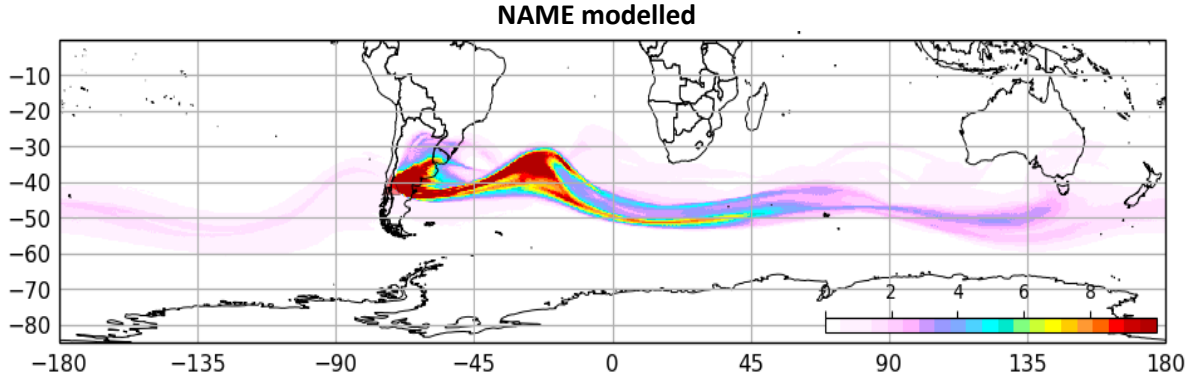

Figure 6.7b: i) from Clarisse et al. (2012) showing a composite image of maximum observed SO_2 columns (DU) for the Puyehue eruption from IASI satellite measurements (note that the satellite images are available approximately every 12 hours and hence the composite image doesn't show a smooth continuous plume). The value for each grid cell equals the maximum observed SO_2 columns in that grid cell for a given time period after the eruption. ii) maximum simulated SO_2 columns (DU) from NAME, calculated as in a) but with higher temporal resolution of 30 min (resulting in a smoother plume than above) over the time period 4 June until 2 July 2011.

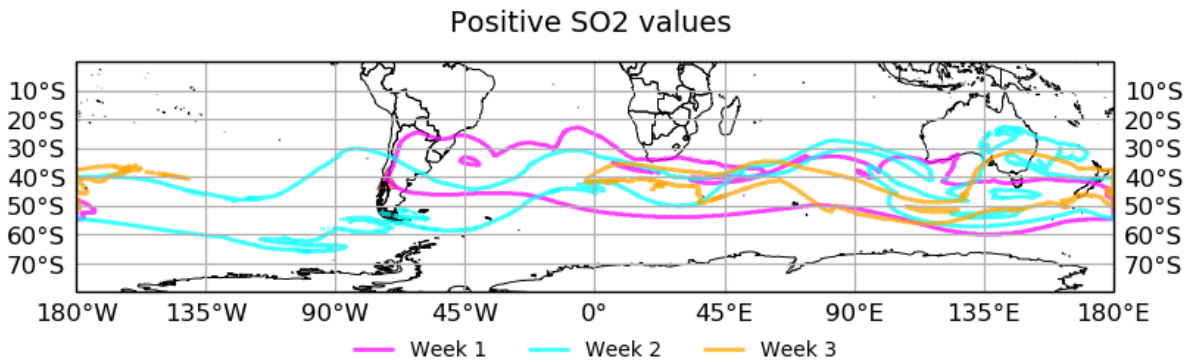

Figure 6.7c: Simulated transport of the SO_2 plume during the first 3 weeks after the eruption onset showing the location of the plume after 1 (pink line), 2 (turquoise line) and 3 (orange line) weeks, respectively.

© Crown Copyright 2021, Met Office

Kasatochi Aug 2008

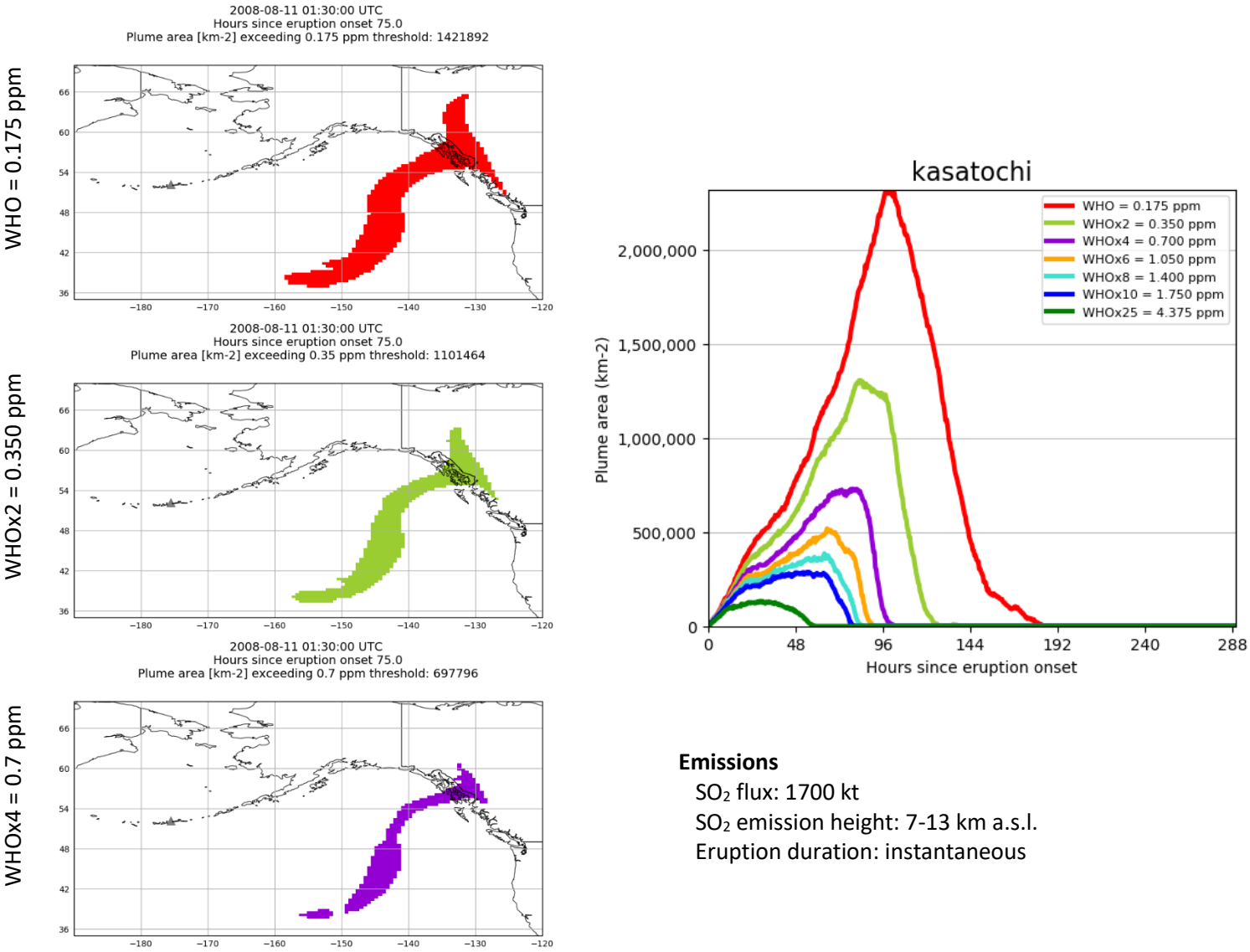

Emissions

SO_2 flux: 1700 kt

SO_2 emission height: 7-13 km a.s.l.

Eruption duration: instantaneous

Figure 6.8a: Maps and time series of the plume area (km^2) which exceeded various SO_2 concentration (ppm) thresholds for the Kasatochi 2008 eruption.

Threshold (ppm)	Number of hours exceeding threshold	Maximum plume extent (km^2)
WHO	186	2,321,411
WHOx2	138	1,306,395
WHOx4	103	730,075
WHOx6	92	518,647
WHOx8	86	386,146
WHOx10	81	288,124
WHOx25	59	132,807

Table 6.10: The number of hours exceeding the various SO_2 concentration (ppm) thresholds, and the maximum plume area (km^2), for the Kasatochi 2008 eruption.

© Crown Copyright 2021, Met Office

The Kasatochi eruption cloud resulted in several reported aircraft encounters. Guffanti et al. (2010) report that: "By 11 August 2008 when Kasatochi's cloud had begun to move over Canada and parts of the northern conterminous United States, dozens of pilots were reporting sulfurous odors in the cockpit and layers of visible haze at altitudes above about 8 km asl (about 26,000 ft km) that were thought to be ash clouds. For example, at about 01:00 UTC on 11 August 2008 the flight crew of a 757 over northern British Columbia, Canada, smelled sulfurous odor and saw a yellowish-brown haze layer from the flight deck at approximately 10 km asl (34,000 ft)."

The location of the aircraft encounter is indicated by the red star in Figure 6.8b. The modelled plume in Figure 6.8a is valid for 01:30 UTC on 11 August corresponding to the time of the aircraft encounter and shows exceedance of all 3 lowest ppm thresholds (WHO: red areas, WHOx2: green areas, WHOx4: purple areas) in the area of the aircraft encounter. The WHOx6 and higher thresholds were not exceeded in the area of the encounter (not shown). The maximum modelled ppm value in the area around the aircraft encounter is 0.77 ppm (WHOx4.4) at an altitude of 11-11.5 km. As previously mentioned, most humans are likely to smell SO_2 gas at around 5 times the WHO threshold (though this varies between WHOx0.5 and WHOx25).

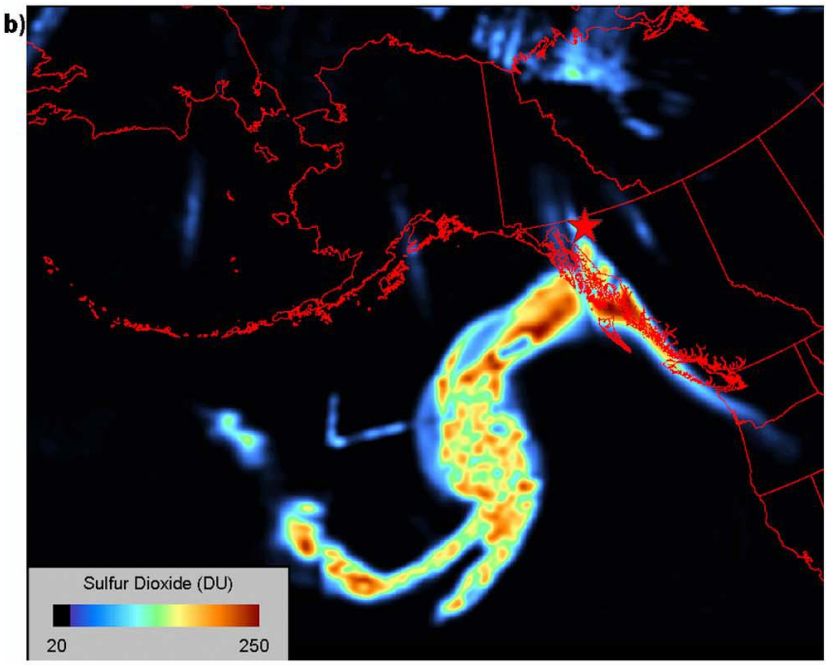

Figure 6.8b: From Guffanti et al. (2010) showing Kasatochi's SO_2 gas cloud as indicated by an OMI satellite image at 23:00 UTC on 10 August 2008. Location of the aircraft encounter over northern British Columbia is indicated by a red star.

It should be noted that for this eruption, which injected the largest amount of SO_2 into the upper troposphere and lower stratosphere (UTLS) since 1991, the satellite retrievals provided a large range of DU values (up to ~2000 DU) and a large spread in probable total amounts of SO_2 (ranging from 1 - 3 Tg). The reason that the various satellite retrievals give different estimates it that they assumed different SO_2 plume heights which strongly affect the estimated DU and total mass values, as well as dealing differently with for example non-linear effects (Clarisse et al., 2012). The NAME model simulation shown here are based on a set of satellite retrievals which lie approximately in the centre of the distribution of probable values (1.7 Tg of SO_2). However, the large spread in satellite retrieval values indicate that there are significant uncertainties related to this eruption.

© Crown Copyright 2021, Met Office

Raikoke June 2019

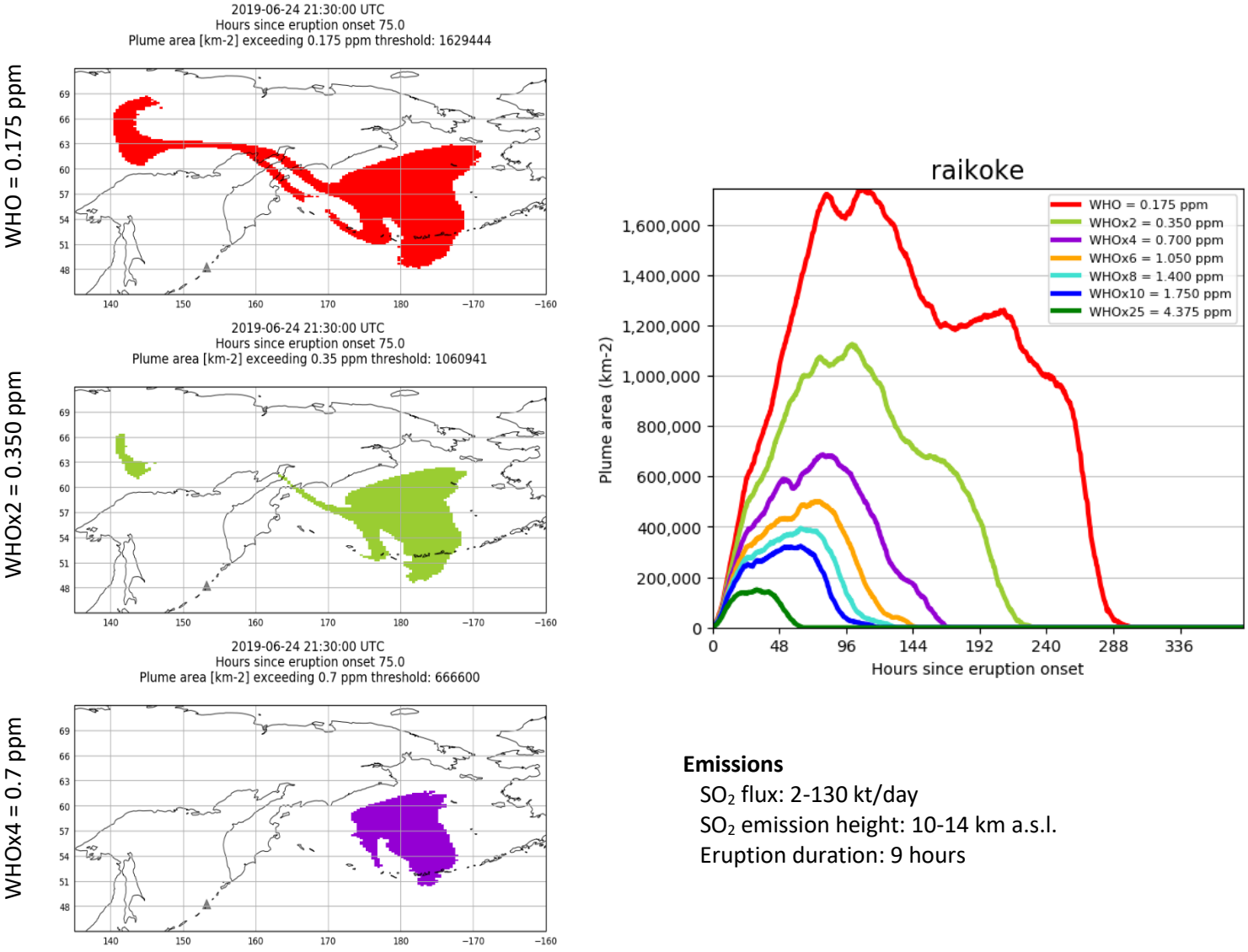

Emissions

SO_2 flux: 2-130 kt/day

SO_2 emission height: 10-14 km a.s.l.

Eruption duration: 9 hours

Figure 6.9: Maps and time series of the plume area (km^2) which exceeded various SO_2 concentration (ppm) thresholds for the Raikoke 2019 eruption.

Threshold	Number of hours exceeding threshold	Maximum plume extent (km^2)
WHO	324	1,745,551
WHOx2	238	1,125,841
WHOx4	172	1,125,841
WHOx6	149	501,852
WHOx8	134	395,469
WHOx10	121	323,823
WHOx25	66	150,878

Table 6.11: The number of hours exceeding the various SO_2 concentration (ppm) thresholds, and the maximum plume area (km^2), for the Raikoke 2019 eruption.

© Crown Copyright 2021, Met Office

6.6 Evaluation of Dobson Unit thresholds

Whilst satellite observations will likely be essential in determining when a significant SO_2 emission has occurred, applying a health threshold in Dobson Units (DU) requires a conversion between concentration in ppm and DU. DU is not a recognised unit for health impacts, and health thresholds are most often reported in volumetric or mass concentration units such as ppm or $\mu g/m^3$. DU values are a measure of vertical column abundance while ppm is a concentration measure, and as such the two are not directly interchangeable as they measure different quantities. Figure 6.10 shows how the conversion from a fixed ppm concentration to an equivalent DU value varies with plume vertical thickness and altitude. The figure shows the SO_2 vertical total column amounts in DU for an SO_2 plume with internal uniform concentration of 0.175 ppm (WHO), for different thicknesses at different heights in the atmosphere, assuming a standard atmosphere. For a fixed plume altitude, the DU value increases linearly with plume thickness. For a fixed plume thickness, the DU values increase non-linearly as the plume altitude decreases due to the fact that the volumetric SO_2 concentration in ppm becomes equivalent to higher mass concentrations (in mg/m^3) as the density of the air increases and there are more molecules in the same volume of air.

The figure shows that the conversion from ppm to DU is highly sensitive to the assumed plume altitude and thickness. The proposed concentration thresholds expressed in DU (WHO=~5 DU, WHOx10=55 DU, WHOx25=140 DU) are only applicable for a specific set of circumstances (10 km plume altitude and 1000 m thick plume thickness as defined by the VASAG). The match between the concentration thresholds and DU levels does not hold at other altitudes or depths of the plume.

Even if a good estimate for the height of the SO_2 plume was available from e.g., satellite observations or other measurements, then the plume thickness assumption is still a critical factor as Figure 9.1 shows. For an SO_2 plume at 10 km altitude, the DU levels equivalent to a concentration of 0.175 ppm vary from ~3 DU for a 500 m thick plume to about ~12DU for a 2000 m thick plume, and ~20 DU for a 3500 m thick plume. Observations of plume thickness are much sparser and more difficult to obtain than observations of plume altitude.

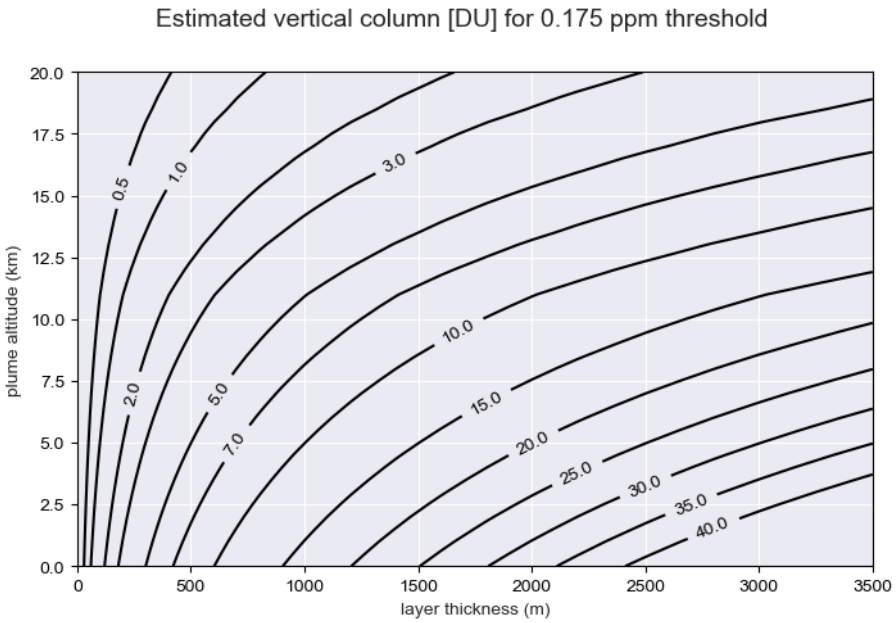

Figure 6.10: SO_2 vertical total column amounts in Dobson Units (DU; contour labels) for an SO_2 plume with internal concentration of 0.175 ppm, of different thicknesses at different heights in the atmosphere, assuming a standard atmosphere.

© Crown Copyright 2021, Met Office

Figure 6.11 and 6.12 show time series of the extent of the plume obtained by applying the proposed thresholds both in ppm and DU, for the 8 eruptions considered. For the assumption of a plume at 10 km altitude and 1 km thickness to be correct, the dashed lines (thresholds in DU) should line up close to the solid line (thresholds in ppm) of the same colour. This is the case for only a minority of the eruptions and then only for some of the thresholds and for certain periods of time, e.g., Merapi and Kasatochi. However, for the other eruptions the assumption of a 10 km plume altitude and 1 km plume thickness are incorrect (dashed and solid lines don't match) and the conversion from ppm to DU based on those specific assumptions does not hold.

For all eruptions, except Puyehue, applying the assumption of a 10 km plume and 1 km thickness to obtain the DU threshold results in a much broader plume than using the corresponding ppm threshold. In other words, the plume areas covered by the ~5 DU threshold is often much larger than the plume area covered by the 0.175 ppm threshold. This is because the actual plume altitude is lower than 10 km, or the actual plume thickness is larger than 1 km, or a combination of the two.

For the smaller eruptions (Etna, Kliuchevskoi and Fogo) the 0.175 ppm threshold (red solid line) is closer to the 11 DU threshold (green dashed line). This is because the plume altitudes for these eruptions are closer to 5 km. From Figure 6.10 we find that for a plume with concentrations of 0.175 ppm, a plume altitude of 5 km and plume thickness of 1 km we obtain a value of ~10 DU.

These results show that the use of a threshold in Dobson Unit (DU) is complicated as it is highly sensitive to the height and thickness of the SO_2 plumes. Therefore, a single DU threshold does not equate to a fixed concentration and cannot be applied equally to all eruptions. DU observations can only be converted to concentrations when observational constraints on both plume height and thickness are available, and with an accompanying look-up table for selecting the appropriate DU threshold based on the plume observations. Suitable observational data will need to be available for various parts of the plume, as the altitude and thickness can vary across the plume. Constraining plume thickness is particularly challenging as there are very limited measurements of this available.

In summary, a threshold in Dobson Unit (vertical column abundance) is complicated, as a single threshold cannot be applied to all eruptions or even for all times and locations in a single eruption, and as such the use of a DU threshold is not advised.

© Crown Copyright 2021, Met Office

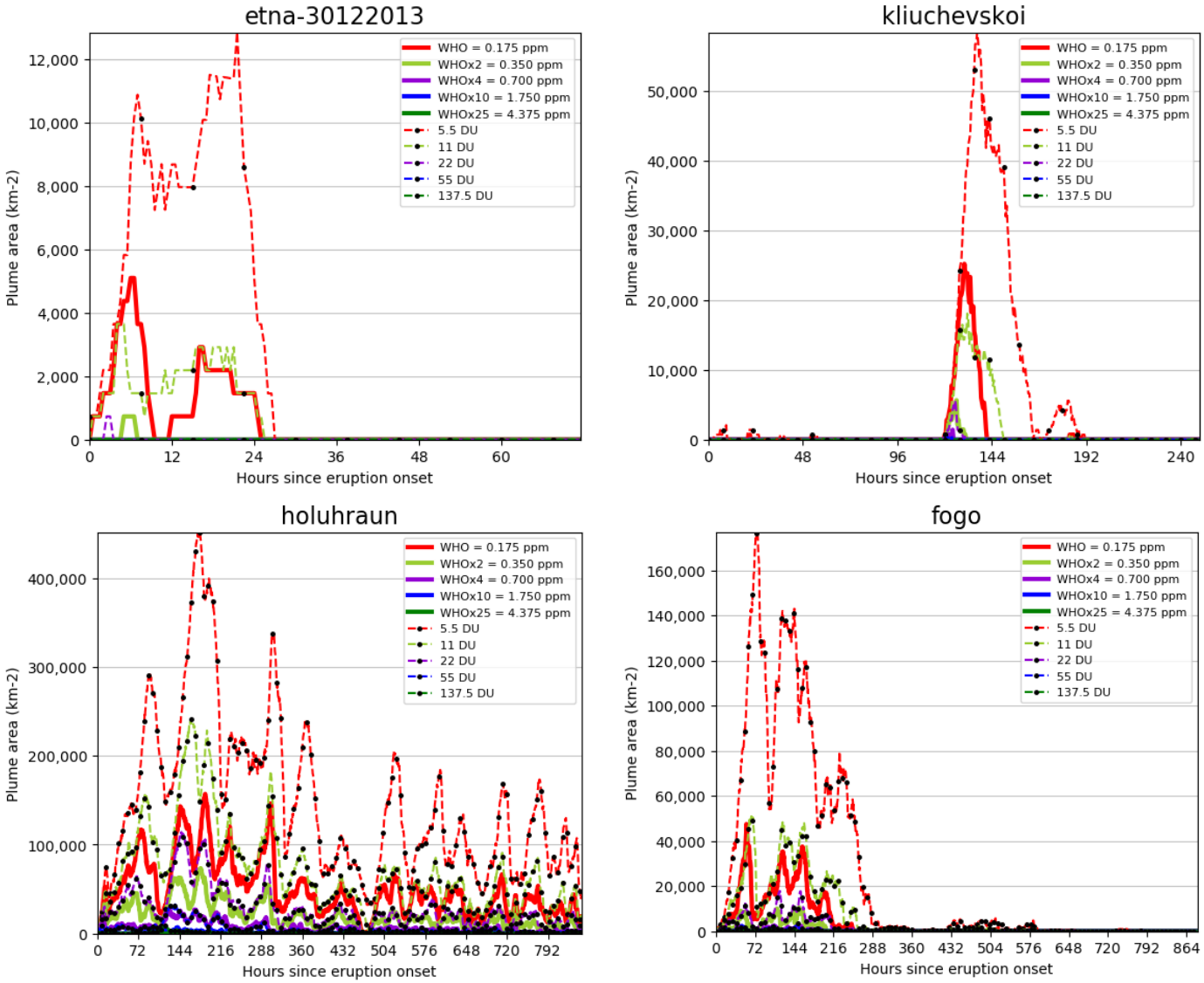

Figure 6.11: Time series of the plume area (km^2) which exceeded various SO_2 ppm and Dobson Unit (DU) thresholds for the Etna, Kliuchevskoi, Holuhraun and Fogo eruptions.

© Crown Copyright 2021, Met Office

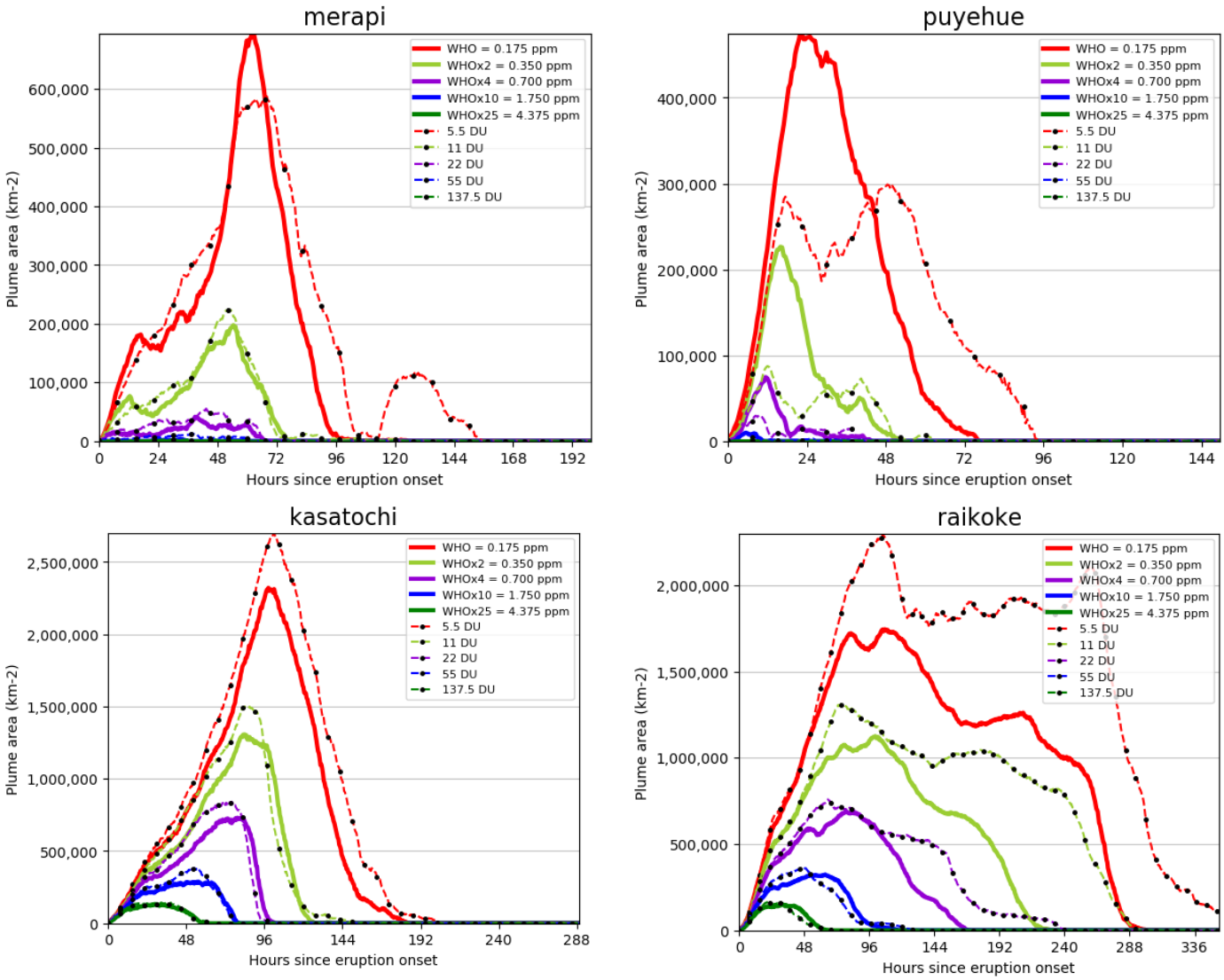

Figure 6.12: Time series of the plume area (km^2) which exceeded various SO_2 ppm and Dobson Unit (DU) thresholds for the Merapi, Puyehue, Kasatochi and Raikoke eruptions.

© Crown Copyright 2021, Met Office

6.7 Comparisons of SO_2 and ash plume extents

Comparisons of the SO_2 and ash plume extents for a few of the eruptions considered in the assessment have been made. The results for Raikoke are included in Figure 6.13. The volcanic ash plume extent is shown by the issued volcanic ash advisory (VAA) polygons (black dashed line) overlaid on the SO_2 plume extent for the lowest threshold (WHO: 0.175 ppm; red area).

There is no dominant plume extent, i.e., the SO_2 plume extents are at times smaller than the ash plume extent, and other times larger. This is also the case for the other eruptions considered (not shown).

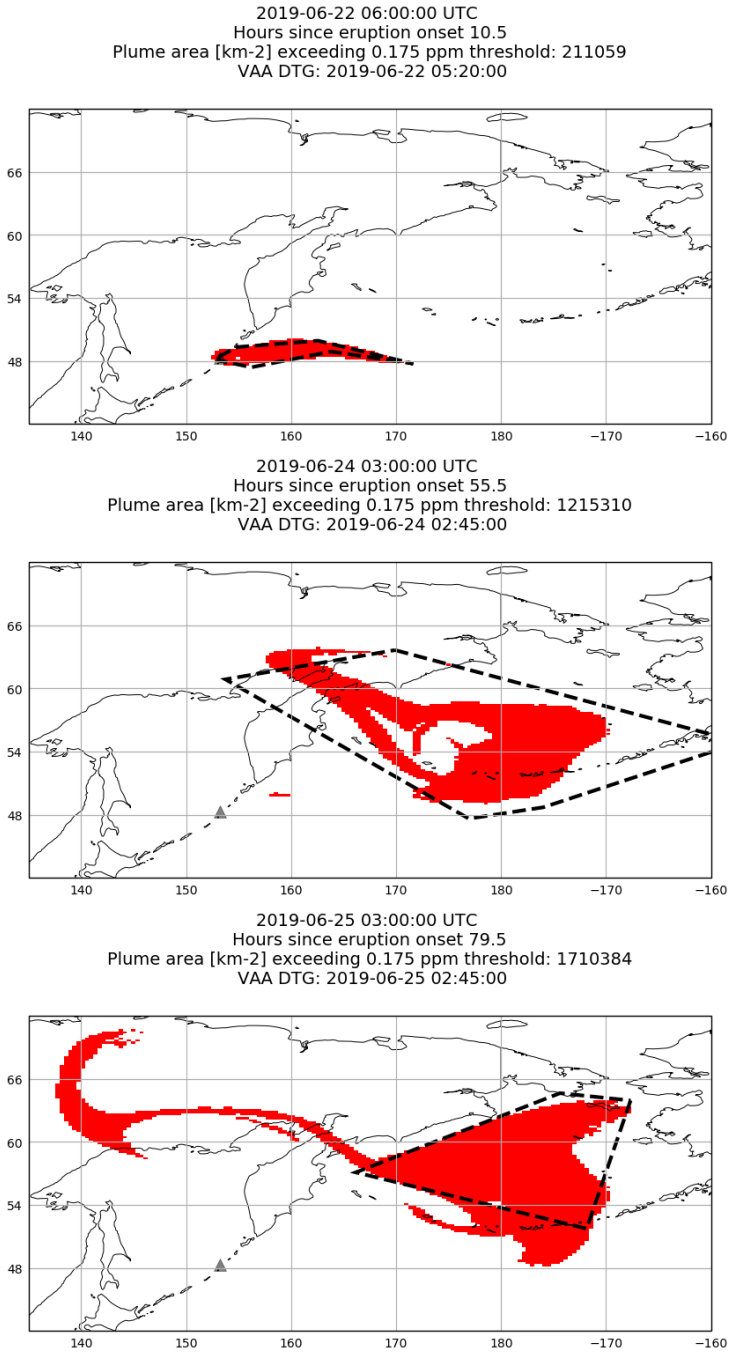

Figure 6.13: Comparison of SO_2 plume extent (red area) and the issued volcanic ash advisory (VAA) polygon (black dashed line) for the Raikoke June 2019 eruption.

© Crown Copyright 2021, Met Office

6.8 Summary

The time period and area over which the SO_2 thresholds are exceeded strongly depends on the eruption characteristics (the amount, duration and height of the SO_2 which is released). Eruptions which release large quantities of SO_2 over a short period of time and at high altitudes give the most extensive plume areas and duration of exceedance. Effusive eruptions which release SO_2 over a significant period of time can lead to prolonged time periods of exceedance, but emissions from this type of activity is generally at lower altitude where SO_2 is removed from the atmosphere more efficiently than at higher altitudes, and the plume exceedance areas are therefore smaller.

Applying the WHO threshold (0.175 ppm) can result in large areas of the plume exceeding this threshold as shown in Figure 6.14 and Table 6.12. For the two largest, explosive eruption case studies considered here (Kasatochi and Raikoke) the vertical dashed lines in Figure 6.14 show the time when the last VAA was issued, indicating that after 5 days the volcanic ash was no longer expected to be an aviation hazard. However, the SO_2 concentrations exceed the WHO threshold for much longer. The difference is partly due to the longer atmospheric residence time of volcanic SO_2 compared to volcanic ash. This is illustrated for the Kasatochi eruption in Figure 6.15 which shows that the amount of ash in the atmosphere, as determined from satellite data, rapidly declined during the first few days after the eruption, while there was still a detectable amount of tropospheric SO_2 left after a week.

Figure 6.16 summarises the results for all eruptions when applying the six higher thresholds (WHOx2-WHOx25) and illustrates the impact of using higher thresholds compared to WHO (Figure 6.15). Table 6.13 and 6.14 show the percentage decrease of the plume areas and time periods over which the six thresholds are exceeded relative to the WHO threshold. This shows that by applying the WHOx2 threshold the maximum plume extent is reduced by ~40% for the two largest eruptions (Raikoke and Kasatochi) while the number of hours exceeding the threshold is reduced by 26% for these large events. Applying the WHOx6 threshold reduces the maximum plume extent by ~70-80% for the two large eruptions, and the number of hours exceeding the threshold is reduced by ~50%. For the moderate size explosive eruptions (Merapi and Puyehue) these reductions are even larger.

Figures 6.17 and 6.18 illustrate the difference in the spatial extent of the cumulative SO_2 plume area exceeding each of the seven SO_2 concentration thresholds for the Raikoke and Puyehue eruptions, respectively. Note that the cumulated area shows the total plume area exceeding a given threshold summed over the entire model simulation period and not on a single day.

It is apparent from these results that SO_2 advisories based on the WHO threshold are likely to cover a larger area and for a longer duration than the equivalent ash advisories for the minimum Quantitative Volcanic Ash (QVA) concentration. Whilst we cannot provide advice on the appropriateness of the other thresholds with respect to health or engineering endpoints, the results illustrate that using higher thresholds changes the impacts on airspace and reduces the areas covered. This suggests that a multiple threshold approach similar to that being introduced for QVA would be worth considering. If the WHO threshold is taken as the minimum concentration threshold, appropriate additional thresholds based on this work could be placed between WHO and WHOx6 (just above the average human odour threshold). A multi-threshold approach could allow various actions to be considered, similar to the Safety Risk Assessment approach to that introduced in Europe for volcanic ash. Further consideration of this and the relevance of other thresholds is needed by the WG-MISD.

© Crown Copyright 2021, Met Office

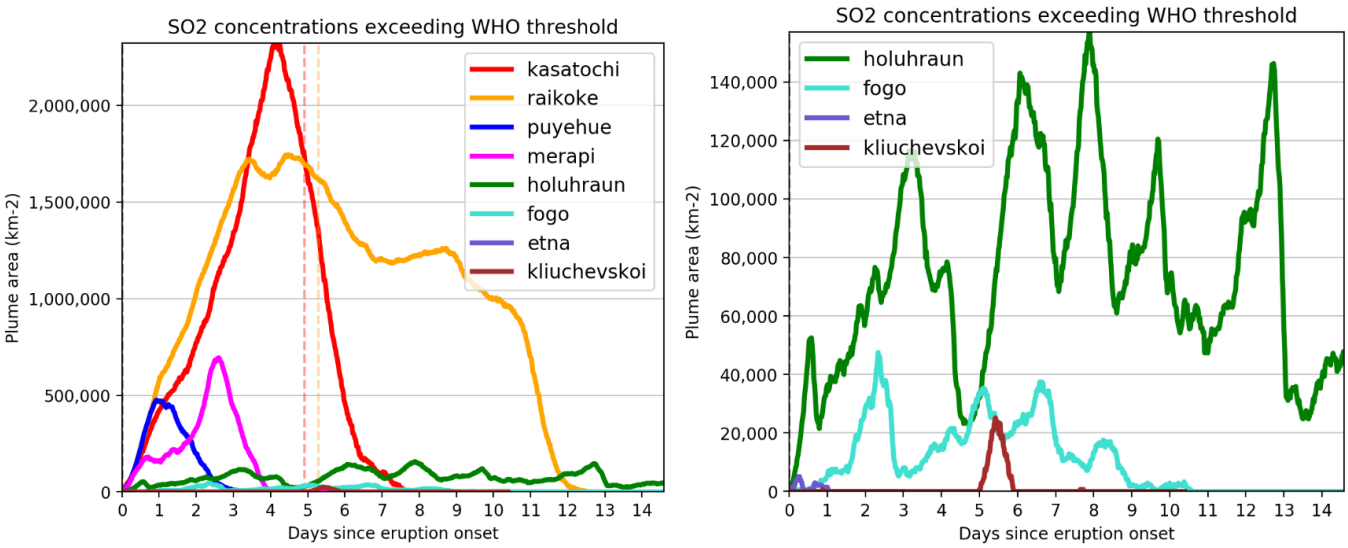

Figure 6.14: Time series of the plume area (km^2) which exceeded the WHO SO_2 ppm threshold for (left) all eight eruption considered in the assessment, and (right) a zoom-in for the four small eruptions.

Volcano	**Number of days exceeding WHO threshold**	**Maximum plume extent (km^2)**
Etna	1	5100
Kliuchevskoi	1	25,177
Merapi	5	694,526
Puyehue	3	474,896
Kasatochi	8	2,321,411
Raikoke	14	1,745,551
Holuhraun	35*	157,085
Fogo	12*	47,563

Table 6.12: The duration and maximum plume extent for exceedance of the WHO threshold, for all eruptions considered. *Effusive eruptions with continuous release over many days.

© Crown Copyright 2021, Met Office

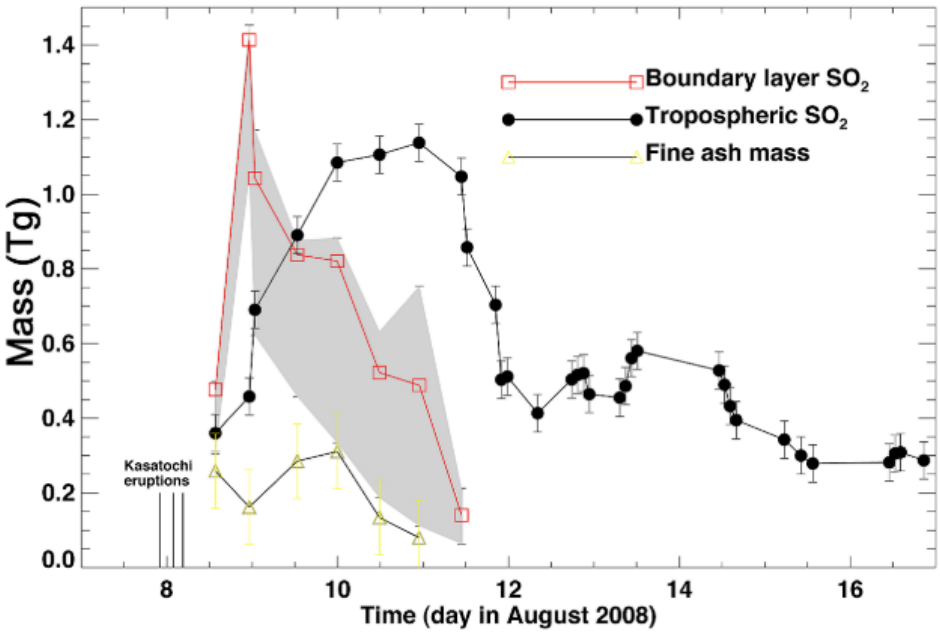

Figure 6.15: The variation of SO_2 and ash mass with time for the first 7 days after the Kasatochi eruption, determined from satellite data. Note that the satellite observations of volcanic ash are limited after a few days when the ash clouds are thin and dispersed. Figure from Prata et al. (2010).

	Etna	Kliuchevskoi	Holuhraun	Fogo	Merapi	Puyehue	Kasatochi	Raikoke
WHOx2	86%	78%	53%	78%	72%	52%	44%	35%
WHOx4	-	94%	82%	95%	94%	84%	69%	35%
WHOx6	-	-	89%	98%	98%	93%	78%	71%
WHOx8	-	-	93%	99%	99%	97%	83%	77%
WHOx10	-	-	95%	99%	99%	98%	88%	82%
WHOx25	-	-	99%	-	-	-	94%	91%

Table 6.13: Percentage reduction in maximum plume extent relative to the WHO threshold.

	Etna	Kliuchevskoi	Holuhraun	Fogo	Merapi	Puyehue	Kasatochi	Raikoke
WHOx2	91%	54%	0%	32%	44%	31%	26%	26%
WHOx4	-	87%	2%	59%	43%	43%	45%	47%
WHOx6	-	-	18%	83%	51%	60%	51%	54%
WHOx8	-	-	35%	95%	67%	78%	54%	59%
WHOx10	-	-	54%	99%	79%	89%	56%	63%
WHOx25	-	-	94%	-	-	-	68%	80%

Table 6.14: Percentage reduction in number of hours exceeding the threshold relative to the WHO threshold.

© Crown Copyright 2021, Met Office

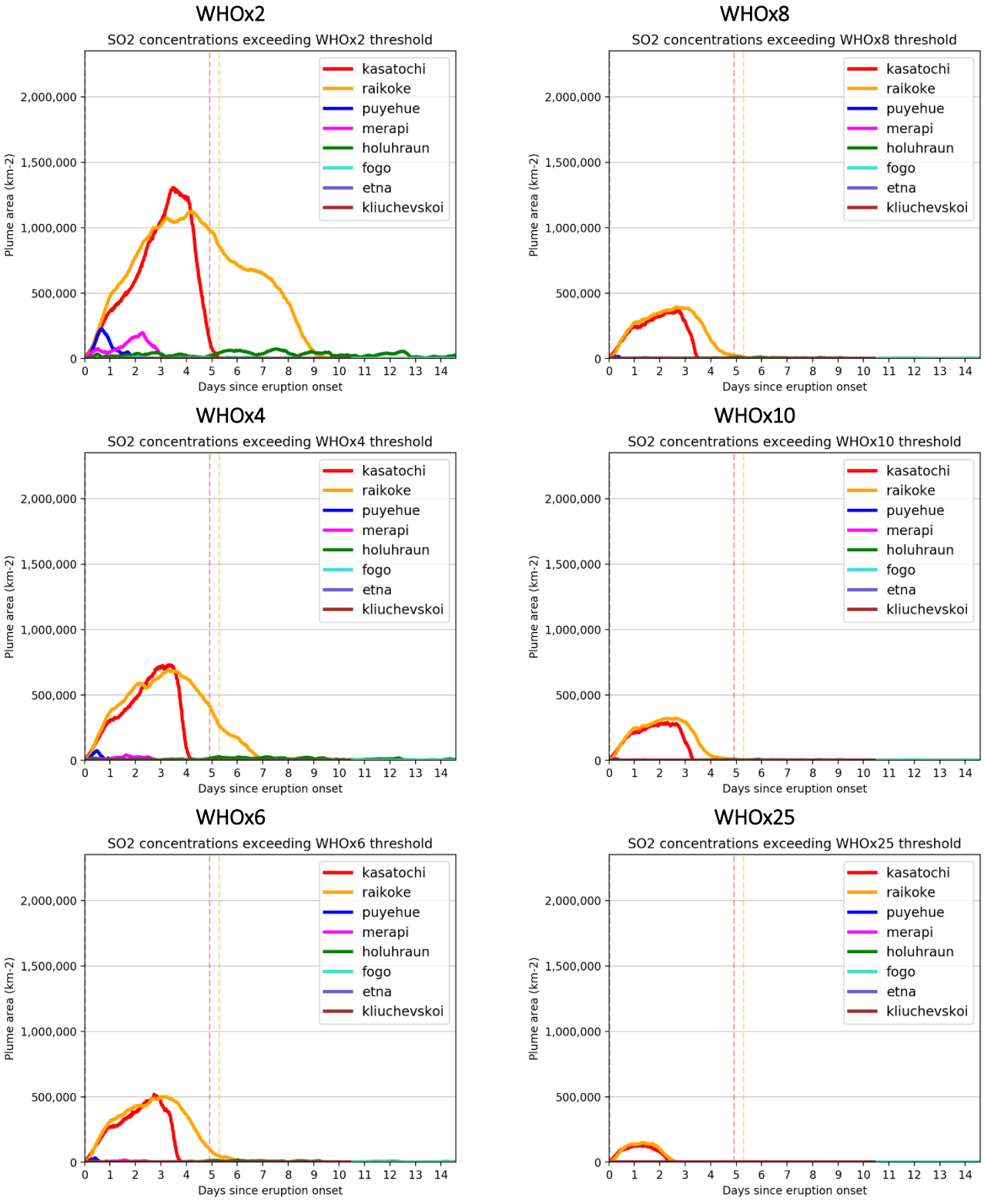

Figure 6.16: Time series of the plume area (km^2) which exceeded various SO_2 ppm thresholds.

© Crown Copyright 2021, Met Office

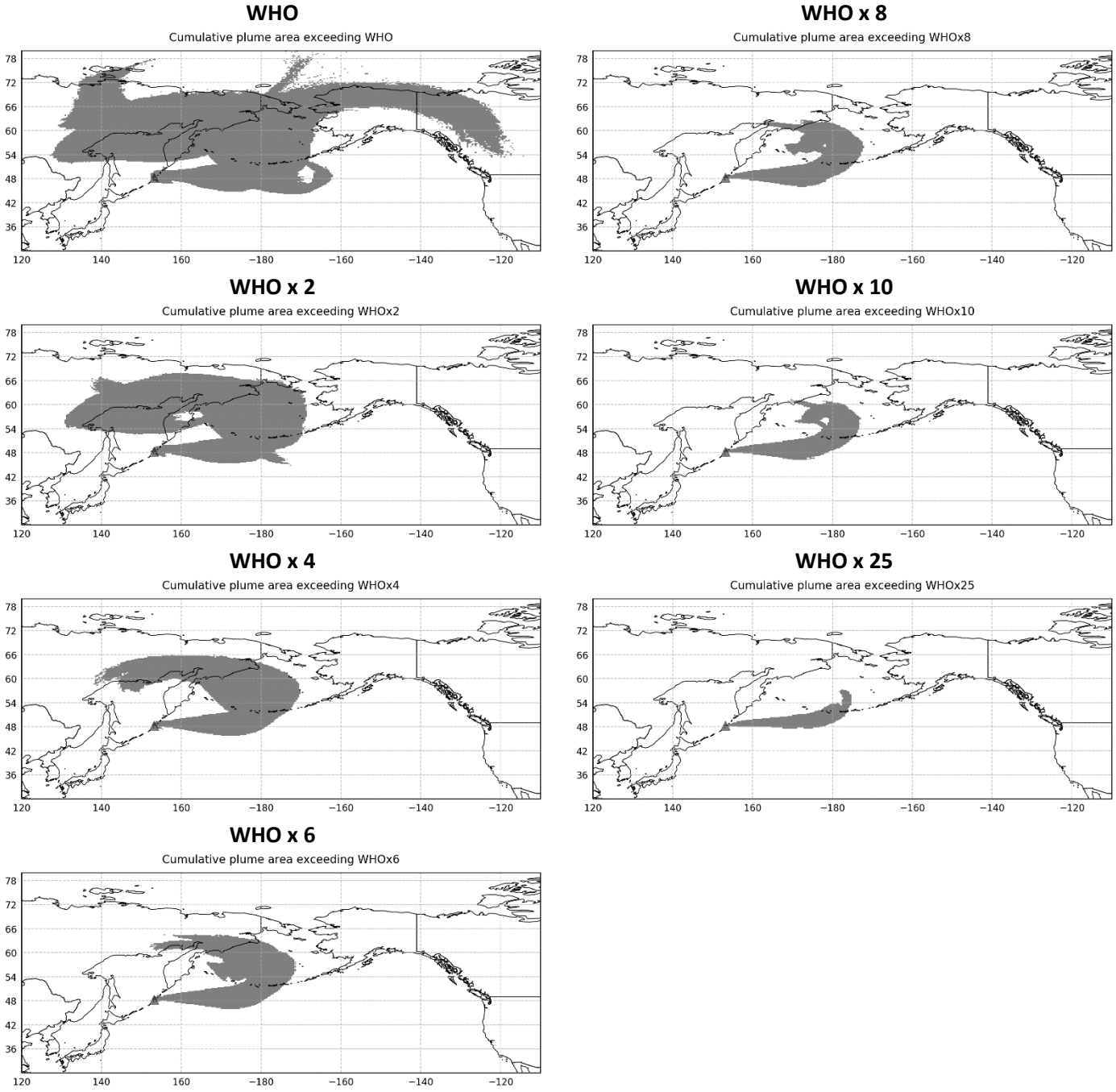

Figure 6.17**:** Cumulative SO_2 plume area exceeding each of the seven SO_2 concentration thresholds for the Raikoke eruption. The cumulated area shows the total plume area exceeding a given threshold summed over the entire model simulation period (and not on a single day).

© Crown Copyright 2021, Met Office

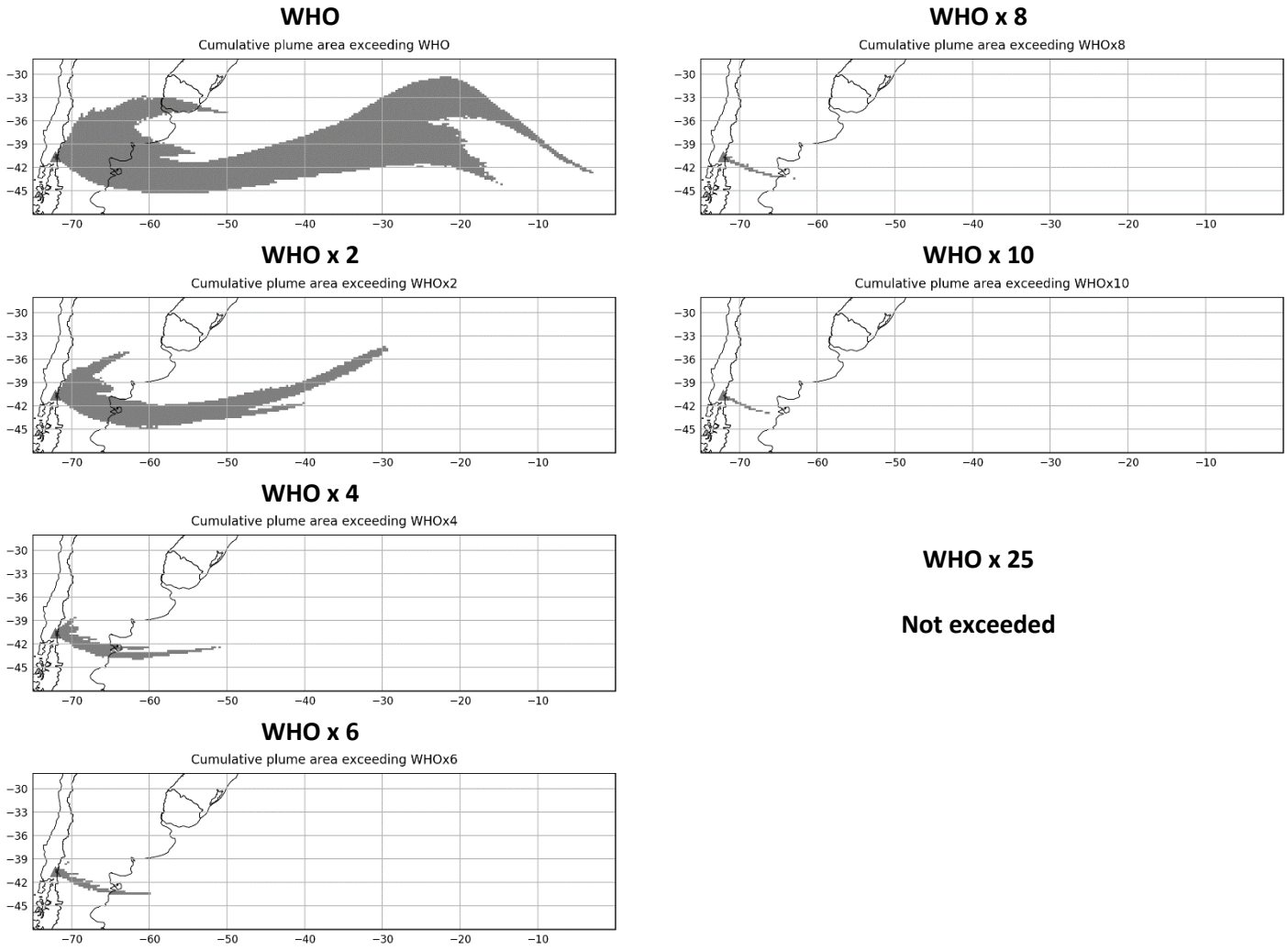

Figure 6.18**:** Cumulative SO_2 plume area exceeding each of the seven SO_2 concentration thresholds for the Puyehue eruption. The cumulated area shows the total plume area exceeding a given threshold summed over the entire model simulation period (and not on a single day).

© Crown Copyright 2021, Met Office

7 Forecasting Systems

A forecasting system must be able to deliver timely, accurate, robust, up-to-date information multiple times per day. To produce an optimal operational forecast of the presence of volcanic SO_2 in the atmosphere a forecasting system must make the best possible use of observations and use an accurate model to predict the onwards transport, dispersion, and removal of the gas. The forecast products generated will need to meet the requirements of the aviation industry. Many of the requirements needed to deliver a volcanic SO_2 forecast are the same as those for a volcanic ash forecast, however there are some differences and practical considerations which will need to be addressed to set up a new service.

7.1 Detection and Communication

Lines of communication to disseminate information on the presence of volcanic SO_2 in the atmosphere to the responsible forecasting centre will be required. It is currently the responsibility of the volcano observatories to provide time-evolving observations of volcanic ash eruptions to the responding VAAC(s). This information is provided in the Volcano Observatory Notice for Aviation (VONA), which includes information on the location and summit height of the erupting volcano, timings of the event (start and end times, and pauses in activity) and the plume height, if available. Consultation will be needed on whether the current communication framework for volcanic ash clouds is also appropriate for volcanic SO_2 forecasting, and whether the VONA in its current form could be used to record information on the releases of SO_2. Given the potential for volcanic SO_2 to be transported significant distances, information from local responding volcano observatories may need to be disseminated to a central data repository, to allow individual centres access to data in a common format.

It should also be remembered that many of the world's volcanoes remain un-monitored at ground-level. As such, consideration should be given to the use of a global satellite observation system for detection and communication, such as the Support to Aviation Control Service (SACs) and the NOAA/CIMSS VOLCAT system, which deliver automated near real-time alerts on SO_2 and volcanic ash clouds (Brenot et al., 2014, Pavalonis et al., 2018), see Section 4 for further discussion on these services. Data from satellite retrievals may also be used to initialise the modelling system through direct data assimilation. This avoids the need to manually set eruption parameters at the source, but there are still limitations with this approach, as discussed in Section 5.

7.2 Forecast Delivery

If we assume that volcanic SO_2 forecasts will, at a minimum, need to meet the same requirements as volcanic ash forecasts (Table 3.3) then the forecasting system will need to:

- Provide forecasts with a temporal resolution of 3 hours that are updated every 6 hours.
- Depict concentrations with a vertical resolution of 50FL, between the surface and 5000 ft (FL600). As SO_2 does not sediment (fall out of the atmosphere due to gravity), releases from high altitude explosive eruptions may remain above this maximum flight level.
- Forecasts could also benefit from indicating the top height and depth of the SO_2 cloud.
- Track the volcanic SO_2 cloud over its entire lifetime. Volcanic SO_2 can reside in the atmosphere for much longer than volcanic ash (several weeks), as such volcanic clouds containing significant quantities of SO_2 can travel greater distances from the volcano (see Section 6). The period over which advisories need to be issued may be much longer than for a volcanic ash event, and predictions might need to be delivered on a global scale.

© Crown Copyright 2021, Met Office

Some consideration should be given to the area of responsibility of the responding operational centre. Volcanic SO_2 clouds can encircle the globe; to provide an optimal forecast the model simulations must track the meteorological and chemical processes along its path, which dictate its location and concentration in the atmosphere. The issuance of consistent advice can prove challenging when volcanic clouds reside over multiple VAAC areas. Given the longevity of volcanic SO_2 this may prove to be a more frequent occurrence than for responses for volcanic ash clouds.

Forecast products (advisories and/or data) generated by an operational modelling system will need to meet the requirements of the aviation industry, e.g., depicting regions with concentrations above defined critical thresholds. For a quantitative assessment of SO_2 concentrations, consideration of the output units will be required. Concentrations of SO_2 can be expressed as an atmospheric column load in Dobson Units (DU), in units of mass per volume (e.g., $\mu g\ m^{-3}$) or in volumetric units such as parts per million (ppm). In Section 6 suitable threshold concentration values and units are discussed, and it is shown that model output must be able to provide concentrations of SO_2 in the atmosphere in ppm, for all levels in the atmosphere.

Predictions of the transport and dispersion of any pollutant in the atmosphere always suffer from uncertainties in the forecast meteorology, the representation of atmospheric processes in the model, and the source parameters. Following the proposed Initial Operating Capability requirements for quantitative volcanic ash products, we suggest that a future SO_2 service would also need to generate probabilistic output, for example with ensemble meteorology and source parameter datasets to capture uncertainty. Forecast products will need to be carefully designed to communicate this information, for example issuance of 'Percentage Probability of Exceedance' for each of the concentration threshold(s).

Finally, any future forecasting system would benefit from near real time validation with well constrained observations of volcanic SO_2 to ensure their accuracy, see further discussion in Section 8.

© Crown Copyright 2021, Met Office

8 Forecast Trial

To test the components identified and described in the preceding sections, a 4-day trial of a global volcanic SO_2 forecast was conducted in April 2021. Two eruptions from 2021 were considered as part of the trial: Etna, Italy and La Soufriere, St Vincent. Internal and external tools and data available at the times of these eruptions and in the week of the trial were used to assess the readiness status of the components of a global volcanic SO2 forecast. These included existing automated alerting systems to inform that an eruption has started, satellite detection and retrieval products for volcanic plumes, SO_2 flux estimation techniques, atmospheric models, and general information shared via subject-specific email lists and respected Twitter accounts. A summary of the tools and data used is provided in Table 8.1 and detailed descriptions of most have been provided in the rest of this report. The NAME model (de Leeuw et al. 2021) was used for all the forecast simulations, but the findings are generally applicable to similar models. Information on the model set-up is provided in Table 8.2.

Satellite data were a key component of the response and both Geostationary (GEO) sensors and Low Earth Orbit (LEO) sensors were utilised. GEO sensors, such as SEVIRI, have the advantage of high temporal frequency updates of the same area. LEO sensors such as TROPOMI and IASI are generally more sophisticated, having more channels in the ultra-violet (UV) or infrared (IR), and hence provide improved detection and quantitative data for SO_2, but only overpass an area once or twice a day.

We note that no specific development of capabilities was conducted ahead of the trial and that current data availability and access is not a guide to any future developed service. Also, that currently different National Meteorological Services will have access to different and/or additional tools/data. The trial was designed to explore the basic feasibility of a forecast using the components identified in this report. The findings of the trial are designed to inform what an operational capability would require and identify areas needing further development, it does not reflect levels of practicality and should not be interpreted as a test of a basic service.

A summary of the actions and approach used in responding to each eruption is provided in the following sections. The overarching findings and their implications are then discussed.

Data/Tool	**Etna**	**La Soufriere**
Alerts	VONA from INGV SACS VAA from VAAC Toulouse	VOLCAT SACS VAA from VAAC Washington
Satellite Data	TROPOMI (SACS, Met Office, Twitter) IASI (Met Office, SACS, Twitter) MSG SEVIRI (Met Office SO_2 retrieval) VIIRS (VOLCAT)	VIIRS (VOLCAT) TROPOMI (SACS, Twitter, email) IASI (SACS, Twitter, email) GOES-16 ABI (VOLCAT) AIRS (Twitter, email) CALIOP (email)
Social Media and email lists	Twitter	ssircvolcano email list volcanicclouds email list Twitter
Model(s)	NAME in a limited area configuration 10km NWP from MetUM	NAME in a limited area configuration 10km NWP from MetUM
Data fusion information	PlumeTraj (University of Manchester/VPLUS project)	C-IFS data assimilation (via Windy.com)

Table 8.1: Summary of the data and tools used for the eruptions considered in the trial.

© Crown Copyright 2021, Met Office

Set-up variable	Etna	La Soufriere
Domain size	10°E - 60°E 20°N - 50°N	70°W – 30°E 5°S – 25°N
Horizontal grid resolution	0.15° x 0.1° (lon, lat)	0.4° x 0.4° (lon, lat)
Vertical Extent	23 km agl	23 km agl
Particle release rate	500,000 per hr	50,000 per hr
Emission duration	2 hr 36 min	Continuous
Total number of Lagrangian particles	1.3 million	For a 24-hr forecast issued ~36 hrs after the start: ~3 million
Output concentration averaging period	1 hour	1 hour

Table 8.2: The NAME atmospheric dispersion model at v8.0 was used in both case-studies with different limited area domains. The Lagrangian framework was used, together with the atmospheric chemistry scheme. The only emitted species in all the simulations was sulphur dioxide, with background concentrations of hydrogen peroxide and ozone also initialised.

8.1 Case-study 1: 28 Feb 2021 eruption of Etna

The eruption of Etna on 28 February 2021 (Figure 8.1) was one of a sequence of eruptions during the early part of 2021. These relatively small eruptions are known as paroxysms due to their sudden, short bursts of explosive activity. This particular paroxysm was chosen due to long-range detection of the SO_2 plume by satellite sensors in the following days. Etna is a well-studied volcano with a sophisticated volcano observatory, so this was considered a good example of an eruption where a lot of information and observations would likely be available.

Two attempts at producing an SO_2 forecast for the eruption were made. The first represented the information that was available at 09:30 UTC on 28 February in the first 1-2 hours after the eruption. The second represented information available ~6 hours later at 16:00 UTC. These are hereafter referred to as Forecast1 and Forecast2. Table 8.3 contains the eruption source parameters used for the model in each forecast.

At 09:30 UTC the information available comprised:

- Two VONA issued by INGV (Istituto Nazionale di Geofisica e Vulcanologia) as the State Volcano Observatory (SVO) for Etna. The first at 08:11 UTC confirming the start of activity and reporting a volcanic cloud height of “around 6 km”. The second at 08:35 UTC stating that the “estimated volcanic cloud height is more than 9 km at the top” and that the ash cloud was moving toward the east.
- Two VAA/VAG issued by VAAC Toulouse at 08:31 and 09:16 UTC. The second states “ash cloud height estimated around FL330”.
- Geostationary satellite images from the SEVIRI instrument on MSG generated using the Met Office’s SO_2 detection and retrieval algorithms.
- An IASI overpass at 08:39 UTC processed by the Met Office showing the start of an SO_2 plume at the location of Etna (very few pixels).
- Radiosonde data from Sicily showing that the wind direction above 6 km was to the east, but below this was to the south.

No automated alerts had been received and no information on SO_2 mass flux was available at this time. Based on in-house familiarity with previous eruptions of Etna (including work done as part of this report) and the pattern from the recent preceding paroxysms, the forecast-trial team chose to set an eruption duration of 2 hours and a total erupted mass of 10 kt of SO_2. An emission height

© Crown Copyright 2021, Met Office

range of 6-10 km was set based on the information provided in the VONA and the assumption that SO_2 is usually emitted at the top of an eruption column.

ESP	Forecast1 (09:30)	Forecast2 (16:00)
Volcano location	Etna summit	Etna summit
Start time (UTC)	08:11	08:11
Stop time (UTC)	Start time + 2 hrs	10:47
Emission height range	6-10 km asl	10-12.5 km asl
SO_2 emission mass	10 kt	14 kt

Table 8.3: Eruption source parameters (ESP) used to initialise the NAME model for the two forecasts. See text for details on how these were decided.

Figure 8.1: Photo of the 28 February 2021 Etna eruption from the west (@parrinelloluigi on Twitter).

At 10:47 UTC a VONA was issued implying that the main explosive phase had finished. At 12:57 UTC an automated alert from the SACS (Support to Aviation Control) service was received by email which contained an estimated plume mass loading of 13.879 kt SO_2 based on a TROPOMI overpass at 11:18 UTC. These two pieces of information confirmed the validity of the starting assumptions for Forecast1 for the duration and mass emitted. In a real situation the responsible forecast centre would likely have generated updated forecasts based on these data as they were received. Here we waited slightly longer, because by 16:00 UTC (~8 hours after the eruption start) visual comparison of hourly forecast data to 15-minute geostationary imagery revealed a growing divergence in the location of the forecast plume compared to observations (Figure 8.2). The location of the front of the forecast plume to the east lagged the transport of the observed plume and was located slightly further south. A forward trajectory run was conducted using the NAME model to evaluate wind directions every kilometre above sea level from 9 to 13 km. This showed that the winds at 10-13 km were a much closer match to the direction of travel seen in the satellite observations than those at 6-9 km. Consequently, for Forecast2, the emission height range was raised (Table 8.3).

© Crown Copyright 2021, Met Office

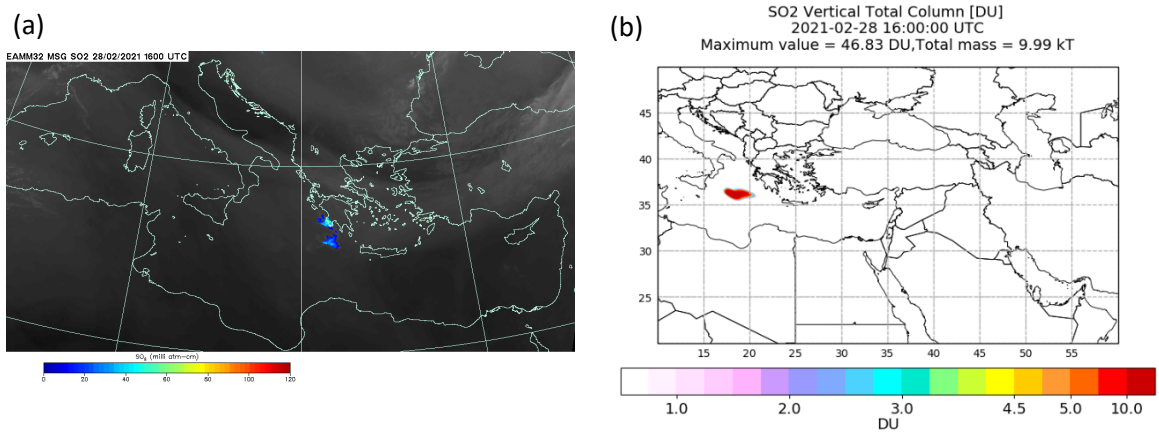

Figure 8.2: Location of the Etna SO_2 plume at 1600 UTC in (a) the MSG SEVIRI retrieval and (b) the Forecast1 model simulation.

With the benefit of later satellite observations being available at the time of the trial, evaluation of the Forecast1 results against later observations confirmed the poor match, with the model plume clearly diverging geographically from satellite observations 10-12 hrs after the eruption start. The Forecast1 plume travelled south-east over Africa, whereas the observed plume travelled closer to Cyprus and across the eastern end of the Mediterranean. The Forecast2 simulation, with revised height, end-time, and emissions, gave a much better agreement.

It is worth noting that the first high-resolution low earth orbiter (LEO) data to help visually constrain the longer-range transport uncertainty (using traditional human comparison techniques) were not available until a 19:05 overpass from IASI. This is approximately 11 hours after the start of the eruption. This is because the plume in the 11:18 TROPOMI imagery was small in extent and similar enough to the modelled plume that any gross errors in the forecast plume could not be seen by eye. New data-fusion techniques provide the opportunity to reduce this time gap and utilise information from early overpasses. To explore what might be possible in the future if real-time data feeds were developed, we engaged with researchers in the VPLUS project (UK NERC research project, University of Manchester) ahead of the forecast trial. They provided additional supplementary data for the 28 February using PlumeTraj (Queißer et al. 2019), see Section 4.1 for details of this technique. These time and height resolved emissions data were based on the same TROPOMI overpass at 11:18 UTC that was reported in the SACS alert and had a total emission of 14 kt. The forecast simulation with the PlumeTraj input produced results similar to Forecast2, but with better definition of some features early on, which translated to improved longer term positioning of the outer plume edge (Figure 8.3).

In a final step, the WHO SO_2 threshold of 0.175 ppm was applied to the forecast data. Using the PlumeTraj initialised simulation as the best estimate, the threshold is exceeded for approximately 20 hours and reaches the eastern end of the Mediterranean at 36° E (although only covers a very small area by this time). For a period, the island of Crete is completely covered. In contrast, the VAA/VAG issued by VAAC Toulouse specifies no ash after 18:00 UTC (~10 hours from eruption start) and only extends to 17.5° E. This confirms the conclusions in Section 5 that even for small eruptions, forecasts for SO_2 based on the WHO threshold could last longer in duration and cover a wider area than the corresponding VAA/VAG. The plume from the eruption remained detectable by satellites for considerably longer, reaching Japan on the 4 March and the west coast of the USA on 6 March. It finally dropped below detection levels on 10 March just prior to reaching the UK. A train of SO_2 plumes from subsequent Etna eruptions can also be seen following behind in the global SO_2 satellite

© Crown Copyright 2021, Met Office

data. This provides strong support for adopting a quantitative forecast approach, rather than a qualitative “detectable” approach.

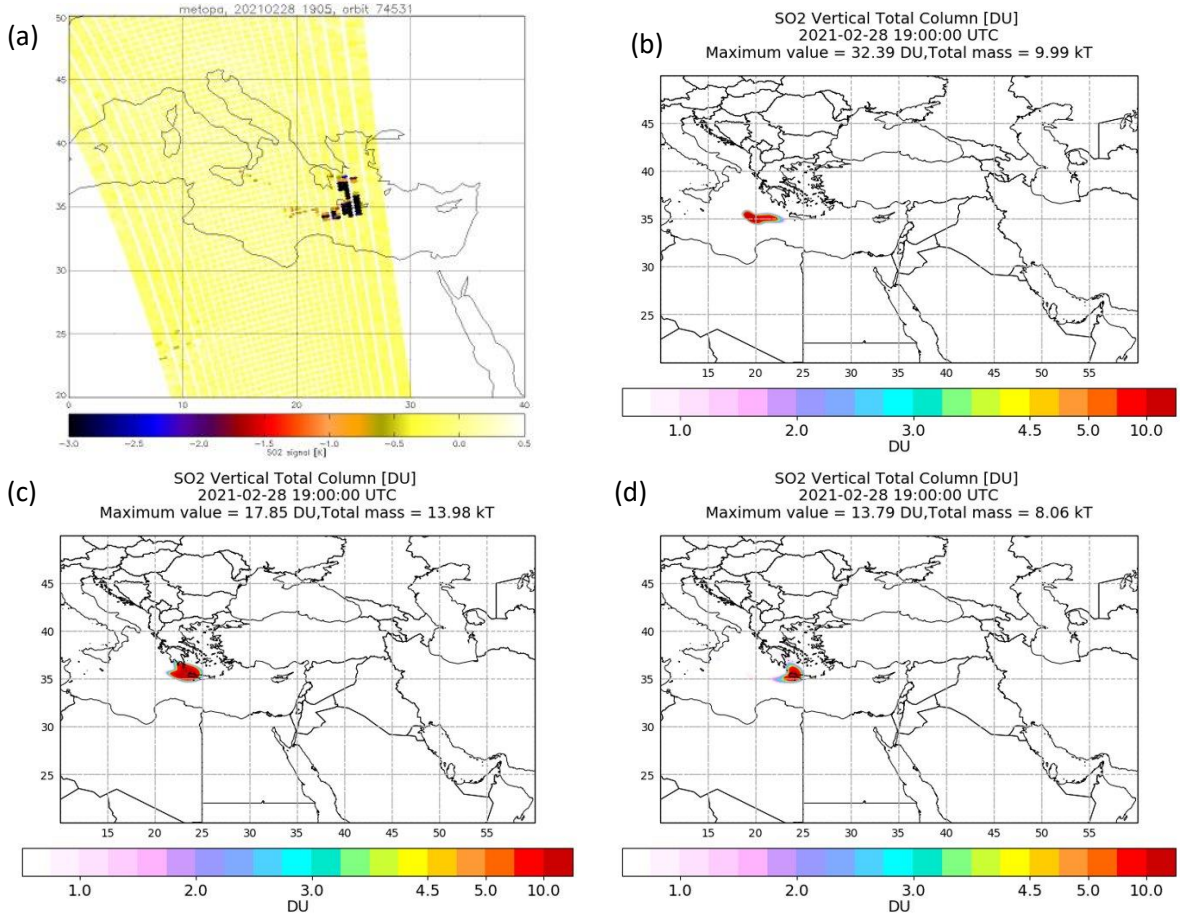

Figure 8.3: Comparison of (a) the IASI overpass at 19:05 UTC to the output from the three simulations at 19:00 UTC: (b) Forecast1, (c) Forecast2 and (d) the simulation initialised from PlumeTraj.

8.2 Case-study 2: 9 April 2021 eruption of La Soufriere

The eruption of La Soufriere in St Vincent began on 9 April (Figure 8.4) three days before the start of the trial. The eruption was considerably larger than that of Etna and consisted of successive explosive phases over several days. The size and duration of the eruption and level of interest in the ash and SO_2 plumes meant that this represented a good chance to test capabilities in near to real-time.

Initial information was more limited for this eruption compared to Etna. For example, there were no VONA that we were able to find, and we were unable to identify the responsible volcano observatory. (It may be that VONA were produced but not publicly available, this is further discussed in the findings below). Washington VAAC issued a VAA at 12:58 UTC for “possible volcanic ash emission”, with a subsequent VAA at 14:33 UTC confirming ash up to FL400. The first satellite-based alert was from the VOLCAT system and was issued at 12:50 UTC on 09/04/21 for volcanic ash using geostationary data. This was followed by an alert for volcanic sulphur dioxide at 17:00 UTC on 09/04/21. The first alerts received from the SACS service were at 15:17 UTC on 10/04/21 for volcanic ash (based on an overpass at 11:53 UTC) and 19:15 UTC on 10/04/21 for volcanic sulphur dioxide

© Crown Copyright 2021, Met Office

(based on a TROPOMI overpass at 16:48 UTC), both more than 24 hours after the start of the eruption. Multiple alerts were issued by both systems thereafter.

Only one forecast was attempted for the eruption with an issue time of 00:00 UTC on 11 April 2021. In this case, two different estimates of source flux were used in different simulations (Table 8.4). In Forecast A, the eruption source flux was based on the best estimates from satellite data on day 2 of the eruption and used 400 kt from the start until 00:00 UTC on 11/04/21. In Forecast B, in an attempt to reflect 'real-time' conditions during an emergency response, we considered how we might constrain the source flux without observations. Here we used an empirical relationship (based on historical data) to constrain the source strength which assumes that the flux of SO_2 can be related to the plume height, see the Modelling Volcanic SO_2 Clouds Report for details on this approach.

The Forecast A flux is based on emissions estimates shared by Fred Prata and Simon Carn on the ssircvolcano email list (a list which is geared to the climate impacts of eruptions rather than other purposes). AIRS data and TROPOMI data both gave a total mass of approximately 400 kt, although the timing of the data used to make these estimates varied by nearly 12 hours during which the volcano continued to erupt (AIRS overpass at 05:12 UTC on 10/04/21 and TROPOMI overpass at 16:51 UTC on 10/04/21). Without further information on the dynamics of the eruption on the 10/04/21, it was not possible to assess whether the agreement of these estimates showed that the majority of SO2 had been emitted prior to 05:00 or was a reflection of the uncertainty in the two techniques. Revised estimates produced on the 11th were within the range 200-450 kt. These estimates are over an order of magnitude larger than the Etna case.

For both simulations, the source fluxes were determined from the data available up until about 36 hours after eruption onset (to replicate a forecast in near real-time). The flux was calculated by assuming a constant emission rate over 36 hours for a total mass of 400 kt. As the eruption was ongoing and the flux after 36 hours was not constrained by observations, a constant flux at the same rate was applied during the forecast period.

Figure 8.4: Photograph of La Soufrière's second explosive eruption in St. Vincent and the Grenadines on April 9, 2021. (Photo by Nadia Huggins, accessed at https://globalvoices.org/2021/04/20/as-st-vincents-la-soufriere-erupts-again-experts-say-its-not-over-yet/).

© Crown Copyright 2021, Met Office

ESP	Forecast A	Forecast B	
		Source 1	Source 2
Volcano location	-61.18, 13.33	-61.18, 13.33	61.18, 13.33
Start time (UTC)	12:40 UTC 09/04/21	12:40 UTC 09/04/21	17:00 UTC 09/04/21
Stop time (UTC)	n/a	17:00 UTC 09/04/21	n/a
Emission height range	12-18 km asl	10-12 km asl	10-18 km asl
SO_2 emission flux	11.1 kt/hr	0.92 kt/hr	2.37 kt/hr

Table 8.4: Eruption source parameters (ESP) used to initialise the NAME model for the La Soufriere eruption forecasts. See text for details on how these were decided.

Constraining the height of the plume was also challenging. Washington VAAC provided top heights for ash plumes that varied between FL380 and FL550 on the 9th and 10th, equivalent to around 12.5 km to 18.5 km. The first VOLCAT SO_2 alert gave SO_2 height estimates in the range 10-18 km, which was supported in further alerts on the 9th and 10th. An initial estimate provided on the ssircvolcano email list based on GOES-17 near-limb imagery suggested a top height starting at 14-15km which rose to 16-17 km by 19:10 UTC on the 9th. Considering all the available data, a height range of 12-18 km was used for Forecast A. Forecast B used a similar height range linked to the empirical relationship but applied a lower height for the initial eruption phase based on satellite estimates and a desire to not overestimate the flux in the first few hours (Table 8.4). Both choices are a considerable simplification of the pulsing behaviour observed. CALIOP data obtained on the 10th but shared on the 11th supported the evidence for the presence of ash layers between 12-18.5 km asl.

Figure 8.5 shows the modelled vertical total column for SO_2 in Dobson Units from Forecast A. Four forecast times on 11/04/21 are depicted: 00:00 (T+0), 06:00 (T+6), 12:00 (T+12) and 18:00 (T+18). The large extent of the plume reflects the emissions from the preceding 36 hours. Comparison of the T+18 forecast to composite TROPOMI data (Figure 8.6) suggests that representation of the extent of the plume is very good, but that the modelled internal plume structure is not quite right, in particular the high mass in the bifurcated plume to the southeast of the source at T+12 and T+18. This is likely due to the crude representation of the eruption as one persistent source.

Taking the modelled concentration data and applying the WHO threshold produces the outputs shown in Figure 8.7. For simplicity we have not attempted to depict the flight levels that these correspond to here, but this would be a necessary step for a forecast centre. Comparison to the temporally closest VAG issued by Washington VAAC (Figure 8.8) demonstrates that in this case, with the limited amount of information available, the area covered by the SO_2 forecast threshold would have been smaller than that covered by the VAA.

© Crown Copyright 2021, Met Office

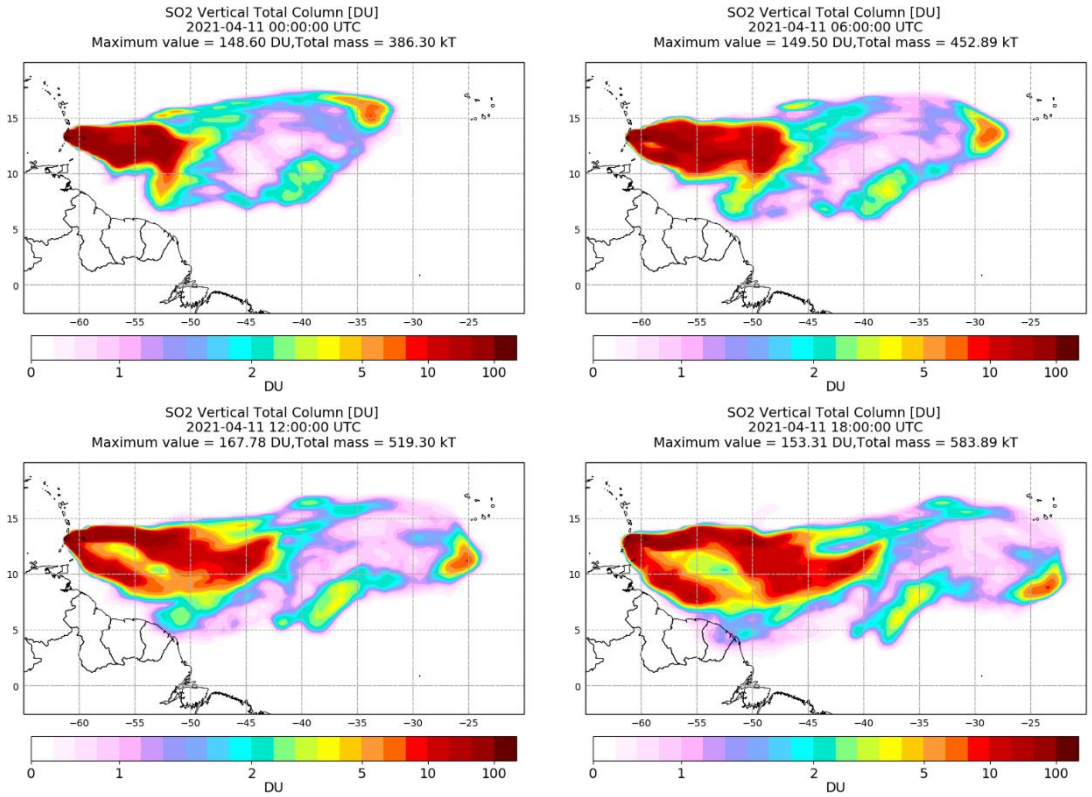

Figure 8.5: Modelled SO_2 forecast in Dobson Units for 00:00 UTC on 11/04/2021, showing outputs for forecast times of T+0, T+6, T+12 and T+18 from Forecast A.

© Crown Copyright 2021, Met Office

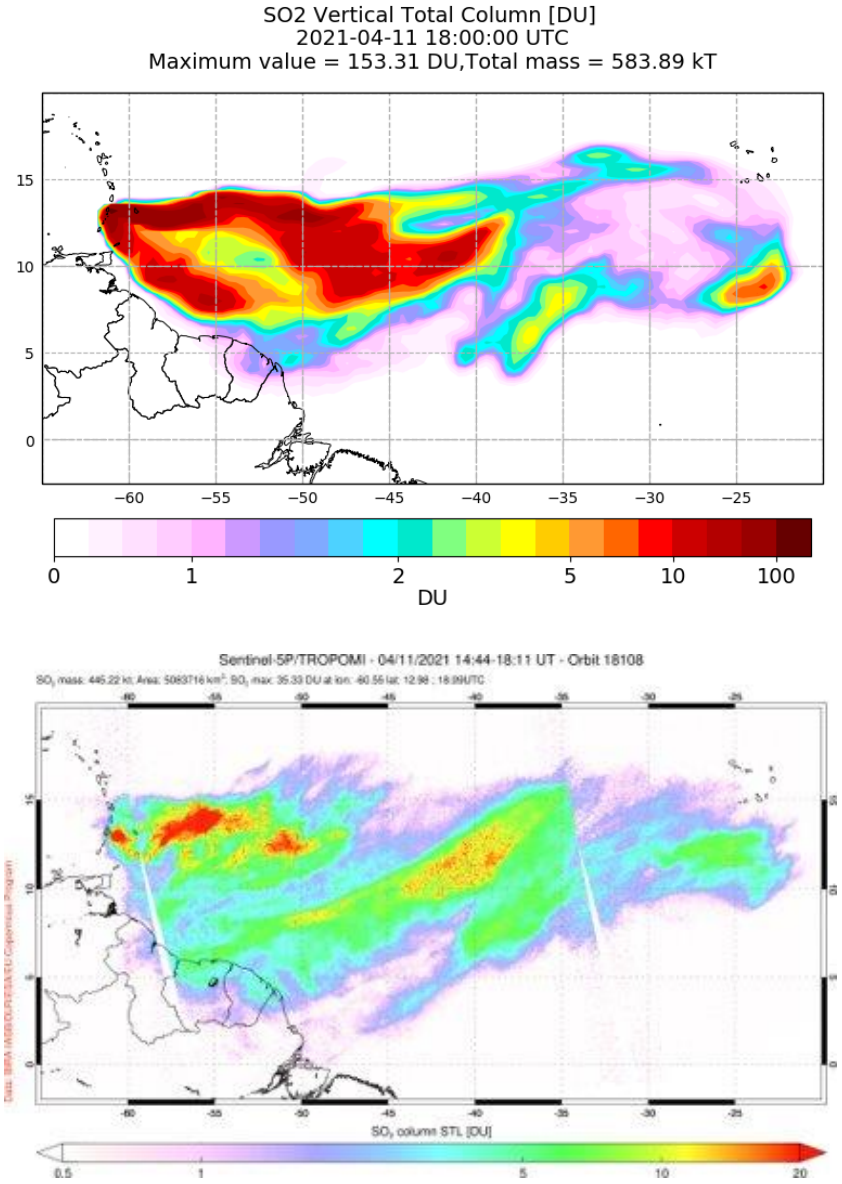

Figure 8.6: Comparison of (top) Forecast A T+18 forecast to (bottom) combined TROPOMI data from three overpasses, the latest being at a comparable time. Note the different colour scales used.

© Crown Copyright 2021, Met Office

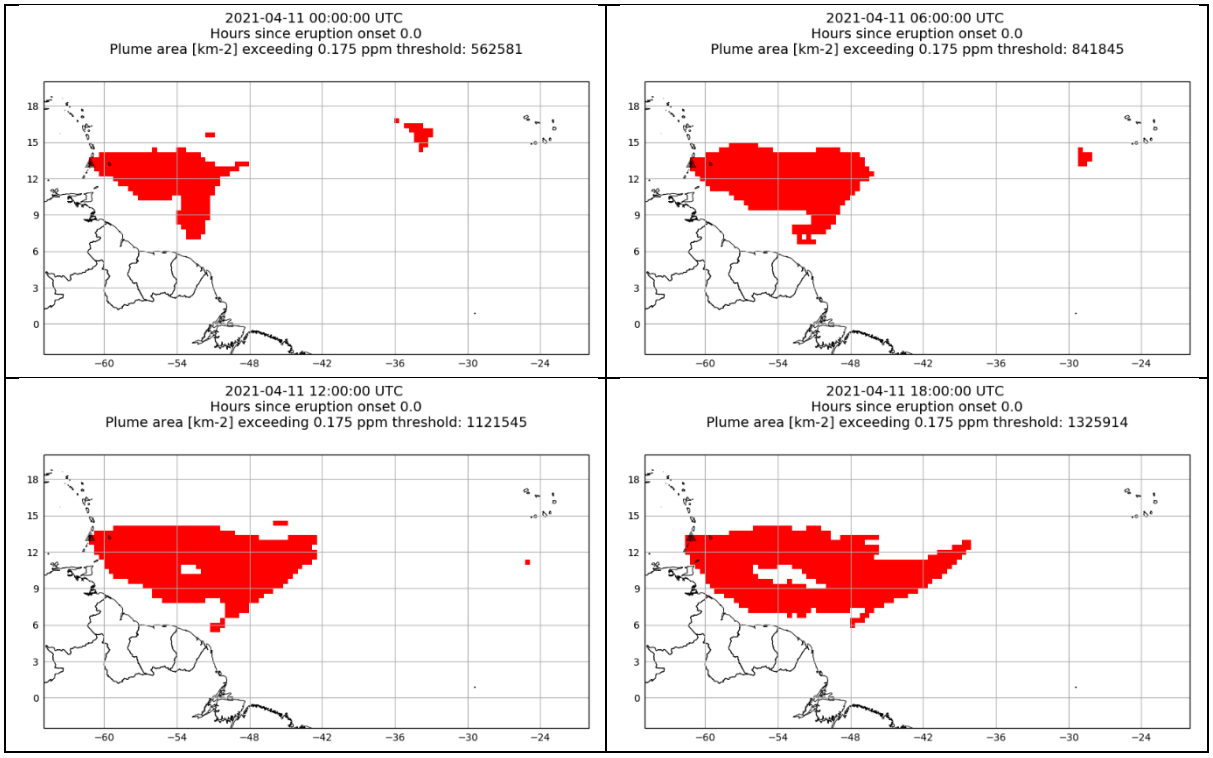

Figure 8.7: Equivalent to Figure 8.5 but showing the area where the WHO threshold for SO_2 of 0.175 ppm is exceeded somewhere in the atmosphere.

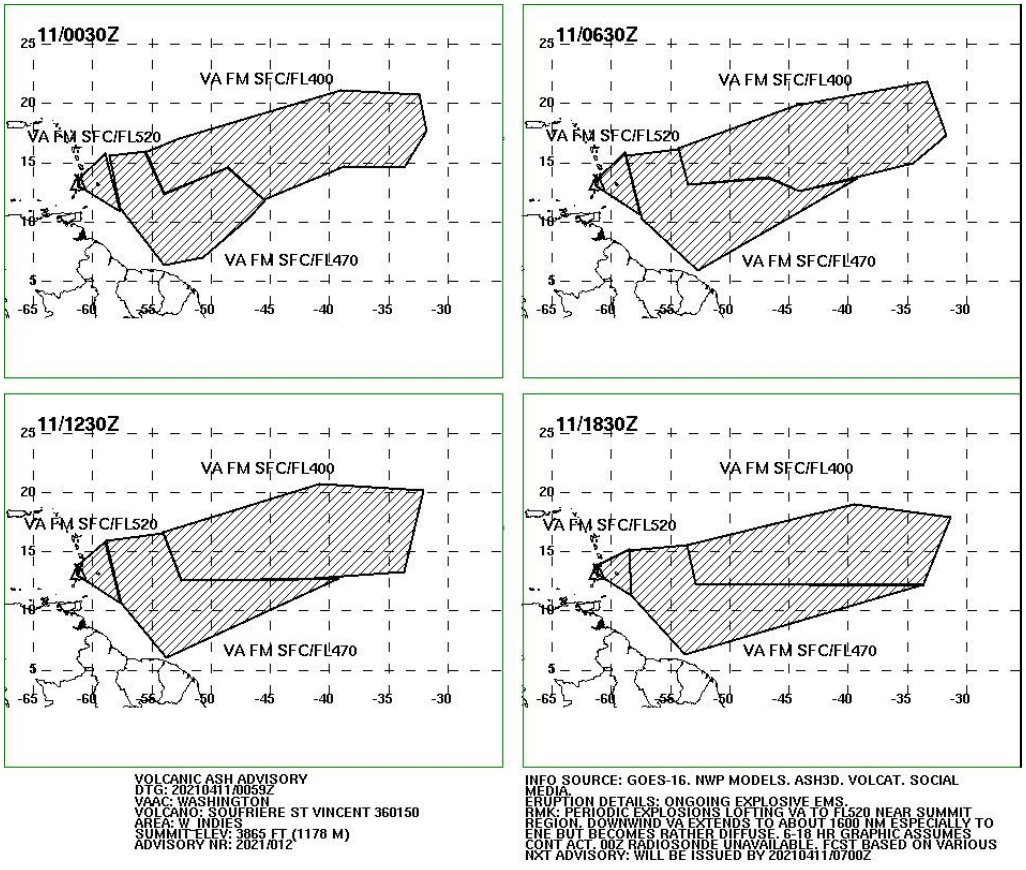

Figure 8.8: The VAG issued by Washington VAAC at 00:59Z on 11/04/2021, which is the closest temporal match to Figures 8.5 and 8.7. Maximum downwind extent is approximately -32E.

© Crown Copyright 2021, Met Office

8.3 Findings from the trial

The results of the trial and our experiences in producing the forecasts for the two case-studies provide useful guidance on the requirements for a future volcanic SO_2 forecast service. Although we have only considered two eruptions that represent a limited sub-set of the different types of volcanic event possible, we believe that the findings are applicable to a wider set of events.

Based on the findings from the trial and the information presented in the rest of this report an assessment of the specific components and requirements of a service are considered below.

8.3.1 Alerting

Finding out that an eruption has started will be one of the key challenges for a forecast centre. Manually looking at satellite data feeds over known volcanoes (which is currently a key function in many VAACs) can be very labour intensive. Good links to the state volcano observatories (SVO) alongside automated alerting processes will be essential.

In the Etna case, the start of the eruption was promptly notified by the SVO via a VONA. This demonstrates the huge value of the VONA process. Although the VONA structure is geared to volcanic ash and there is no requirement for SO_2 to be mentioned, much of the information in the VONA is relevant to SO_2 forecasting. Current procedures for the creation and dissemination of the VONA vary around the world and this is an area of active work by ICAO, WMO and the Volcano Observatory Best Practice process. The fact that we could not find the VONA for La Soufriere highlights the value that would come from establishing a global “clearing house” for all issued VONA (as suggested in Section 7). This would not only enable the lead centre to easily access the VONA, but also provide continuity for back up and training purposes. If an SO_2 forecast for aviation were to be introduced, the inclusion of additional SO_2 information in the VONA (height, mass etc) would be a useful additional component.

Existing automated systems (VOLCAT, SACS etc) use satellite data to warn of anomalous SO_2 detections and it is easy to subscribe to these alerts. However, the processing time of satellite data means that there is a delay between a satellite overpass and the issuance of an alert. This can be on the order of hours. (This delay is not always clear when looking at past events when only the overpass time is given on images or alerts.) Based on the information that was available to us in near real-time for the La Soufriere eruption, the earliest that a plume forecast could have been initialised based on the VOLCAT SO_2 alert was 17:00 UTC on 09/04/21 (approx. 5 hours after the start). (The first automated alert for the Etna eruption was also received about 5 hours after the start of the eruption). However, an earlier alert for volcanic ash from VOLCAT demonstrates that faster awareness of an eruption is possible and that improvements to alerting systems to utilise both ash and SO_2 alerts will ensure the earliest notification. With current capabilities, a human forecaster will still be needed to filter and assess false alerts before triggering any response, but further developments are likely to reduce the number of false alerts.

Other alerting techniques for volcanic eruptions, e.g., infrasound, were not considered, but are being explored under other IAVW channels.

8.3.2 Estimation of source parameters

Once a centre is aware of an eruption, it will need to produce a quantitative forecast. This may be before high-quality satellite flux data are available. For volcanic ash when no observed flux data are available, an established empirical relationship can be used to determine a first estimate of the mass eruption rate based on the eruption height (e.g., Mastin et al. 2009). No equivalent published

© Crown Copyright 2021, Met Office

relationship exists for SO_2. This could be a serious limitation at the start of an eruption, although new work reported in Section 3.3.1 suggests that there may be potential here.

For the Etna case, we were fortunate that the eruption occurred in the morning, so that the early plume transport coincided with a UV LEO sensor overpass. For a night-time eruption, there would have been a considerable delay before any information was available. Even so, the Etna case highlights the advantage of "local knowledge" and an understanding of the behaviour of the erupting volcano to define initial emission fluxes. This is particularly valuable in the initial hours after an eruption when no information on SO_2 flux may be available. For the first Etna forecast a best estimate flux was used based on historical behaviour. It was only for the second forecast, once the LEO overpass data had been processed that we were able to use observed fluxes.

In the La Soufriere case, our lack of direct access to processed SO_2 satellite data from the major sensors, as well as lack of in-house tools to use such data in data-fusion approaches, meant that we were entirely reliant on flux estimates provided by experienced researchers via email. In an operational 24/7 context it is not feasible or appropriate to rely on such information via ad-hoc email lists and social media. For an operational service, a forecast centre would need to develop, as part of the wider operational capability, its own tools to generate equivalent SO_2 flux data from a range of sensors (TROPOMI, AIRS, IASI etc). It is envisaged that community-based discussion and data-sharing will still have a valuable role in understanding complex eruptions and interpreting the available data.

The fact that reasonable estimates of the SO_2 mass flux directly from satellites are already generally available on the same day as the eruption, which is not currently the case for ash, is a significant benefit from existing research capabilities. Combined with the existence of models and prototype data-fusion techniques, this makes quantitative SO_2 forecasting very achievable. The challenge is the delay in getting sufficient overpass data to make the estimate, as these data currently come from the low earth orbiters. The delay varies depending on time of day of the eruption (many overpasses are close to local noon) and the latitude (there are more overpasses at higher latitudes). Consequently, operational application of algorithms to the current geostationary (GEO) satellite sensors should be explored to determine whether they can provide a usable quick first estimate. Work is also needed to ensure the best use of planned future GEO sensors, which will have improved capabilities (Section 4).

The modelled concentrations of SO_2 in the atmosphere are strongly dependent on the vertical emission profile used in addition to the mass flux. For a pulsing eruption such as La Soufriere or the 2019 Raikoke eruption, emitting over a representative height range is the sensible approach to capture the areal extent of the SO_2 plume, but this could mean that modelled concentrations are lower than reality. Adequate constraint of the SO_2 plume height is therefore going to be of similar importance to constraining the flux. A variety of satellite approaches provide potential for constraining heights (lidar, limb-sounders and sophisticated retrieval techniques applied to UV and IR LEO data, see Section 4), but timeliness of availability is a current limitation.

The Etna case highlighted the value of data-fusion techniques such as PlumeTraj and that these will be an essential component of a future forecasting system if accurate and timely forecasts are to be issued. We did not have any techniques directly available to us for the La Soufriere case, but this case-study highlighted the role that data assimilation could have in producing a forecast, as well as some of the current challenges around this approach (see below). Human interpretation of the data was necessary in both cases (input and output respectively), so although data-fusion is one area where full automation may be possible, it may not be desirable.

© Crown Copyright 2021, Met Office

As new observations and data become available, satellite-based estimates evolve with time. This means that the source parameters used in later model forecasts need to be able to be revised with time.

8.3.3 Modelling

For the trial, we used the NAME model with a limited area domain that was defined by hand for each case-study as part of the process. For an operational service this is not ideal, as the forecast transport direction and extent are not known at the start. The run-time of a model simulation is influenced by the domain extent and the grid resolution and, for a Lagrangian model, the number of model particles released and hence the emission duration. For the La Soufriere case-study, we were forced to reduce the horizontal resolution (chemistry and output grids) and particle release rate to achieve suitable run times. Optimisation of model(s) and increased computer resources to cope with a range of eruption scenarios will be a necessary development step for a future SO_2 forecast centre.

To enable qualitative and quantitative comparison to both GEO and LEO satellite data, higher time-resolution output is required from the models than the likely forecast time-steps (e.g., hourly versus a 3 or 6 hour forecast step). This has potential overheads for model run duration and data storage, which will be an important consideration. Identical requirements will exist for quantitative volcanic ash.

For the La Soufriere eruption, we had access to the ECMWF CAMS model output in real-time via the windy.com website and past data via stills and animations on Twitter. The CAMS forecast included representation of the SO_2 plume solely through a data assimilation process with some known limitations for volcanic SO_2 (see Section 5.4.1). Figure 8.9 shows a comparison for 1800 on 11 April between the CAMS forecast and the NAME simulation. Although direct comparison between the models proved challenging due to the different plotting scales used, this small qualitative multi-model ensemble was useful for highlighting uncertainties. Sharing of model prediction data and interpretation in real-time between centres could therefore offer considerable benefits. In personal communications, ECMWF conveyed that they believe the La Soufriere plume was overestimated in the CAMS forecasts in comparison to satellite data.

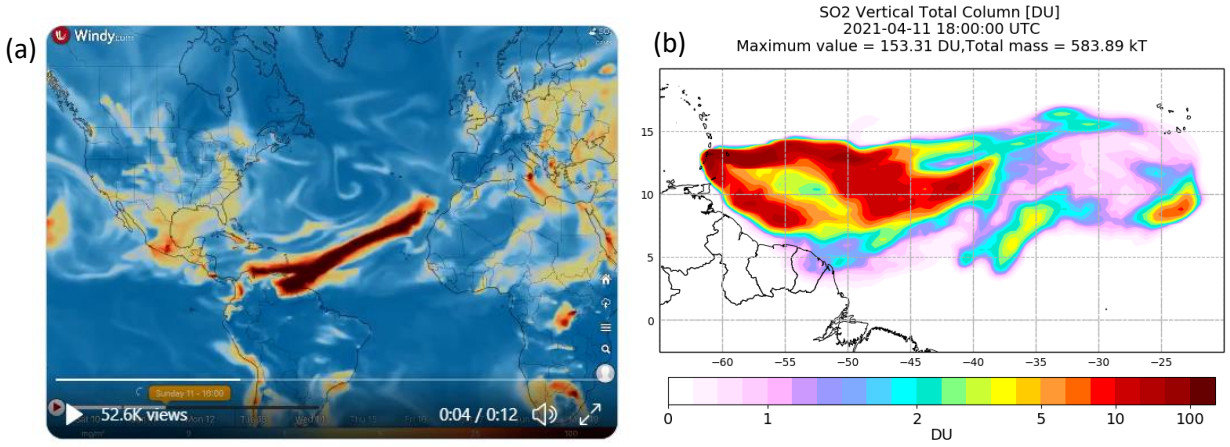

Figure 8.9: (a) CAMS total column SO_2 forecast initialized on 10 April 12 UTC with assimilated TROPOMI observations (assuming 500hPa injection height). Visualized by Windy.com. Still image for 18:00 UTC on 11 April from video shared by Mark Parrington, ECMWF on Twitter (@m_parrington) on 10 April. (b) NAME SO_2 forecast for 18:00 UTC on 11 April.

© Crown Copyright 2021, Met Office

8.3.4 Comparison to ash forecasts

The longevity of an SO_2 plume in the atmosphere compared to an ash plume means that SO_2 forecasts may need to be issued for considerably longer than the equivalent ash forecasts and cover a wider area. In the Etna case, for example, the observable ash signal disappeared much quicker than the SO_2 signal. This meant that within the validity timeframe of the VAAs, where ash was limited to only the area close to Italy, SO_2 was detected near Greece. The WHO SO_2 threshold was also exceeded for much longer than the validity period of the VAAs. Forecasts based on the WHO SO_2 threshold would need to have been issued for around 24 hours, whereas the VAA only lasted about 4 hours until 12:00 UTC.

For the La Soufriere eruption, there was a closer alignment between the extent and duration of the ash and SO_2 forecasts in the period that was selected. However, the SO_2 plume continued to travel east and remained detectable for many days, so a forecast centre would need to have been proactive in checking and confirming when amounts went below the designated threshold.

The implication is that an SO_2 forecast response could last much longer than the equivalent ash forecast requirement and certainly a centre would need to continue to track the SO_2 plume to confirm that it was not exceeding whatever concentration threshold(s) was mandated. The lowest quantitative volcanic ash threshold aligns approximately with detectability thresholds for older sensors, whereas this is not the case for the proposed SO_2 thresholds. Comparison of satellite data to forecasts for SO_2 will therefore require a slightly different approach from the community. There are likely parallels here with the new concentration levels for volcanic ash and future enhanced satellite detection capabilities for ash.

8.3.5 Forecast Validation

Satellite data will be the primary tool for validating forecasts. The trial showed that although LEO sensors dominate the literature for estimating SO_2 fluxes, the overpasses can be too few and far between for rapid real-time validation. Instead, the GEO satellite data were very useful for rapid identification of errors in the plume dispersion/transport. In the Etna case, the high-frequency MSG GEO data were essential for validating the location of the SO_2 cloud and hence demonstrating that the first forecast was deviating from reality. The sporadic nature of the LEO data was not sufficient for this purpose. Although the retrieved quantitative GEO data were of lower quality than the equivalent LEO data, they provided detection and information on the transport at high temporal resolution (15 minutes), which is what is needed. The two types of satellites provide complementary information, and both will be essential. Exploring what GEO SO_2 data are available or could be produced will be a key step for a forecast centre (some consideration of this is given in Section 4).

The strengths and weaknesses of different sensors and their data need to be well understood. Differences in sensitivity, detection limits (e.g., between UV and IR sensors) and resolution mean that different sensors can give a wide range of SO_2 Dobson Unit (DU) values for the same times (see Section 4). This can be seen, for example, by comparing the different products available on the SACS website and was noticed during the trial. This is one reason why defining a threshold based on an observed DU is problematic. The other, fundamental challenge is comparing model estimates of concentration to satellite retrievals of column loads.

All the validation conducted here was purely qualitative and based on comparison by eye between model data and satellite images to identify/correct gross errors. Differences in projections between the images and forecasts can make this challenging. For quantitative validation purposes, a forecast centre will need the data files as well as the images. The SACS service has recently introduced netCDF files that correspond to its alerts, which is a useful first step, but timing of their availability

© Crown Copyright 2021, Met Office

will depend on overpass times and post-processing. We were not able to utilise these files during the trial.

In addition to satellite data, ground based SO_2 sensors are deployed by volcano observatories and research groups at a number of volcanoes worldwide. These may be fixed or used in a more ad-hoc fashion along traverses. In an ideal world, a forecast centre would also have access to all ground-based monitoring data for SO_2 and there would be good understanding of how these data validate against satellite observations. Research aircraft flights in volcanic plumes would also provide useful data to validate both models and satellite retrievals. Facilitating access in near real-time to all such data will be a significant challenge and require engagement and buy-in from the global volcanological community. No such data were available in near real-time during the trial.

8.3.6 Availability of satellite data

Satellite data will be crucial for the alerting, derivation of ESPs, data-fusion and forecast validation during any SO_2 eruption as highlighted above. Whilst there are lots of satellite data available, the access to it is currently very disparate and not in one place. This would be an issue for an operational centre in terms of quality assurance and confidence in 24/7 availability and use of data. For an operational service, direct feeds of data may need to be brought in house. Certainly, the means to calculate fluxes in near real-time from a variety of sensors will be needed.

Websites and alerting systems such as VOLCAT and SACS are hugely useful, but the long-term maintenance and reliance on research-project supported tools should be a concern. These services are now of a maturity where they could be brought into (or replicated) in an operational centre(s) (and indeed VOLCAT is used this way for volcanic ash), but this will require satellite and technological expertise and working with current providers.

There is also a lot of knowledge within the satellite research community and a willingness to share information and data as shown by the email lists. However, relying on the research community to provide data will not be sufficient or appropriate for a 24/7 operation. A centre will need to consider how it can best utilise this community and draw on its expertise in quiet time and during events but identify what system aspects may need to be replicated in-house.

© Crown Copyright 2021, Met Office

9 Recommendations

This report outlines the capabilities required to provide an operational forecast of volcanic SO_2 to the aviation industry. Here we make recommendations on the components and developments needed to deliver such a service. Many of the areas identified as requiring scientific and technological development are identical for quantitative forecasting of volcanic ash so there are many synergies that can and should be exploited.

Significant quantities of volcanic SO_2 can be released into the atmosphere by both effusive and explosive eruptions. Effusive (lower energy) fissure eruptions can release large volumes of gas at ground-level and may be accompanied by very little ash. Forecasts will need to be delivered for these events, as well as explosive eruptions that can release both SO_2 and ash at higher altitudes.

To predict the location and concentration of volcanic SO_2 in the atmosphere an operational capability will need to:

- Be fast, accurate and robust enough to deliver multiple forecasts per day.
- Represent temporally varying source conditions: timings of release, plume height(s) and depth(s), and release rate(s) (SO_2 flux).
- Use a suitable model to predict the onwards transport, dispersion, and removal of SO_2 in the atmosphere, including depletion by chemical processes.
- Be able to represent surface and high-altitude releases, local and global transport.
- Incorporate observations of SO_2 from satellite sensors.
- Generate forecasts on an appropriate domain, to represent the long-range transport and dispersion of SO_2.
- Provide 4D gridded datasets.

Three main scientific components are essential to the delivery of such an SO_2 service: models, observations, and data fusion techniques. Robust communication procedures that provide timely alerts and the delivery of observations to the responding centre will be crucial. Techniques for estimating source parameters from observations, the use of sophisticated data fusion methods for ingesting observations into models directly, and new verification procedures will also all be essential.

We now provide a summary of the requirements, readiness state, and key areas for future work under each of these areas. Finally, forecast delivery aspects, including concentration thresholds, are considered.

Models

The key requirements for an SO_2 service are:

- A model capable of representing the chemistry and transport of the SO_2 plume, which can be run over a large domain (potentially global) and produce timely (e.g., in less than hour) three-dimensional results.
- The appropriate NWP and/or meteorological data assimilation for said model (offline or online respectively) at a resolution appropriate for the type of event.
- The ability to cope with complex and evolving source parameters, and for the sources used in later model forecasts to be revised with time as new information becomes available.

Models exist with the capabilities to generate the required data and there have been significant developments in modelling systems used to simulate the transport and transformation of atmospheric SO_2 for air quality forecasting and research. However, the choice and optimisation of

© Crown Copyright 2021, Met Office

model(s) and computer resources to cope with a range of eruption scenarios and aviation needs will be a necessary development step for a forecast centre.

For validation purposes, higher time-resolution output is required from models than the likely forecast time-steps (e.g., hourly versus a 3 or 6 hour forecast step). This has potential overheads for model run duration and data storage, which will be an important consideration. Identical requirements will exist for quantitative volcanic ash.

Satellite observations and data

Satellite observations are essential in a forecasting context for:

- Near-real time alerting and awareness.
- Model initialisation in near-real time.
- Validation, assessment and improvement of forecast and models.

A combination of satellite data from low earth orbiting (LEO) and geostationary satellites (GEO) is required to provide a robust system considering both timeliness and quality of the satellite observations. To meet the service requirements a centre will need:

- Operational access to existing global automated eruption alerts based on satellite observations (and other techniques) and/or the development of equivalent functionality in-house.
- Direct data streams from a considerable range of Geostationary and Low Earth Orbit sensors with the capability to detect SO_2. This includes existing processed data streams produced by ESA, NASA, etc, and could build on software technologies such as VOLCAT.
- Algorithms to further process these data streams and produce quantitative estimates of SO_2 mass flux and plume height data within suitable operational time windows.
- Visualisation and analysis software for quantitative comparison of satellite and model data, to enable validation and quality assurance.

Current processing algorithms for SO_2 retrievals may need to be enhanced and made operational to ensure that data are available as quickly as possible after an overpass/detection. A key step for a forecast centre will be exploring what current and future Geostationary SO_2 data are available to enable more frequent source estimation and forecast validation.

Detailed education and understanding of the differences in sensitivity, detection limits (e.g., between UV and IR sensors) and resolution will be needed for staff to enable appropriate interpretation of the wide range of SO_2 Dobson Unit values given for the same times by different sensors. The impacts on source estimation, data fusion and validation will all need to be considered.

Use of other observations such as near-source, aircraft based etc will also be important, but satellite observations will dominate and are key.

Detection and Alerting

The requirement here is for rapid awareness of potentially hazardous SO_2 plumes.

The current VONA process provides a mechanism for the communication of critical information about volcanic eruptions to the VAACs. It would seem logical to extend this to include SO_2. This will not only provide fast notification but also local information on the eruption source parameters, whilst also providing a more holistic summary of the eruptive activity.

© Crown Copyright 2021, Met Office

For an SO_2 capability, key recommendations for future developments around the VONA include:

- Access in real-time to all issued VONA via a global repository.
- The VONA to contain additional information about SO_2 emissions.

Satellite data are also essential for detection and alerting on a global scale. Existing automated systems use satellite data to warn of anomalous SO_2 detections and it is recommended that alerts for volcanic ash and SO_2 should be used in combination for both SO_2 and volcanic ash forecast services.

These satellite-based alerting services are now of a maturity where they should be brought into (or replicated) in an operational centre(s) rather than relying on research-supported tools for operational response. This will require satellite and technological expertise and working with current providers and researchers. Further development work, e.g., to reduce the number of false alarms, would be beneficial.

Eruption source parameters

To produce a quantitative forecast, a centre will need to know how much SO_2 is being emitted into the atmosphere, i.e., its mass flux. A variety of techniques exist for defining SO_2 emissions (all of which rely on observations) and it is already possible to generate reasonable estimates of the SO_2 mass flux directly from satellites and other observations. For well monitored volcanoes, and particularly effusive eruptions, ground-based measurements may be more accurate than satellite estimates so good links to the volcano observatories will be key.

For a global operational service, covering many unmonitored volcanoes, a forecast centre(s) would also need to develop and implement, as part of the wider operational capability, its own tools to generate SO_2 flux data from a range of satellite sensors.

One challenge is the delay in getting sufficient overpass data to make the estimate, as these data currently come from the low earth orbiters. The delay varies depending on time of day of the eruption and the plume latitude. Consequently, operational application of algorithms to the current geostationary (GEO) satellite sensors should be explored to determine whether they can provide a usable more-timely first estimate. Work is also needed to ensure the best use of planned future GEO sensors, which will have improved capabilities

Adequate constraint of the SO_2 plume height and thickness is of similar importance to constraining the flux. A variety of satellite approaches provide potential for constraining heights (see Section 4), but timeliness of data availability is a current limitation. These challenges are similar to those for forecasting volcanic ash and are not new. The VAACs have established techniques for e.g., determining eruption heights, etc, which will directly translate into SO_2 forecasting.

It is envisaged that community-based discussion and data-sharing will still have a valuable role in understanding complex eruptions and interpreting the available data.

Data fusion techniques

A global SO_2 forecast system would greatly benefit from the use of one or more data fusion methods to achieve more accurate and timely forecasts by bringing together observations and modelling. Many research studies have demonstrated the benefit of various techniques and shown that forecasts are improved by applying a data fusion approach. The forecast trial case-studies (Section 8) also highlighted the value of data-fusion techniques.

© Crown Copyright 2021, Met Office

As each data fusion method has its advantages and limitations (Section 5) it is recommended that a forecast system includes not just one but several different techniques. For example, simple and quick trajectory techniques might be most useful in the first few hours of the eruption to constrain the source term from a single satellite image, while a more comprehensive and computationally demanding inversion or data assimilation might be most suitable when more observations are available at a later stage.

A combined method could also be favourable where both the underlying emission source term is optimised with inverse methods as well as the simulated concentrations fields with data assimilation, with an addition of post-processing tools (e.g., bias correction) which could be applied as a fully independent approach. Such a system does not yet exist and would need thorough research, optimisation, validation, system development and testing.

Most current techniques are limited and exist as research capabilities. Development and resource will therefore be needed to build on these and pull suitable capabilities through into operations. There are many similarities here with the work needed for quantitative volcanic ash and potential efficiencies and benefits from combining approaches across the two applications.

Forecast Delivery

The impact of providing forecasts for fixed concentration thresholds has been explored. This shows that:

- For larger SO_2 eruptions, the choice of the WHO concentration threshold will result in SO_2 advisories needing to be issued for considerably longer (days) and covering a wider area than the equivalent ash advisories. The consequent impact on aviation will depend on the action required in response to the advisory.
- A multiple threshold approach with additional higher thresholds may therefore be desirable if suitable additional concentration levels and aviation procedures can be agreed upon.
- Use of a DU threshold is not recommended, because the corresponding atmospheric concentration is highly sensitive to the height and thickness of the SO_2 plume and not a fixed value.

There are a variety of options as to how a global forecast could be logistically delivered, for example:

1. One centre delivers a global service (with back-up).
2. Multiple centres that have responsibility for eruptions occurring in designated volcanic zones (or defined limited areas) and continue forecasting for the entire life of the plume.
3. Multiple centres that have responsibility for eruption plumes in defined limited areas and hand over at area boundaries.

The choice has a fundamental impact on some of the requirements outlined above, which should be considered. Table 9.1 attempts to summarise some of the advantages and disadvantages of each option. In all cases, personnel with expertise in SO_2 monitoring and atmospheric modelling, as well as an understanding of volcanic processes, should be a priority.

© Crown Copyright 2021, Met Office

Option	Pros	Cons
Option 1: One centre responsible for whole globe	Global consistency in approach. Resource to develop necessary capabilities and techniques focussed on one centre.	Single centre needs access to extensive global satellite data. Very challenging/possibly impossible to build and maintain local knowledge and connections with all volcano observatories. Needs a single database (or communications route) to be established for access to all VONA. Responding to multiple eruptions in different parts of the globe may be onerous. No back up and/or realistic minimum is two global centres.
Option 2: Multiple centres forecasting entire plume from designated volcanoes	Local familiarity and knowledge easier to maintain. Easier to establish links to regional volcano observatories and access to VONA. More localised focus on detection. Single centre provides entire prediction.	Each centre needs to develop and maintain all of the outlined capacities, with corresponding resource overheads. Approaches, models and tools will vary between centres. Varying plume extents requires global capability.
Option 3: Multiple centres forecasting for defined regions	As Option 2, but also: Models can be set-up to run on fixed limited area domains. Satellite and observations data are only required for the specific region. Communications and relationships are simplified in a limited region.	As Option 2, but also: High likelihood of discrepancies in SO_2 concentration at area boundaries. Customers need to patch multiple products to represent the whole plume.

Table 9.1: Advantages and disadvantages of different ways that a global forecast service could be implemented.

© Crown Copyright 2021, Met Office

Acknowledgements

The report has benefited from thorough review by Matthew Hort (Met Office).

The authors would like to thank the following from the Met Office: Paul Agnew for providing tuition on chemical processes in the atmosphere, Florent Malavelle for advice on climate models, and Eleanor Smith for providing advice on atmospheric composition modelling systems. John Eyre, Simon Keogh, Pete Francis and Cameron Saint for providing useful feedback and guidance on the satellites section. Helen Webster for providing feedback on the data fusion section.

We express our gratitude to Nickolay Krotkov (NASA/GSFC), Mike Pavolonis (NOAA/NESDIS), and Hugues Brenot (Royal Belgian Institute for Space Aeronomy) for providing insights on the most up-to-date satellite alerting systems and the methods they rely on, and to Hans de Leeuw (University of Cambridge) for insightful discussions and his generosity in providing figures 3.3 and 6.10.

References

Athanassiadou, M., Francis, P.N., Saunders, R.W., Atkinson, N.J., Hort, M.C., Havemann, S., Thelen, J-C., and Bush, M., A case study of sulphur dioxide identification in three different volcanic eruptions, using Infrared satellite observations (IASI), Meteorol. Appl. 23: 477–490, 2016.

Bannister, R., A review of operational methods of variational and ensemble-variational data assimilation. Q. J. R. Meteorol. Soc., 143, 607–633, 2017.

Barsotti, S., Probabilistic hazard maps for operational use: the case of SO2 air pollution during the Holuhraun eruption (Bárðarbunga, Iceland) in 2014–2015, Bulletin of Volcanology, 82, 56, 2020.

Beckett, F., Witham, C., and Devenish, B., Statistical Assessment of Dispersion Model Sensitivity, Deliverable report D8.5 of the EU FUTUREVOLC project, 2015.

Benedetti, A., J. W. Kaiser, J.-J. Morcrette, R. Eresmaa, and S. Lu, Simulations of volcanic plumes with the ECMWF/MACC aerosol system, Dec. 2011, ECMWF Tech. Memo. 653, 2011.

Berglen, T. F., T. K. Berntsen, I. S. A. Isaksen, and J. K. Sundet, A global model of the coupled sulfur/oxidant chemistry in the troposphere: The sulfur cycle, J. Geophys. Res., 109, D19310, doi:10.1029/2003JD003948, 2004.

BIRA-IASB, S5P/TROPOMI SO2 ATBD, Royal Belgian Institute for Space Aeronomy, https://sentinels.copernicus.eu/documents/247904/2476257/Sentinel-5P-ATBD-SO2-TROPOMI, 2020.

Bluth, G.J.S., Schnetzler, C.C., Krueger, A.J., Walter, L.S., The contribution of explosive volcanism to global atmospheric sulphur dioxide concentrations. Nature, 366, 327-329, 1993.

Boichu, M. and Clarisse, L., Improving volcanic sulfur dioxide cloud dispersal forecasts by progressive assimilation of satellite observations, Geophys. Res. Lett., 41, 2637–2643, doi:10.1002/2014GL059496, 2014.

Boichu, M., Chiapello, I., Brogniez, C., et al., Current challenges in modelling far-range air pollution induced by the 2014–2015 Bárðarbunga fissure eruption (Iceland), Atmos. Chem. Phys., 16, 10831–10845, 2016.

Boichu, M., L. Clarisse, D. Khvorostyanov, and C. Clerbaux, Improving volcanic sulfur dioxide cloud dispersal forecasts by progressive assimilation of satellite observations, Geophys. Res. Lett., 41, 2637–2643, doi:10.1002/2014GL059496, 2014.

© Crown Copyright 2021, Met Office

Boichu, M., Menut, L., Khvorostyanov, D., Clarisse, L., Clerbaux, C., Turquety, S., and Coheur, P-F., Inverting for volcanic SO2 flux at high temporal resolution using spaceborne plume imagery and chemistry-transport modelling: the 2010 Eyjafjallajokull eruption case study, Atmos. Chem. Phys., 13, 8569–8584, 2013.

Brenot, H., N. Theys, L. Clarisse, J. van Geffen, J. van Gent, M. Van Roozendael, R. van der A, D. Hurtmans, P.-F. Coheur, C. Clerbaux, P. Valks, P. Hedelt, F. Prata, O. Rasson, K. Sievers, and C. Zehner, Support to Aviation Control Service (SACS): an online service for near-real-time satellite monitoring of volcanic plumes, Nat. Hazards Earth Syst. Sci. 14, 1099–1123, 2014.

CAMS, 2020, https://atmosphere.copernicus.eu/solving-challenges-modelling-volcanic-eruptions.

Carboni, E., Grainger, R. G., Mather, T. A., Pyle, D. M., Thomas, G. E., Siddans, R., Smith, A. J. A., Dudhia, A., Koukouli, M. E., and Balis, D., The vertical distribution of volcanic SO2 plumes measured by IASI, Atmos. Chem. Phys., 16, 4343–4367, https://doi.org/10.5194/acp-16-4343-2016, 2016.

Carn, A.A., Clarisse, L., Prata, A.J., Multi-decadal satellite measurements of global volcanic degassing, Journal of Volcanology and Geothermal Research 311, 99–134, 2016.

Carn, S. A., V. E. Fioletov, C. A. McLinden, C. Li, and N. A. Krotkov, A decade of global volcanic SO2 emissions measured from space, Sci. Rep. 7, 44095, 2017.

Carn, S. A., Multi-Satellite Volcanic Sulfur Dioxide L4 Long-Term Global Database V3, Greenbelt, MD, USA, Goddard Earth Science Data and Information Services Center (GES DISC), https://doi.org/10.5067/MEASURES/SO2/DATA404, 2019.

Carn, S., L. Clarisse, and A. Prata, Multi-decadal satellite measurements of global volcanic degassing, J. Volcanol. Geotherm. Res. 311, 99–134, 2016.

Carn, S.A., Fioletov, V.E., McLinden, C.A., Li, C., and Krotkov, N.A., A decade of global volcanic SO2 emissions measured from space, Scientific Reports, 7:44095, 2017.

Chai, T., Crawford, A., Stunder, B., Pavolonis, M. J., Draxler, R., and Stein, A., Improving volcanic ash predictions with the HYSPLIT dispersion model by assimilating MODIS satellite retrievals, Atmos. Chem. Phys., 17, 2865–2879, https://doi.org/10.5194/acp-17-2865-2017, 2017.

Clarisse, L., Hurtmans, D., Clerbaux, C., Hadji-Lazaro, J., Ngadi, Y., and Coheur, P.-F., Retrieval of sulphur dioxide from the infrared atmospheric sounding interferometer (IASI), Atmos. Meas. Tech., 5, 581–594, https://doi.org/10.5194/amt-5-581-2012, 2012.

Corradini, S., L. Merucci, and A. J. Prata, Retrieval of SO2 from thermal infrared satellite measurements: Correction procedures for the effects of volcanic ash, Atmos. Meas. Tech. 2, 177–191, 2009.

Costa, A., Suzuki, Y.J., Cerminara, M., Devenish, B.J., Esposti Ongaro, T., Herzog, M., Van Eaton, A.R., Denby, L.C., Bursik, M., de Michieli, M., et al., Results of the eruptive column model inter-comparison study, Journal of Volcanology and Geothermal Research, 326, 2-25, 2016.

Crawford, A. M., B. J. B. Stunder, F. Ngan, and M. J. Pavolonis, Initializing HYSPLIT with satellite observations of volcanic ash: A case study of the 2008 Kasatochi eruption, J. Geophys. Res.Atmos.,121, 10,786–10,803,doi:10.1002/2016JD024779, 2016.

D'Amours, R., Malo, A., Servranckx, R., Bensimon, D., Trudel, S., and Gauthier-Bilodeau, J-P., Application of the atmospheric Lagrangian particle dispersion model MLDP0 to the 2008 eruptions of

© Crown Copyright 2021, Met Office

Okmok and Kasatochi volcanoes, Journal of Geophysical Research, 115, D00L11, doi:10.1029/2009JD013602, 2010.

de Leeuw, J., Schmidt, A., Witham, C. S., Theys, N., Taylor, I. A., Grainger, R. G., Pope, R. J., Haywood, J., Osborne, M., and Kristiansen, N. I., The 2019 Raikoke volcanic eruption: Part 1 Dispersion model simulations and satellite retrievals of volcanic sulfur dioxide, Atmos. Chem. Phys., https://doi.org/10.5194/acp-2020-889, 2021.

Denlinger, R., Pavolonis, M., Sieglaff, J., A robust method to forecast volcanic ash clouds. J. Geophys. Res., 117, D13208, 2012.

Dhomse, S.S., Emmerson, K.M., Mann, G.W., Bellouin, N., Carslaw, K.S., Chipperfield, M.P., Hommel, R., Abraham, N.L., Telford, P., Braesicke, P., Dalvi, M., Johnson, C.E., O'Connor, F., Morgenstern, O., Pyle, J.A., Deshler, T., Zawodny, J.M. and Thomason, L.W., Aerosol microphysics simulations of the Mt. Pinatubo eruption with the UMUKCA composition climate model, Atmospheric Chemistry and Physics, 14, 11221–11246, 2014.

Doutriaux-Boucher, M., P. Dubuisson, R. Saunders, and S. Watkin, Volcanic SO2 detection by satellite using infrared radiometers, Met Office Forecasting Research Technical Report No. 487, https://digital.nmla.metoffice.gov.uk/IO_754240fc-f3c5-432e-8be5-f20ab5290ff3/, 2006.

Eckhardt, S., Prata, A.J., Seibert, P., Stebel, K., and Stohl, A., Estimation of the vertical profile of sulfur dioxide injection into the atmosphere by a volcanic eruption using satellite column measurements and inverse transport modelling, Atmos. Chem. Phys., 8, 3881–3897, 2008.

Egan, S.D., Stuefer, M., Webley, P.W., Cahill, C.F., Dean, J., WRF-Chem modeling of sulfur dioxide emissions from the 2008 Kasatochi Volcano, Annals of Geophysics, Fast Track 2, doi: 10.4401/ag-6626, 2014.

Flemming, J. and Inness, A., Volcanic sulfur dioxide plume forecasts based on UV satellite retrievals for the 2011 Grímsvötn and the 2010 Eyjafjallajökull eruption, Journal of Geophysical Research: Atmospheres, 118, 10,172–10,189, doi:10.1002/jgrd.50753, 2013.

Folch, A., Mingari, L., Gutierrez, N., Hanzich, M., Macedonio, G., Costa, A., FALL3D-8.0: a computational model for atmospheric transport and deposition of particles, aerosols and radionuclides – Part 1: Model physics and numerics, Geosci. Model Dev., 13, 1431–1458, 2020.

Fu, G., Prata, F., Lin, H. X., Heemink, A., Segers, A., and Lu, S., Data assimilation for volcanic ash plumes using a satellite observational operator: a case study on the 2010 Eyjafjallajökull volcanic eruption, Atmos. Chem. Phys., 17, 1187–1205, https://doi.org/10.5194/acp-17-1187-2017, 2017.

Fu, G., Heemink, A., Lu, S., Segers, A., Weber, K., Lin, H.X., Model-based aviation advice on distal volcanic ash clouds by assimilating aircraft in situ measurements, Atmos. Chem. Phys., 16, 9189–9200, 2016.

Fu, G., Lin, H., Heemink, A., Segers, A., Lu, S., Palsson, T., Assimilating aircraft-based measurements to improve forecast accuracy of volcanic ash transport, Atmos. Environ., 115, 170–184, 2015.

Fu, G., Lin, H.X., Heemink, A., Lu, S., Segers, A., Velzen, N.V., Lu, T., Xu, S., Accelerating volcanic ash data assimilation using a mask-state algorithm based on an ensemble Kalman filter: A case study with the LOTOS-EUROS model (version 1.10), Geosci. Model Dev., 10, 1751–1766, 2017b.

© Crown Copyright 2021, Met Office

Ge, C., Wang, J., Carn, S., Yang, K., Ginoux, P., Krotkov, N., Satellite-based global volcanic SO2 emissions and sulfate direct radiative forcing during 2005–2012, J. Geophys. Res. Atmos., 121, 3446–3464, 2016.

Gíslason, S.R., Stefánsdóttir, G., Pfeffer, M.A., Barsotti, S., Jóhannsson, Th., Galeczka, I., Bali, E., Sigmarsson, O., Stefánsson, A., Keller, N.S., Sigurdsson, Á., Bergsson, B., Galle, B., Jacobo, V.C., Arellano, S., Aiuppa, A., Jónasdóttir, E.B., Eiríksdóttir, E.S., Jakobsson, S., Guðfinnsson, G.H., Halldórsson, S.A., Gunnarsson, H., Haddadi, B., Jónsdóttir, I., Thordarson, Th., Riishuus, M., Högnadóttir, Th., Dürig, T., Pedersen, G.B.M., Höskuldsson, Á., Gudmundsson, M.T., Environmental pressure from the 2014–15 eruption of Bárðarbunga volcano, Iceland Geochem. Persp. Let., 1, 84-93 2015.

Guffanti, M., D. J. Schneider, K. L. Wallace, T. Hall, D. R. Bensimon, and L. J. Salinas, Aviation response to a widely dispersed volcanic ash and gas cloud from the August 2008 eruption of Kasatochi, Alaska, USA, J. Geophys. Res., 115, D00L19, doi:10.1029/2010JD013868, 2010.

Guffanti, M., T. J. Casadevall, and K. Budding, Encounters of aircraft with volcanic ash clouds: A compilation of known incidents, 1953–2009, U.S. Geological Survey Data Series 545, https://pubs.usgs.gov/ds/545/, 2010.

Halmer, A., Schmincke, H.U., Graf, H.F., The annual volcanic gas input into the atmosphere, in particular into the stratosphere: a global data set for the past 100 years, Journal of Volcanology and Geothermal Research, 115, 511, 2002.

Hansell, A. and Oppenheimer, C., Health Hazards from Volcanic Gases: A Systematic Literature Review, Archives of Environmental Health, 59(12):628-39, 2005.

Harvey, N.J., Dacre, H.F., Webster, H.N., Taylor, I.A., Khanal, S., Grainger, R.G., Cooke, M.C., The Impact of Ensemble Meteorology on Inverse Modeling Estimates of Volcano Emissions and Ash Dispersion Forecasts: Grímsvötn 2011. Atmosphere, 11, 1022. https://doi.org/10.3390/atmos11101022, 2020.

Heard, I.P.C., Manning, A.J., Haywood, J.M., Witham, C., Redington, A., Jones, A., Clarisse, L. and Bourassa, A., A comparison of atmospheric dispersion model predictions with observations of SO2 and sulphate aerosol from volcanic eruptions, Journal of Geophysical Research, doi:10.1029/2011JD016791, 117, D00U22, 2012.

Heaviside, C., Witham, C.S., Vardoulakis, S., Potential health impacts from sulphur dioxide and sulphate exposure in the UK resulting from an Icelandic effusive volcanic eruption, Science of the Total Environment, 774, 145549, 2021.

Heng, Y., Hoffmann, L., Griessbach, S., Rößler, T., and Stein, O., Inverse transport modeling of volcanic sulfur dioxide emissions using large-scale simulations, Geosci. Model Dev., 9, 1627–1645, https://doi.org/10.5194/gmd-9-1627-2016, 2016.

Hughes, E. J., J. Yorks, N. A. Krotkov, A. M. da Silva, and M. McGill, Using CATS near-real-time lidar observations to monitor and constrain volcanic sulfur dioxide (SO2) forecasts, Geophys. Res. Lett., 43, 11,089–11,097, doi:10.1002/ 2016GL070119, 2016.

Hughes, E.J., L.C. Sparling, S.A. Carn, and A.J. Krueger, Using horizontal transport characteristics to infer an emission height time-series of volcanic SO2, J. Geophys. Res., 117, D18307. DOI: 10.1029/2012JD017957, 2012.

© Crown Copyright 2021, Met Office

Huijnen, V., Flemming, J., Chabrillat, S., Errera, Q., Christophe, Y., Blechschmidt, A-M., Richter, A., Eskes, H., C-IFS-CB05-BASCOE: stratospheric chemistry in the Integrated Forecasting System of ECMWF, Geosci. Model Dev., 9, 3071–3091, 2016.

Hyman, D., M. Pavolonis, and J. Sieglaff, A novel approach to estimating time-averaged volcanic SO2 fluxes from infrared satellite measurements, Remote Sensing, submitted 2021.

Hyman, D.M. and M.J.Pavolonis, Probabilistic retrieval of volcanic SO2 layer height and partial column density using the Cross-track Infrared Sounder (CrIS), Atmos. Meas. Tech. 13, 5891–5921, 2020.

Inness, A., Ades, M., Balis, D., Efremenko, D., Flemming, J., Hedelt, P., Koukouli, M.-E., Loyola, D., and Ribas, R., The CAMS volcanic forecasting system utilizing near-real time data assimilation of S5P/TROPOMI SO2 retrievals, Geosci. Model Dev. Discuss., https://doi.org/10.5194/gmd-2021-219, in review, 2021.

Ishii, K., Hayashi, Y., Shimbori, T., Using Himawari-8, estimation of SO2 cloud altitude at Aso volcano eruption on October 8, 2016, Earth, Planets and Space, 70:19, 2018.

Johnson, B., et al., In situ observations of volcanic ash clouds from the FAAM aircraft during the eruption of Eyjafjallajökull in 2010, J. Geophys. Res., 117, D00U24, doi:10.1029/2011JD016760, 2012.

Jones, A., Thomson, D., Hort, M., and Devenish, B., The U.K. Met Office's Next-Generation Atmospheric Dispersion Model, NAME III, https://doi.org/10.1007/978-0-387-68854-1_62, 2007.

Kleinbeck, S., Schäper, M., Juran, S. A., Kiesswetter, E., Blaszkewicz, M., Golka, K., Zimmermann, A., Brüning, T., and Van Thriel, C., Odor Thresholds and Breathing Changes of Human Volunteers as Consequences of Sulphur Dioxide Exposure Considering Individual Factors, Safety and Health at Work, 2, 4, P355-364, https://doi.org/10.5491/SHAW.2011.2.4.355, 2011.

Klüser, L., Erbertseder, T., and Meyer-Arnek, J., Observation of volcanic ash from Puyehue–Cordón Caulle with IASI, Atmos. Meas. Tech., 6, 35–46, https://doi.org/10.5194/amt-6-35-2013, 2013.

Knowland, K.E., Keller, C.A. and Lucchesi, R., File Specification for GEOS-CF Products. GMAO Office Note No. 17 (Version 1.1), 37 pp, available from https://gmao.gsfc.nasa.gov/pubs/docs/Knowland1204.pdf, 2020.

Kristiansen, N. I., D. Arnold, C. Maurer, J. Vira, R. Radulescu, D. Martin, A. Stohl, K. Stebel, M. Sofiev, C. O'Dowd, G. Wotawa, Improving model simulations of volcanic emission clouds and assessing model uncertainties, Natural Hazard Uncertainty Assessment: Modeling and Decision Support, Geophysical Monograph 223, First Edition, edited by Karin Riley, Peter Webley, and Matthew Thompson, American Geophysical Union. Published 2017 by John Wiley & Sons, Inc., 2017.

Kristiansen, N. I., Stohl, A., Prata, A. J., Richter, A., Eckhardt, S., Seibert, P., Hoffmann, A., Ritter, C., Bitar, L., Duck, T. J., and Stebel, K., Remote sensing and inverse transport modeling of the Kasatochi eruption sulfur dioxide cloud, J. Geophys. Res., 115, 1–18, doi:10.1029/2009JD013286, 2010.

Krotkov, N. A., M. R. Schoeberl, G. A. Morris, S. Carn, and K. Yang, Dispersion and lifetime of the SO2 cloud from the August 2008 Kasatochi eruption, J. Geophys. Res., 115, D00L20, doi:10.1029/ 2010JD013984, 2010.

© Crown Copyright 2021, Met Office

Lamotte, C., Guth, J., Marécal, V., and Cussac, M., Modeling study of the impact of SO2 volcanic passive emissions on the tropospheric sulfur budget, Atmos. Chem. Phys. Discuss. [preprint], https://doi.org/10.5194/acp-2020-1040, in review, 2020.

Lopez, T., Carn, S., Wener, C., Fee, D., Kelly, P., Doujkas, M., Pfeffer, M., Webley, P., Cahill, C., Schneider, D., Evaluation of Redoubt Volcano's sulfur dioxide emissions by the Ozone Monitoring Instrument, Journal of Volcanology and Geothermal Research 259, 290–307, 2013.

Lu, S., Heemink, A., Lin, H. X., Segers, A., and Fu, G., Evaluation criteria on the design for assimilating remote sensing data using variational approaches, Mon. Weather Rev., 0, 1–11, doi:10.1175/mwr-d-16-0289.1, 2017.

Lu, S., Lin, H. X., Heemink, A. W., Fu, G., and Segers, A. J.: Estimation of Volcanic Ash Emissions Using Trajectory-Based 4-D-Var Data Assimilation, Mon. Weather Rev., 144, 575–589, doi:10.1175/mwr-d-15-0194.1, 2016.

Lu, S., Lin, H. X., Heemink, A., Segers, A., and Fu, G.: Estimation of volcanic ash emissions through assimilating satellite data and ground-based observations, J. Geophys. Res.-Atmos., 121, 10971–10994, doi:10.1002/2016JD025131, 2016b.

Maerker, K. C., P. V. Rix, and J. Van Geffen, Trajectory matching and dispersion modeling of volcanic plumes utilizing space-based observations, paper presented at USEReST 2008, the 2nd Workshop on USE Remote Sensing Techniques for Monitoring Volcanoes and Seismogenic Areas, Inst. of Electr. and Electron. Eng., Naples, Italy, 11–14 Nov, 2008.

Malavelle, F., Haywood, J., et al., Strong constraints on aerosol–cloud interactions from volcanic eruptions, Nature, vol 546: 485, 2017.

Marenco, F., Sulphur dioxide monitoring from space, Space Applications and Nowcasting Technical Memo 7, 2021.

Marti, A. and Folch, A., Volcanic ash modelling with NMMB-MONARCH-ASH model: Quantification of offline modelling errors. Atmos. Chem. Phys.,18, 4019–4038, 2018.

Martin, E., S. Bekki, C. Ninin, and Bindeman, I., Volcanic sulfate aerosol formation in the troposphere, J. Geophys. Res. Atmos., 119, 12,660–12,673, doi:10.1002/2014JD021915, 2014.

Martin, E., Volcanic Plume Impact on the Atmosphere and Climate: O- and S-Isotope Insight into Sulfate Aerosol Formation, Geosciences, 8, 198, doi:10.3390/geosciences8060198, 2018.

Mastin, L. G., Guffanti, M., Servranckx, R., Webley, P., Barsotti, S., Dean, K., Durant, A., Ewert, J.W., Neri, A., Rose, W.I., Schneider, D., Siebert, L., Stunder, B., Swanson, G., Tupper, A., Volentik, A., Waythomas, C.F., A multidisciplinary effort to assign realistic source parameters to models of volcanic ash-cloud transport and dispersion during eruptions, J. Volcanol. Geotherm. Res.,186, 10–21, 2009.

Maters, E. C., Delmelle, P., Rossi, M. J., and Ayris, P. M., Reactive uptake of sulfur dioxide and ozone on volcanic glass and ash at ambient temperature. Journal of Geophysical Research: Atmospheres, 122, 10,077–10,088, https://doi.org/10.1002/2017JD026993, 2017.

Mills, M. J., et al., Global volcanic aerosol properties derived from emissions, 1990–2014, using CESM1(WACCM), J. Geophys. Res. Atmos., 121, 2332–2348, 2016.

© Crown Copyright 2021, Met Office

Mingari, L., Folch, A., Prata, A. T., Pardini, F., Macedonio, G., and Costa, A., Data Assimilation of Volcanic Aerosols using FALL3D+PDAF, Atmos. Chem. Phys. Discuss. [preprint], https://doi.org/10.5194/acp-2021-747, in review, 2021.

Morton, B.R., Taylor, G.I., Turner, J.S., Turbulent gravitational convection from maintained and instantaneous source. Phil. Trans. Roy. Soc. Lond. A 234, 1–23, 1956.

Moxnes, E., N. Kristiansen, A. Stohl, L. Clarisse, A. Durant, K. Weber, and A. Vogel, Separation of ash and sulfur dioxide during the 2011 Grímsvötn eruption, J. Geophys. Res. Atmos., 119, 7477–7501, doi:10.1002/2013JD021129, 2014.

Muser, L.O., Hoshyaripour, G.A., Bruckert, J., Horváth, A., Malinina, E., Wallis, S., Prata, F.J., Rozanov, A., von Savigny, C., Vogel, H. and Vogel, B., Particle aging and aerosol–radiation interaction affect volcanic plume dispersion: evidence from the Raikoke 2019 eruption, Atmos. Chem. Phys., 20, 15015–15036, 2020.

Newhall, C.G., and Self, S., The volcanic explosivity index (VEI): An Estimate of Explosive Magnitude for Historical Volcanism, Journal of Geophysical Research, 87, 1231-1238, 1982.

Osores, S., Ruiz, J., Folch, A., and Collini, E., FALL3D-ETKF- V1.0, Zenodo, https://doi.org/10.5281/zenodo.3066310, 2019.

Osores, S., Ruiz, J., Folch, A., and Collini, E., Volcanic ash forecast using ensemble-based data assimilation: an ensemble transform Kalman filter coupled with the FALL3D-7.2 model (ETKF–FALL3D version 1.0), Geosci. Model Dev., 13, 1–22, https://doi.org/10.5194/gmd-13-1-2020, 2020.

Pardini, F., Burton, M., Arzilli, F., La Spina, G., Polacci, M., SO2 emissions, plume heights and magmatic processes inferred from satellite data: the 2015 Calbuco eruptions. J. Volcanol. Geotherm. Res. 361, 12–24, 2018.

Pardini, F., Burton, M., Vitturi, M. de'Michieli, Corradini, S., Salerno, G., Merucci, L., Di Grazia, G., Retrieval and intercomparison of volcanic SO2 injection height and eruption time from satellite maps and ground-based observations. J. Volcanol. Geotherm. Res. 331, 79–91. https://doi.org/10.1016/j.jvolgeores.2016.12.008, 2017.

Pardini, F., Corradini, S., Costa, A., Esposti Ongaro, T., Merucci, L., Neri, A., Stelitano, D., and de' Michieli Vitturi, M., Ensemble-Based Data Assimilation of Volcanic Ash Clouds from Satellite Observations: Application to the 24 December 2018 Mt. Etna Explosive Eruption, Atmosphere, 11, 359, https://doi.org/10.3390/atmos11040359, 2020.

Pattantyus, A.K., Businger, S., Howell, S.G., Review of sulfur dioxide to sulfate aerosol chemistry at Kīlauea Volcano, Hawai'i. Atmospheric Environment 185 262–271, 2018.

Pavolonis, M. J., Sieglaff, J., & Cintineo, J., Automated detection of explosive volcanic eruptions using satellite-derived cloud vertical growth rates. Earth and Space Science, 5, 903–928. https://doi.org/10.1029/ 2018EA000410, 2018.

Pelley, R., Cooke, M., Manning, A., Thomson, D., Witham, C., Hort, M., Initial Implementation of an Inversion Technique for Estimating Volcanic Ash Source Parameters in Near Real time using Satellite Retrievals; Forecasting Research Technical Report; Met Office: Exeter, UK, Volume 604. 2015.

Peuch, V-H., Engelen, R., Flemming, J., Hiojnen, V., and Inness, A., Atmospheric composition in ECMWF's Integrated Forecasting System, ECMWF Newsletter No. 143, pp. 20–25, 2015.

© Crown Copyright 2021, Met Office

Pisso, I., Sollum, E., Grythe, H., Kristiansen, N.I., Cassiani, M., Eckhardt, S., Arnold, D., Morton, D., Thompson, R.L., Groot Zwaaftink, C.D., Evangeliou, N., Sodemann, H., Haimberger, L., Henne, S., Brunner, D., Burkhart, J.F., Fouilloux, A., Brioude, J., Philipp6, A., Seibert, P. and Stohl, A.,The Lagrangian particle dispersion model FLEXPART version 10.4, Geosci. Model Dev., 12, 4955–4997, 2019.

Plu, M., L. Robertson, D. Arnold, R. Baró, A. Carvalho, J. Letertre-Danczak, V.-H. Peuch, C. Maurer, M.D. Mulder, M. Hirtl, B. Scherllin-Pirscher, A. Uppstu, M. Sofiev, G. Bigeard, B. Sič, L. El Amraoui, N. Frebourg, EUNADICS-AV DELIVERABLE (D -N°: D26) Case studies with multi-source data assimilation, https://knmiprojects.archiefweb.eu/?subsite=eunadics#archive, 2019.

Prata, A. J., G. Gangale, L. Clarisse, and F. Karagulian, Ash and sulfur dioxide in the 2008 eruptions of Okmok and Kasatochi: Insights from high spectral resolution satellite measurements, J. Geophys. Res., 115, D00L18, doi:10.1029/2009JD013556, 2010.

Prata, A. J., S. A. Carn, A. Stohl, and J. Kerkmann, Long range transport and fate of a stratospheric volcanic cloud from Soufriere Hills volcano, Montserrat, Atmos. Chem. Phys. Discuss., 7(2), 4657–4672, doi:10.5194/acpd-7-4657-2007, 2007.

Prata, A. T., Mingari, L., Folch, A., Macedonio, G., and Costa, A., FALL3D-8.0: a computational model for atmospheric transport and deposition of particles, aerosols and radionuclides – Part 2: Model validation, Geosci. Model Dev., 14, 409–436, https://doi.org/10.5194/gmd-14-409-2021, 2021.

Prata, F., S. Carn, L. Clarisse, N. Theys, and J.-P. Vernier, Raikoke SO2 masses derived from satellite sensors, WMO-SPARC-SSiRC Volcano Response team, short note, 2019.

Queißer, M., Burton, M., Theys, N. et al., TROPOMI enables high resolution SO2 flux observations from Mt. Etna, Italy, and beyond. Sci Rep 9, 957. https://doi.org/10.1038/s41598-018-37807-w, 2019.

Redington A.L., Derwent R.G., Witham C.S. and Manning A.J., Sensitivity of modelled sulphate and nitrate aerosol to cloud, pH and ammonia emissions, Atmospheric Environment, 43, 3227-3234, 2009.

Remy, S., Huijnen, V., Mann, G., Sengupta, K., Chabrillat, S., Coupling of IFS-GLOMAP and IFS-CB05-BASCOE, ECMWF Report, CAMS43_2019SC3_D43.1.5.4_201901_ICBG_v1, 2019.

Rolph, G.D., Draxler, R.R., De Pena, R., Modeling sulfur concentrations and depositions in the United States during ANATEX, Atmospheric Environment, 26A, 1, 73-93, 1992.

Rolph, G.D., Draxler, R.R., De Pena, R., The use of model-derived and observed precipitation in long-term sulfur concentration and deposition modelling, Atmospheric Environment, 27A, 13, 2017-2037, 1993.

Rose, W., Gu, Y., Watson, I., Yu, T., Blut, G., Prata, A., Krueger, A., Krotkov, N., Carn, S., Fromm, M., et al., The February–March 2000 eruption of Hekla, Iceland from a satellite perspective. Volcanism Earth´s Atmos.2003,139, 107–132, 2003.

Ryan, W.F., The air quality forecast rote: Recent changes and future challenges, Journal of the Air & Waste Management Association, 66:6, 576-596, 2016.

Schmehl, K., Haupt, S., Pavalonis, M., A Genetic Algorithm Variational Approach to Data Assimilation and Application to Volcanic Emissions, Pure Appl. Geophys., 169, 519–537, 2012.

© Crown Copyright 2021, Met Office

Schmidt A., S. Leadbetter, N. Theys, E. Carboni, C. Witham, J. Stevenson, C. Birch, T. Thordarson, S. Turnock, S. Barsotti, L. Delaney, W. Feng, R. Grainger, M. Hort, A. Hoskuldsson, I. Ialongo, E. Ilyinskaya, T. Johannsson, P. Kenny, T. Mather, N. Richards, J. Shepherd, Satellite detection, long-range transport and air quality impacts of volcanic sulfur dioxide from the 2014-2015 flood lava eruption at Bardarbunga (Iceland), Journal of Geophysical Research, DOI: 10.1002/2015JD023638, 2015.

Schmidt, A., Witham, C. S., Theys, N., Richards, N. A. D., Thordarson, T., Szpek, K., Feng, W., Hort, M. C., Woolley, A. M., Jones, A. R., Redington, A. L., Johnson, B. T., Hayward, C. L., and Carslaw K. S., Assessing hazards to aviation from sulfur dioxide emitted by explosive Icelandic eruptions, J. Geophys. Res. Atmos, 119, 14180-14196, DOI:10.1002/2014JD022070, 2014.

Schnetzler, C.C., Bluth, G.J.S., Krueger, A.J., Walter, L.S., A proposed volcanic sulfur dioxide index (VSI), Journal of Geophysical Research, 102, B9, 20,087-20,091, 1997.

Schoeberl, M. R., S. D. Doiron, L. R. Lait, P. A. Newman, and A. J. Krueger, A simulation of the Cerro Hudson SO2 cloud, J. Geophys. Res., 98(D2), 2949–2955, doi:10.1029/92JD02517, 1993.

Schumann, U., Weinzierl, B., Reitebuch, O., Schlager, H., Minikin, A., Forster, C., Baumann, R., Sailer, T., Graf, K., Mannstein, H., Voigt, C., Rahm, S., Simmet, R., Scheibe, M., Lichtenstern, M., Stock, P., Rüba, H., Schäuble, D., Tafferner, A., Rautenhaus, M., Gerz, T., Ziereis, H., Krautstrunk, M., Mallaun, C., Gayet, J.-F., Lieke, K., Kandler, K., Ebert, M., Weinbruch, S., Stohl, A., Gasteiger, J., Groß, S., Freudenthaler, V., Wiegner, M., Ansmann, A., Tesche, M., Olafsson, H., and Sturm, K., Airborne observations of the Eyjafjalla volcano ash cloud over Europe during air space closure in April and May 2010, Atmos. Chem. Phys., 11, 2245–2279, https://doi.org/10.5194/acp-11-2245-2011, 2011.

Scire, J.S., Strimaitis, D.G., Yamartino, R.J., A User's Guide for the CALPUFF Dispersion Model (Version 5), Earth Tech Inc, 2000.

Simpson, D., Benedictow, A., Bergei, H., Bergstrom, R., Emberson, L.D., Fagerli, H., Flechard, C.R., Hayman, G.D., Gauss, M., Jonson, J.E.., Jenkin, M.E., Nyiri, A., Richter, C., Semeena, V.S., Tsyro, S., Tuovinen, J.-P., Veldebenito, A., and Wind, P., The EMEP MSC-W chemical transport model–technical description, Atmos. Chem. Phys., 12, 7825–7865, 2012.

Sofiev, M., Data assimilation, Lecture/presentation slides, Available at https://etrp.wmo.int/pluginfile.php/21447/mod_folder/content/0/Lecture14_15.Sofiev.DA_AQ_20191010.pdf?forcedownload=1 , 2019.

Steensen, B.M., Schulz, M., Wind, P., Valdebenito, A.M., and Fagerli, H., The operational eEMEP model version 10.4 for volcanic SO2 and ash forecasting, Geosci. Model Dev., 10, 1927–1943, 2017.

Stein, A.F., Draxler, R.R., Rolph, G.D., Stunder, B.J.B., Cohen, M.D., Ngan, F., NOAA's HYSPLIT atmospheric transport and dispersion modelling system, BAMS, 2059-2077, 2015.

Stein,A.F., Lamb, D., Draxler, R.R., Incorporation of detailed chemistry into a three-dimensional Lagrangian-Eulerian hybrid model: application to regional tropospheric ozone, Atmospheric Environment, 34, 4361 - 4372, 2000.

Stohl, A., Prata, A., Eckhardt, S., Clarisse, L., Durant, A., Henne, S., Kristiansen, N., Minikin, A., Schumann, U., Seibert, P., Determination of time- and height-resolved volcanic ash emissions and their use for quantitative ash dispersion modeling: The 2010 Eyjafjallajokull eruption. Atmos. Chem. Phys., 11, 4333–4351, 2011.

© Crown Copyright 2021, Met Office

Tang, Y., Tong, D.Q., Yang, K., Lee, P., Baker, B., Crawford, A., Luke, W., Stein, A., Campbell, P.C.., Ring, A., Flynn, J., Wang. Y., McQueen, J., Pan, L., Huang, J., Stajner, I., Air quality impacts of the 2018 Mt. Kilauea Volcano eruption in Hawaii: A regional chemical transport model study with satellite-constrained emissions, Atmospheric Environment, 237, 117648, 2020.

Taylor, I. A., Carboni, E., Ventress, L. J., Mather, T. A., and Grainger, R. G.: An adaptation of the CO2 slicing technique for the Infrared Atmospheric Sounding Interferometer to obtain the height of tropospheric volcanic ash clouds, Atmos. Meas. Tech., 12, 3853–3883, https://doi.org/10.5194/amt-12-3853-2019, 2019.

Theys, N., Campion, R., Clarisse, L., Brenot, H., van Gent, J., Dils, B., Corradini, S., Merucci, L., Coheur, P.-F., Van Roozendael, M., Hurtmans, D., Clerbaux, C., Tait, S., and Ferrucci, F., Volcanic SO2 fluxes derived from satellite data: a survey using OMI, GOME-2, IASI and MODIS, Atmos. Chem. Phys., 13, 5945– 5968, doi:10.5194/acp-13-5945-2013, 2013.

Theys, N., Hedelt, P., De Smedt, I. *et al.* Global monitoring of volcanic SO_2 degassing with unprecedented resolution from TROPOMI onboard Sentinel-5 Precursor. *Sci Rep* **9,** 2643 (2019). https://doi.org/10.1038/s41598-019-39279-y

Urupina, D., Lasnea, J., Romaniasa, M.N., Thiery, V., Dagsson-Waldhauserova, P., Theveneta, F., Uptake and surface chemistry of SO2 on natural volcanic dusts, Atmospheric Environment, 217, 116942, 2019.

Vieno, M., Dore, A.J., Stevenson, D.S., Doherty, R., Heal, M.R., Reis, S., Hallsworth, S., Tarrason, L., Wind, P., Fowler, D., Simpson, D. and Sutton, M.A., Modelling surface ozone during the 2003 heat-wave in the UK, Atmos. Chem. Phys., 10, 7963–7978, 2010.

Vira, J., Carboni, E., Grainger, R. G., and Sofiev, M., Variational assimilation of IASI SO2 plume height and total column retrievals in the 2010 eruption of Eyjafjallajökull using the SILAM v5.3 chemistry transport model, Geosci. Model Dev., 10, 1985–2008, https://doi.org/10.5194/gmd-10-1985-2017, 2017.

Walters, D., Baran, A., Boutle, I., Brooks, M., Earnshaw, P., Edwards, J., Furtado, K., Hill, P., Lock, A., Manners, J., et al., The Met Office Unified Model Global Atmosphere 7.0/7.1 and JULES Global Land 7.0 configurations, Geosci. Model Dev., 12, 1909–1963, 2019.

Wang, J., Park, S., Zeng, J., Ge, C., Yang, K., Carn, S., Krotkov, N., and Omar, A. H., Modeling of 2008 Kasatochi volcanic sulfate direct radiative forcing: assimilation of OMI SO2 plume height data and comparison with MODIS and CALIOP observations, Atmos. Chem. Phys., 13, 1895–1912, doi:10.5194/acp-13-1895- 2013, 2013.

Wilkins, K. L., Watson, I. M., Kristiansen, N. I., Webster, H. N., Thomson, D. J., Dacre, H. F., and Prata, A. J., Using data insertion with the NAME model to simulate the 8 May 2010 Eyjafjallajökull volcanic ash cloud, J. Geophys. Res. Atmos., 121, doi:10.1002/2015JD023895, 2016.

Wilkins, K., Mackie, S., Watson, I., Webster, H, N., Thomson, D., Dacre, H., Data insertion in volcanic ash cloud forecasting. Ann. Geophys. 2014, 2, doi:10.4401/ag-6624, 2014.

Wilkins, K.L., Western, L.M. and Watson, I. M., Simulating atmospheric transport of the 2011 Grímsvötn ash cloud using a data insertion update scheme, Atmospheric Environment, 141, 48-59, https://doi.org/10.1016/j.atmosenv.2016.06.045, 2016.

© Crown Copyright 2021, Met Office

Witham, C.S., Oppenheimer, C., and Horwell, C.J., Volcanic ash-leachates: a review and recommendations for sampling methods, Journal of Volcanology and Geothermal Research, 141, 299– 326, 2005.

Wong, DC., Pleim, J., Mathur, R., Binkowski, F., Otte, T., Gilliam, R., Pouliot, G., Xiu, A., Young, J.O., Kang, D., WRF-CMAQ two-way coupled system with aerosol feedback: software development and preliminary results, Geosci. Model Dev., 5, 299–312, 2012.

World Health Organization, WHO global air quality guidelines: particulate matter (PM2.5 and PM10), ozone, nitrogen dioxide, sulfur dioxide and carbon monoxide. World Health Organization. https://apps.who.int/iris/handle/10665/345329. License: CC BY-NC-SA 3.0 IGO, 2021.

Yang, K., N. A. Krotkov, A. J. Krueger, S. A. Carn, P. K. Bhartia, and P. F. Levelt, Improving retrieval of volcanic sulfur dioxide from backscattered uv satellite observations, Geophys. Res. Lett. 36, 2009.

Zhao, Y., Saunois, M., Bousquet, P et al., Inter-model comparison of global hydroxyl radical (OH) distributions and their impact on atmospheric methane over the 2000–2016 period. Atmos. Chem. Phys., 19, 13701–13723, 2019.

Zhu, Y., Toon, O.B., Jensen, E.J., Bardeen, C.G., Mills, M.J., Tolbert, M.A., Yu, P., and Woods, S., Persisting volcanic ash particles impact stratospheric SO2 lifetime and aerosol optical properties, Nature Communications, 11:4526, 2020.

Zidikheri, M. J., and R. J. Potts, A simple inversion method for deter- mining optimal dispersion model parameters from satellite detections of volcanic sulfur dioxide, J. Geo- phys. Res. Atmos., 120, 9702–9717, doi:10.1002/2015JD023627, 2015.

Zidikheri, M., Lucas, C. and Potts, R., Quantitative verification and calibration of volcanic ash ensemble forecasts using satellite data, J. Geophys. Res. Atmos., 123, doi:10.1002/2017JD027740, 2018.

Zidikheri, M.J. and Lucas, C. Using Satellite Data to Determine Empirical Relationships between Volcanic Ash Source Parameters. Atmosphere, 11, 342, https://doi.org/10.3390/atmos11040342, 2020.

© Crown Copyright 2021, Met Office

Appendix A – List of Acronyms

AIRS: Atmospheric Infrared Sounder
CALIOP: Cloud-Aerosol Lidar with Orthogonal Polarization
CALPUFF: California Puff Model
CAMS: Copernicus Atmospheric Monitoring Service
CESM: Community Earth System Model
C-IFS: Composition Integrated Forecasting System
CMAQ: Community Multiscale Air Quality modelling
DOAS: Differential Optical Absorption Spectroscopy
DU: Dobson Units
ECMWF: European Centre for Medium-Range Weather Forecasts
eEMEP: Emergency European Monitoring and Evaluation Programme model
ESA: European Space Agency
ESP: Eruption Source Parameters
FLEXPART: FLEXible PARTicle dispersion model
GEO: Geostationary, or geosynchronous, satellite
GEOS-CF: Goddard Earth Observing System Composition Forecasting
GLOMAP: Global Model of Aerosol Processes
HadGEM3: Hadley Centre Global Environment Model version 3
HYSPLIT: Hybrid Single-Particle Lagrangian Integrated Trajectory model
IASI: Infrared Atmospheric Sounding Interferometer
IAVW: International Airways Volcano Watch
ICAO: International Civil Aviation Organization
ICON-ART: ICOsahedral Nonhydrostatic model – Aerosols and Reactive Trace gases
IFS-CB05-BASCOE-GLOMAP (ICBG): A Coupled Tropospheric and Stratospheric Aerosol and Chemistry Option for the ECMWF IFS
IMO: Icelandic Met Office
INGV: Instituto Nazionale di Geofisica e Vulcanologia
IR: Infrared
JMA-GATM: Japan Meteorological Agency Global Atmospheric Transport Model
JPPS: Joint Polar Satellite System
LEO: Low Earth Orbit
MetUM: Unified Model of the UK Met Office, an NWP model
MISD: The ICAO Met Panel's Working Group on Meteorological Information and Service Development
MLDP0: Modele Lagrangien de Dispersion de Particules
MOCAGE: Modèle de Chimie Atmosphérique de Grande Echelle
MSG: Meteosat Second Generation, geostationary satellite
MW: Microwave
NAME: Numerical Atmospheric dispersion Modelling Environment
NASA: National Aeronautics and Space Administration
NCAR: National Centre for Atmospheric Research
NOAA: National Oceanic and Atmospheric Administration
NWP: Numerical Weather Prediction, 4D weather forecast data

© Crown Copyright 2021, Met Office

OH: The hydroxyl radical
OMI: Ozone Monitoring Instrument
SACS: Support to Aviation Control Service
SEVIRI: Spinning Enhanced Visible and InfraRed Imager, which is on the MSG satellite
SILAM: System for Integrated modeLling of Atmospheric coMposition
SO_2: Sulphur dioxide
SO_4: Sulphate
TOMS: Total Ozone Mapping Spectrometer
TROPOMI: Tropospheric Monitoring Instrument
UKCA: United Kingdom Chemistry and Aerosol model
UM: Unified Model
UTLS: Upper Troposphere Lower Stratosphere
UV: Ultraviolet
VAA: Volcanic Ash Advisory
VAAC: Volcanic Ash Advisory Centre
VAG: Volcanic Ash Graphic
VEI: Volcanic Explosivity Index
VIIRS: Visible Infrared Imaging Radiometer Suite
VOLCAT: Volcanic Cloud Analysis Toolkit, monitoring system from NOAA/CIMSS
VONA: Volcano Observatory Notice to Aviation
WHO: World Health Organisation
WMO: World Meteorological Organisation
WRF-Chem: Weather Research and Forecasting (WRF) model coupled with Chemistry
ZAMG: Zentralanstalt für Meteorologie und Geodynamik, Chemical weather forecasts, Austria

© Crown Copyright 2021, Met Office